THERMODYNAMICS AND ION BINDING PROPERTIES OF MICELLAR AND POLYELECTROLYTE SYSTEMS APPLICATION OF THE POISSON-BOLTZMANN EQUATION

GUÐMUNDUR GUNNARSSON

LUND 1981

THERMODYNAMICS AND ION BINDING PROPERTIES OF MICELLAR AND POLYELECTROLYTE SYSTEMS. APPLICATION OF THE POISSON-BOLTZMANN EQUATION.

av

Gudmundur Gunnarsson
Civilingenjör
Värmlands nation

Akademisk avhandling som för avläggande av teknologie doktorsexamen vid tekniska fakulteten vid universitetet i Lund kommer att offentligen försvaras å hörsal D, Kemicentrum, lördagen den 5 september 1981 kl 10.15.

Digitized by the Internet Archive
in 2026

https://archive.org/details/IA41553424_0026

THERMODYNAMICS AND ION BINDING PROPERTIES OF MICELLAR AND POLYELECTROLYTE SYSTEMS. APPLICATION OF THE POISSON-BOLTZMANN EQUATION.

GUDMUNDUR GUNNARSSON

1981

Gunnarsson, G (1981)
Thesis, University of Lund.
Division of Physical Chemistry 2.
Chemical Centre, P.O.B. 740.
S-220 07 Lund 7, SWEDEN.

UNIV.
LEIDEN
BIBL.

Organization
LUND UNIVERSITY
Division of Physical Chemistry
Chemical Centre, P.O.B. 740
S-220 07 LUND 7
SWEDEN

Document name
DOCTORAL DISSERTATION

Date of issue
11/8 1981

CODEN:

Author(s)
Gudmundur Gunnarsson

Sponsoring organization

Title and subtitle
THERMODYNAMICS AND ION BINDING PROPERTIES OF MICELLAR AND POLYELECTROLYTE SYSTEMS. APPLICATION OF THE POISSON-BOLTZMANN EQUATION.

Abstract

The ion binding properties of polyelectrolytes are discussed on basis of the Poisson-Boltzmann (PB) equation. Comparison is made between the ion binding properties of spherical, cylindrical and planar polyelectrolytes. Comparison is also made between theory and the ion binding properties of polyelectrolytes as obtained from NMR experiments. In all cases the theory is in agreement with experiments. Thermodynamic functions for polyelectrolytes of different geometries are also discussed on basis of the PB equation and comparison is made between theory and experiments on the proton dissociation enthalpy of poly(acrylic acid). In this case are the theoretical values a factor of two too low.

A model expression for the free energy of a micellar solution is presented. The free energy expression consists essentially of three contributions: 1) the electrostatic free energy, 2) the hydrophobic energy and 3) the entropy of mixing of the micelles. Expressions for chemical potentials of all species in a micellar solution are presented and an equation for the micellar size distribution is derived. When applying the theory the micellar size distribution is either assumed to be monodisperse or allowed to be polydisperse. It is found that the theory can account for changes in the critical micelle concentration (cmc) with salt concentration, counterion valency and hydrocarbon chain length. The decrease in monomer concentration above cmc is also accounted for. The main characteristics of the micellar size distribution for dodecyl sulfate are also reproduced.

Key words

Classification system and/or index terms (if any)

Supplementary bibliographical information

Language
English

ISSN and key title

ISBN

Recipient's notes

Number of pages
115

Price

Security classification

Distribution by (name and address) Gudmundur Gunnarsson, Divison of Physical Chemistry, Chemical Centre, P.O.B. 740, S-220 07 LUND 7, SWEDEN

I, the undersigned, being the copyright owner of the abstract of the above-mentioned dissertation, hereby grant to all reference sources permission to publish and disseminate the abstract of the above-mentioned dissertation.

TABLE OF CONTENTS

LIST OF PAPERS 1

1. INTRODUCTION 2

2. THE POISSON-BOLTZMANN EQUATION AND THE CELL MODEL 5

3. ION BINDING TO POLYELECTROLYTES

3.1 General remarks 10
3.2 Theoretical considerations 11
3.3 Comparison between theory and experiment 22

4. THERMODYNAMIC FUNCTIONS IN POLYELECTROLYTE SYSTEMS

4.1 Fundamental equations 25
4.2 Some numerical examples 30
4.3 Enthalpies of proton dissociation of poly(acrylic acid) 34

5. APPLICATIONS TO MICELLES 37

REFERENCES 42

APPENDIX I 44

APPENDIX II 45

ACKNOWLEDGEMENTS 46

LIST OF PAPERS

The present thesis consists of this summary and the following papers (refered to by Roman numerals in the summary).

I. SURFACTANT ASSOCIATION INTO MICELLES. AN ELECTROSTATIC APPROACH.

G.Gunnarsson, B.Jönsson and H.Wennerström.

J.Phys.Chem., 84, 3114 (1980).

II. ION BINDING TO POLYELECTROLYTES AS DESCRIBED BY THE THEORY OF MANNING AND THE POISSON-BOLTZMANN EQUATION. COMPARISON WITH ^{23}Na NMR RELAXATION RATE EXPERIMENTS.

G.Gunnarsson and H.Gustavsson.

Submitted for publication.

III. ENTHALPIES OF PROTON DISSOCIATION OF POLY(ACRYLIC ACID). COMPARISON BETWEEN EXPERIMENT AND THEORY FOR A POLYELECTROLYTE SYSTEM.

G.Gunnarsson, H.Wennerström, G.Olofsson and A.Zacharov.

J.C.S. Faraday I, 76, 1287 (1980).

IV. MICELLAR SIZE DISTRIBUTIONS FOR IONIC AMPHIPHILES.

G.Gunnarsson and H.Wennerström.
Submitted for publication.

1. INTRODUCTION

Many macromolecules of biological importance are polyelectrolytes, i.e. they contain many ionic residues per molecule (1). One such example is DNA, in which case the distance between charged phosphate groups, projected on the cylindrical axis of the molecule, is only 1.7 Å (2). Other examples of approximately cylindrical polyelectrolytes are the mucopolysaccarides, dermatan-4-sulfate (DS), chondroitin-4-sulfate (CS) and hyaluronic acid (HA), which are important components of connective tissues. For these polyelectrolytes the distances between charged groups are 5 Å, 5 Å and 10 Å, respectively (3).

All of the above mentioned polyelectrolytes, as well as many others, are polyanions and as such they attract positive ions. This results in high degrees of cation binding to these polyanions, a feature which can be studied by many experimental methods. A characteristic feature of polyelectrolytes is that the extent of ion binding is mainly determined by the charge density of the polyelectrolyte (4,5), and is relatively insensitive to the type of ionic group on the macromolecule and to the type of counterions, as long as they are of the same valency. This suggests that the overall ion binding behaviour in these systems is determined by long range electrostatic effects and that chemical specificity is only of secondary importance.

Spherical polyelectrolytes, of which micelles formed from ionic surfactants, see figure 1.1, are typical examples, are also common. Micelles consist typically of 20-100 monomers, a number which depends on the chain length of the surfactant (6,7). The ion binding properties of micelles are in many ways similar to those of cylindrical polyelectrolytes (6). The ion binding properties of micelles are thus determined by long range electrostatic effects. Also determined by these effects is the concentration at

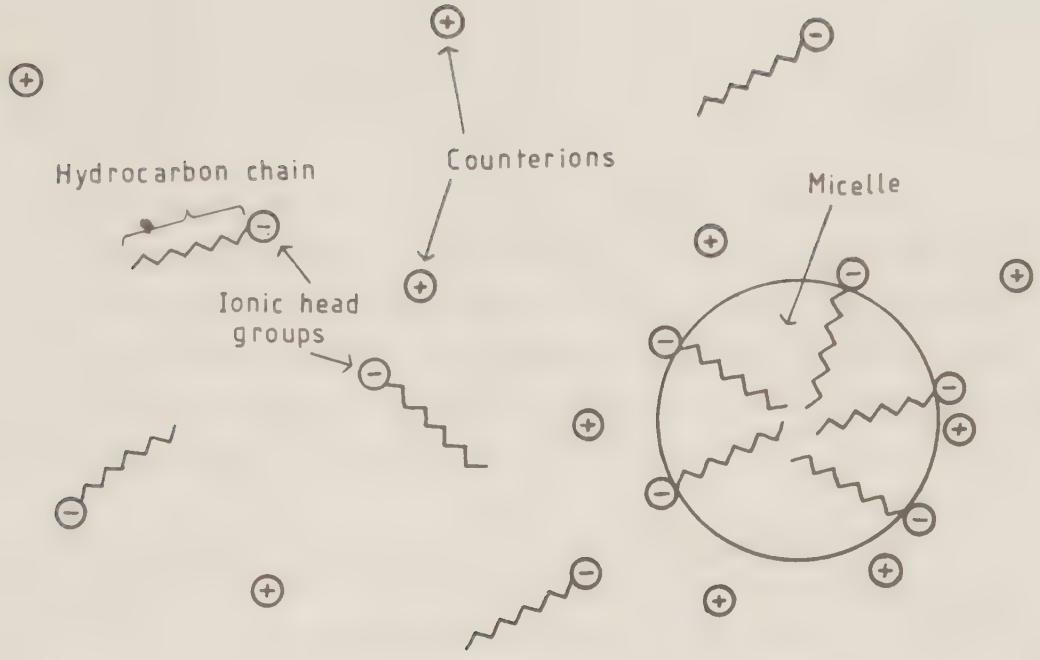

Figure 1.1 Schematic illustration of an ionic surfactant solution containing both monomeric and micellised surfactants. Only few of the monomers in the micelles are indicated.

which they start to form, which is called the critical micelle concentration (cmc). This is manifested in the decrease of the cmc with salt concentration (7). The micellar sizes are also influenced by electrostatic effects, as can be seen from the increase in micellar size with salt concentration (7).

It is thus clear that it is important to understand electrostatic effects in cylindrical polyelectrolyte and micellar systems. Attempting to include all molecular interactions in a description of these systems is not feasible and approximations must therefore be introduced. A first approximation would be to neglect the molecular identity of all species. Assuming furthermore that the solvent is represented by a dielectric continuum and neglecting the correlation between the small ions leads to the Poisson-Boltzmann equation

(8,9,10). An advantage of the PB equation, as compared to the theory of Manning (5), for example, is that it is both applicable to any geometry and it is possible to take the concentration of the polyelectrolyte into account through the cell model (11,23).

This thesis consists of an application of a theory based on the PB equation to the ion binding and thermodynamic properties of polyelectrolytes, such as cylindrical polyanions and micelles. In chapter 2, "The Poisson-Boltzmann equation and the cell model", the PB equation and the basic model is presented. Special attention is payed to the approximations inherent in the PB equation.

The general properties of ion distributions around polyelectrolytes are treated in chapter 3,"Ion binding to polyelectrolytes". In this chapter the ion distribution is related to different methods for measuring the degree of ion binding (I) and comparisons are made with experiments (II).

The presence of a polyelectrolyte and the non uniform charge distributions lead to large excess electrostatic free energies in polyelectrolyte systems (4,13). The excess electrostatic therodynamic functions are discussed in chapter 4, "Thermodynamics of Polyelectrolytes", where comparisons are also made with experiments on the proton dissociation enthalpy of poly(acrylic acid) (III).

The excess electrostatic free energy makes a large contribution to the free energy of micellar solutions (14). Another important contribution, which constitutes the driving force in the micelle forming process, is the hydrophobic effect (14,15). Expressions for the free energy and chemical potentials in micellar solutions are presented in chapter 5, "Applications to micelles". When applying the theory the micellar size distribution is either assumed to be monodisperse (I) or allowed to be polydisperse (IV).

2. THE POISSON-BOLTZMANN EQUATION AND THE CELL MODEL

A polyelectrolyte in solution will attract ions of opposite charge, called counterions, and repell ions of the same charge, called coions. In order to understand the properties of polyelectrolytes one needs to know how the small ions are distributed around the polyelectrolyte. Instead of trying to include all molecular interactions in the model we shall neglect the molecular nature of all species and only electrostatic effects will be taken into account. These effect will be treated within the approximations of the Gouy-Chapman model (8,9).

The fundamental relation in the Gouy-Chapman model is the following equation

$$c_i = c_{io} \exp(-z_i e\phi/kT) \tag{2.1}$$

where z_i is the valence of ion i. This equation relates a curve of constant potential, ϕ, to the average concentration of ion i along that curve, c_i. c_{io} is a constant equal to the average concentration of ion i on the zero potential curve. The average charge density, ρ, is obtained by summing over all ions according to

$$\rho = \sum_i z_i e c_{io} \exp(-z_i e\phi/kT) \tag{2.2}$$

Combining equation 2.2, which is essentially a Boltzmann distribution law, with the Poisson equation of classical electrostatics leads to the Poisson-Boltzmann (PB) equation.

$$-\varepsilon_r \varepsilon_o \nabla^2\phi = \sum_i z_i e c_{io} \exp(-z_i e\phi/kT) \tag{2.3}$$

where ε_o is the permittivity of vacuum. Here is it assumed that the dielectric constant, ε_r, is independent of the electric field. This means that the effects of dielectric saturation are neglected (16). The medium, in this case water, comes into the model only through its dielectric constant, ε_r.

In order to find a solution to the PB equation it is necessary to make some assumptions about the geometry of the polyelectrolyte and its surroundings. It is assumed that the polyelectrolyte can be approximated either by a sphere, by an infinite cylinder of radius r_b or by an infinite plane of thickness $2r_b$, see figure 2.1.

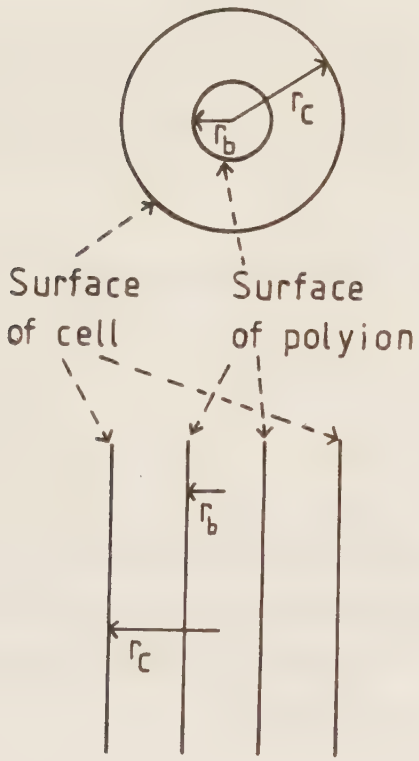

A cross section through the center of a spherical polyion of radius r_b. This also represents a cross section perpendicular to the axis of a cylindrical poyion of radius r_b.

A cross section parallel to the central axis of a cylindrical polyion. This represents also a cross section perpendicular to a planar polyion of thickness $2r_b$.

Figure 2.1. Polyelectrolyte geometries and the cell model.

The charges on the polyelectrolyte are assumed to be uniformly smeared out on its surface, resulting in a constant surface charge density, σ, and its surroundings are assumed to be of the same symmetry as the polyelectrolyte itself. This has the important consequence that the PB equation can then be transformed into a one dimensional form

$$\nabla^2\phi = \frac{1}{r^s}\frac{d}{dr}\left(r^s \frac{d\phi}{dr}\right) = -\frac{e}{\varepsilon_o \varepsilon_r} \sum_i z_i c_{io} \exp\left(-\frac{z_i e\phi}{kT}\right) \qquad (2.4)$$

where r is the distance from the center of the polyelectrolyte. The value of s depends on the symmetry of the problem and is 2, 1 and 0 for spherical, cylindrical and planar geometries, respectively.

The concentration of the polyelectrolyte itself is taken into account through the cell model (11,12). In the cell model the solution is divided into cells, each cell of the same geometry as the polyelectrolyte which it contains. The polyelectrolyte is assumed to be at the center of the cell, where r_c is the distance from the center of the polyelectrolyte to the cell boundary, see figure 2.1. The space between the polyelectrolyte and the cell boundary is filled with water and small ions.

It is convenient to set the electrostatic potential equal to zero at the cell boundary. This gives the following equation

$$\phi(r_c) = 0 \tag{2.5}$$

c_{io} is then the concentration of ion i at the cell boundary. The cell as a whole is assumed to be electrically neutral. Then from Gauss' law follows the further boundary condition.

$$\frac{d\phi}{dr}\Big|_{r_c} = 0 \tag{2.6}$$

Often one is interested in solutions to the PB equation for given values of r_b, r_c and σ and all values of $\tilde{c}_i$, where $\tilde{c}_i$ is the overall concentration of ion i. $\tilde{c}_i$ is expressed as

$$\tilde{c}_i = \int_{V_1} c_i(r)\, dV/V_1$$

$$= \int_{r_b}^{r_c} c_{io} \exp(-z_i e\phi/kT)\, r^s\, dr/\left(\frac{1}{s+1} r_c^{s+1} - \frac{1}{s+1} r_b^{s+1}\right) \tag{2.7}$$

where V_1 is the volume of the aqueous region of the cell. This expression gives the concentration in moles per unit volume of water, which is equivalent to molal units, if the density of water is taken

as 1. The concentration can also be expressed in molar units by substituting for V_1 the whole volume of the cell. Using the electroneutrality of the cell it follows that

$$\sigma = - \varepsilon_r \varepsilon_o \frac{d\phi}{dr} \Big|_{r_b} \qquad (2.8)$$

A problem with the PB equation and the cell model is that one does not know apriori which values of all c_{io} will give the required values of all $\tilde{c}_i$ and of σ. For planes, both with and without salt (17,18), and for cylinders without salt it is possible to solve the PB equation analytically (11,12). For cylinders, with salt, and for spheres, both with and without salt, one must resort to numerical methods to solve the PB equation. The numerical procedure used in this thesis is described in paper I.

Once we have obtained all the c_{io} which correspond to the case that we are interested in, we can then calculate a number of properties of a polyelectrolyte system. In the next chapter we consider the properties of the ion distribution. But before doing that we will discuss the approximations inherent in the PB equation. The PB equation is not in full agreement with a correct statistical mechanical treatment of the model, whereas Monte Carlo (MC) simulations (within statistical fluctuations) are. The difference lies in the fact that the PB equation neglects correlation between the small ions (10,19). This correlation, in the abscence of polyelectrolyte, would determine the activities of the small ions. Typical ion distributions obtained from the PB equation are shown in figure 2.2, where the parameters have been chosen to represent a dodecyl sulfate micelle. Also shown are the results of MC simulations on the same system (20). The calculations are for a sphere with 58 charges. In the MC simulations the polyion has a radius of 18 Å and the small ions have a radius of 1 Å whereas in the PB equation the small ions are all point charges. In order to make the results comparable when solving the PB equation the radius of the sphere is set equal to 19 Å. The neglect of ion-ion correlations leads to somewhat

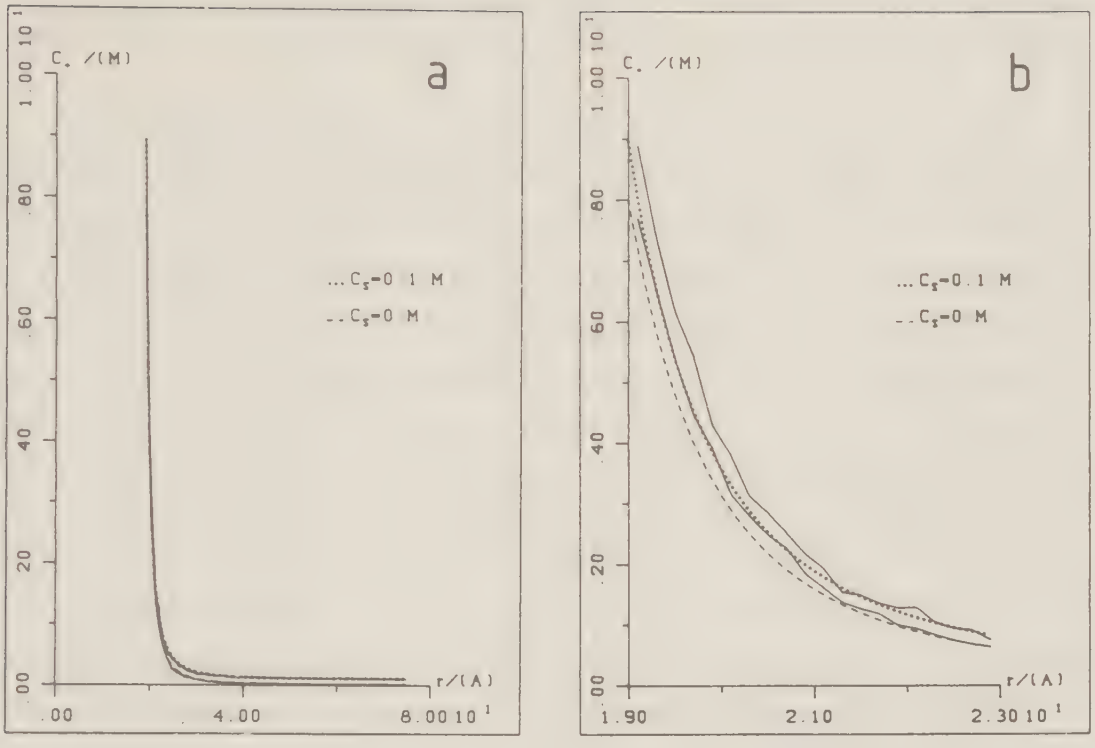

Figure 2.2. a) The radial concentration profile of counterions outside a sphere with 58 charges, with and without salt. The two solid curves are from MC simulations and the two other curves are from solutions of the PB equation. b) Expansion of the radial concentration profile in a) close to the surface. From ref. (20).

too low concentrations of counterions near the surface of the polyelectrolyte. The difference however is very small and shows that the PB equation well describes the distribution of small ions in micellar systems. It is also interesting to note that the assumption of point charges in the PB equation does not significantly influence the results.

As mentioned previously the charges of the polyelectrolyte are assumed to be smeared out on its surface and thus the discrete nature of the head groups of the polyelectrolyte is neglected. MC simulations on planar polyelectrolytes show however that this has a very small effect on the ion distribution (21).

3. ION BINDING TO POLYELECTROLYTES

3.1 General remarks

Due to the high charge density of many polyelectrolytes there will be an accumulation of counterions near the polyelectrolyte. The extent of counterion binding to cylindrical polyelectrolytes has been extensively studied, both by theory and experiments (4,5,22-25). One finds theoretically, in the limit of uniform line charge and infinite dilution a phase transition behaviour at a certain critical charge density ξ_{crit}. When the charge density, ξ, is increased above this value the counterions are said to "condense" on the polyion. This behaviour follows from the PB equation (26) but alternative derivations also exist (5). For more realistic boundary conditions such as a finite cylinder radius and a finite polyion concentration a true discontinuity at ξ_{crit} is no longer present, but the solutions to the PB equation still show qualitatively the same behaviour with respect to the ion distribution (22). The two characteristic features of ion condensation are that in the condensation limit for cylinders ($\xi > \xi_{crit}$)

i) The counterion concentration far from the polyelectrolyte remains unchanged when the charge density at the polyion is changed.

ii) The counterion concentration close to polyion is unaffected by changes in the polyion and salt concentration.

It was recently shown that this qualitative behaviour of the ion distribution is not limited to the cylindrical geometries but that it also applies to the planar case (17,18,28).

Spherical polyelectrolytes differ from the cylindrical and planar systems in that they carry a finite charge. As a consequence some of the limiting properties of the other systems no longer apply.

The above studies on the ion binding properties of cylinders, as described by the PB equation, were either for cylinders at infinite dilution in a salt solution (27) or for salt free cylinders in the cell model (22). When the work reported in this thesis was initiated the PB equation and the cell model had not been applied to the study of the ion binding properties of cylinders at finite polyelectrolyte concentration in the presence of salt. The same was also the case for spherical polyelectrolytes, both with and without salt. This is probably because numerical methods are necessary to solve the PB equation for these systems, (as was described in chapter 2). We therefore started an investigation into ion binding properties of cylinders and spheres as described by the PB equation and the cell model and the results of this investigation as well as the comparison with experiments are reported in this chapter. In all cases it is assumed that the polyion is negatively charged and that $t = 25^{o}C$.

3.2 Theoretical considerations

In figure 3.1 we show how the concentration of counterions at the surface of a cell, c_{+o}, varies with total charge density on the polyelectrolyte, σ, for planar, cylindrical and spherical geometries without salt, where the radii of the sphere and the cylinder have been taken to represent micellar systems. One notices that c_{+o} levels off when the charge density is increased, but that there is no discontinuity. This implies that the counterions tend to accumulate near the surface as the surface charge density, σ, is increased (and therefore also the total counterion concentration), which is typical of ion condensation behaviour. This is further illustrated in figure 3.2 where the apparent surface charge density, σ_{app}, at 3 Å outside

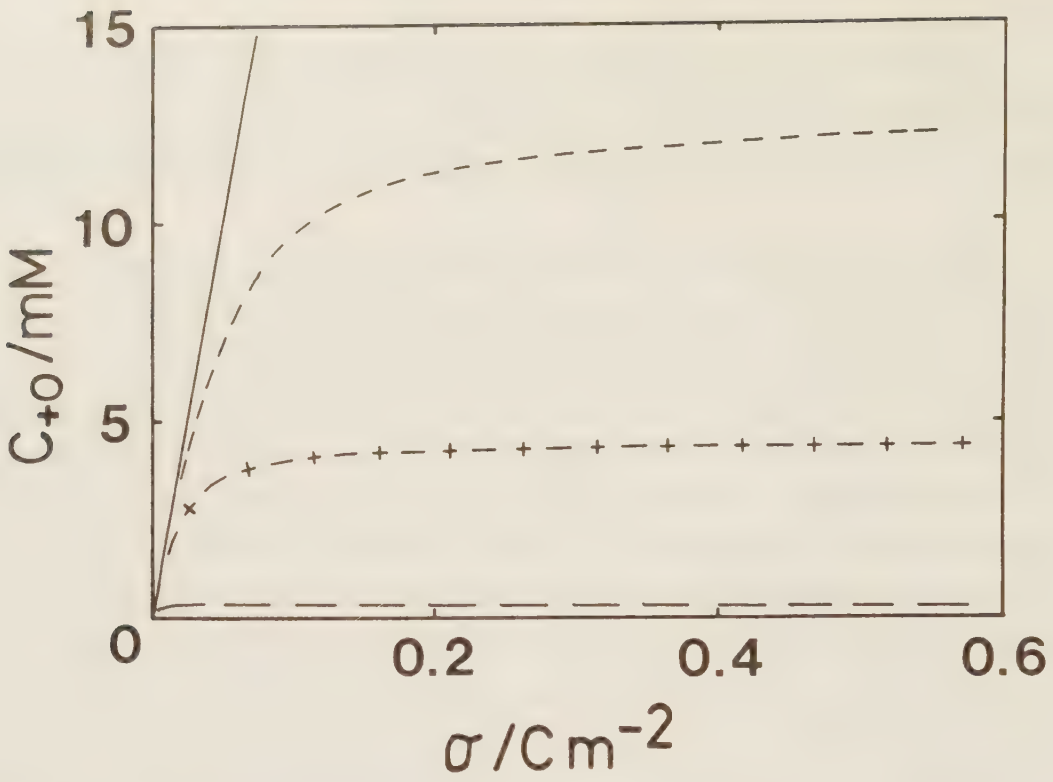

Figure 3.1 The concentration of counterions at the cell boundary, c_{+o}, as a function of the surface charge density, σ, for spheres (- - -), cylinders (- + - +) and planes (— —). The full line shows the hypothetical increase in c_{+o} if there were no interactions between the surface and its counterions. All solutions are free of added salt. The radii of the sphere and cylinder are 18 Å, the radius of the cell is 80 Å and the distance to the cell boundary for the other geometries is adjusted to make the counterion concentration in the water the same for the three cases.

each surface is plotted v.s. σ. For higher values of σ it is seen that σ_{app} increases very slowly with σ. This is because of the accumulation of counterions. From figures 3.1 and 3.2 we see that ion condensation behaviour also applies approximately to spheres. The onset of ion condensation behaviour occurs however at higher charge densities than for cylinders and planes.

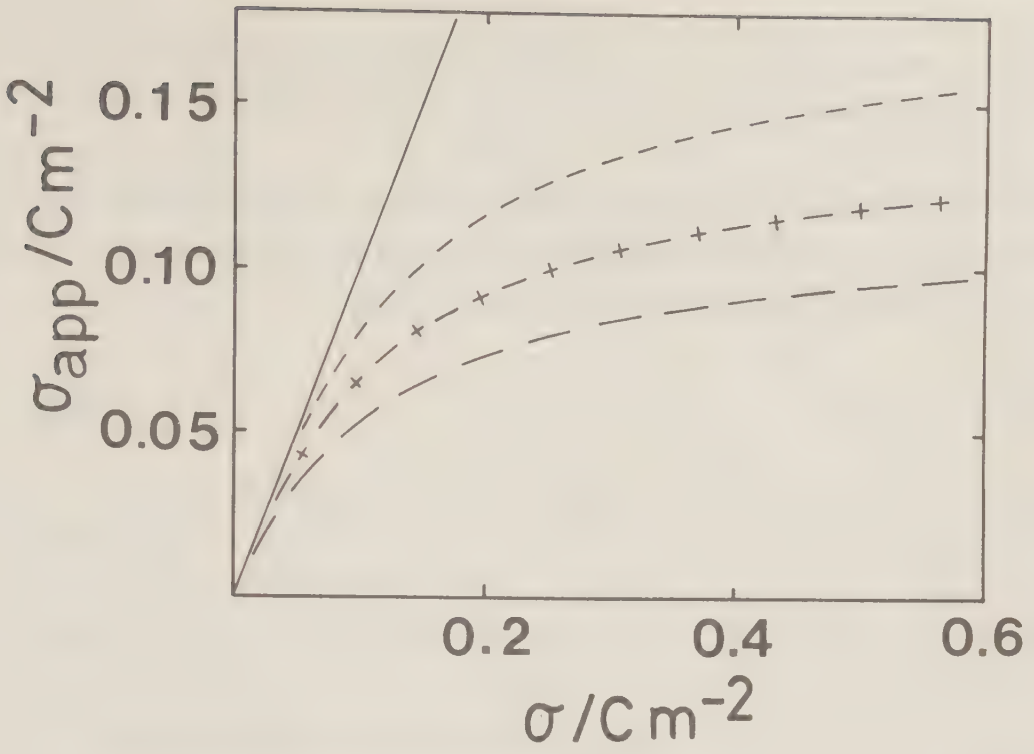

Figure 3.2 The apparent charge density, σ_{app}, at a distance 3 Å from the surface, as a function of the surface charge density, σ, for spheres (- - -), cylinders (- + +) and planes (— —). Parameters are as in figure 3.1.

It is not straightforward to relate the ion distribution around polyelectrolytes to different methods for estimating the degree of ion binding, β, which is defined by

$$\beta = \frac{\text{number of bound counterions}}{\text{number of ionic groups on the polyion}} \qquad (3.1)$$

Here it should be kept in mind that the counterions can come both from the polyion itself as well as added salt. If more than one type of counterions is present it is possible to define β for each type of counterion.

Different experimental methods probe different aspects of the ion distribution. Experimental methods used to measure the degree of ion association can be roughly divided into three classes: those based on

thermodynamic measurements, those based on measurements of transport properties, and those based on spectroscopic measurements.

In a thermodynamic experiment one estimates the activity of the counterions, a_+ which within the approximations of the PB equation and the cell model, is given by

$$a_+ = c_{+o} \tag{3.2}$$

The degree of ion association as measured in a thermodynamic experiment, β_{th}, is therefore (I)

$$\beta_{th} = (\tilde{c}_p + \tilde{c}_{salt} - c_{+o})/\tilde{c}_p \tag{3.3}$$

where $\tilde{c}_p$ and $\tilde{c}_{salt}$ are the concentrations of counterions from the polyelectrolyte and salt, respectively. The value of β_{th} at high polyelectrolyte concentration will depend on the concentration units used.

The osmotic pressure, Π, is given within the cell model by

$$\Pi = kT \sum_i c_{io} \tag{3.4}$$

and the osmotic coefficients, ϕ_p, by

$$\phi_p = \sum_i c_{io} / \sum_i \tilde{c}_i \tag{3.5}$$

In the absence of salt we see that

$$\beta_{th} = 1 - \phi_p \tag{3.6}$$

Thus it is only in salt free solutions that measurements of osmotic coefficients give information on the degree of ion binding.

The presence of a polyelectrolyte will influence the transport properties of small ions, eg. diffusion coefficients. As a first approximation it is often assumed that ions in a region where $|e\phi(r)/kT|>1$ are trapped and moving with the polyion (28). If r_{tr} is defined by $|e\phi(r_{tr})/kT| = 1$ then the degree of ion association as measured through a transport property is given by (I)

$$\beta_{tr} = (s+1) \int_{r_c}^{r_{tr}} c_i(r)\, dr \,/\, (r_c^{s+1}\, \tilde{c}_p) \qquad (3.7)$$

In measurements of spectroscopic properties, such as NMR parameters, often it is only the counterions in the direct vicinity of the polyelectrolyte that have properties different from those in a solution free of the polyelectrolyte. We shall therefore use the following definition for β_{sp}, the degree of ion association as measured in a spectrosopic experiment (I)

$$\beta_{sp} = (s+1) \int_{r_b}^{r_b+\Delta} c_i(r)\, dr \,/\, (r_c^{s+1}\tilde{c}_p) \qquad (3.8)$$

where Δ is of the order of molecular dimensions. Δ in our calculations is often taken as 3 A.

In figure 8 in paper I and figure 3.3 we show how β_{sp} and β_{th} respectively, vary with total concentration of ionic charges in the polyelectrolyte, $\tilde{c}_p$, for planar, cylindrical and spherical polyions without salt and for a spherical polyion at two different salt concentrations. Figure 3.4 shows the corresponding variation in β_{tr} for spherical polyions in salt and salt free solutions. From figures 3.3, 3.4 and 8 in paper I we see that β is independent of the concentration at low polyelectrolyte concentrations both for cylinders and planes in salt free solutions, irrespective of which definition is used. However it seems possible to dilute the counterions away from a sphere in a salt free solution and to reach a uniform distribution for the ions. However the changes in β are not very

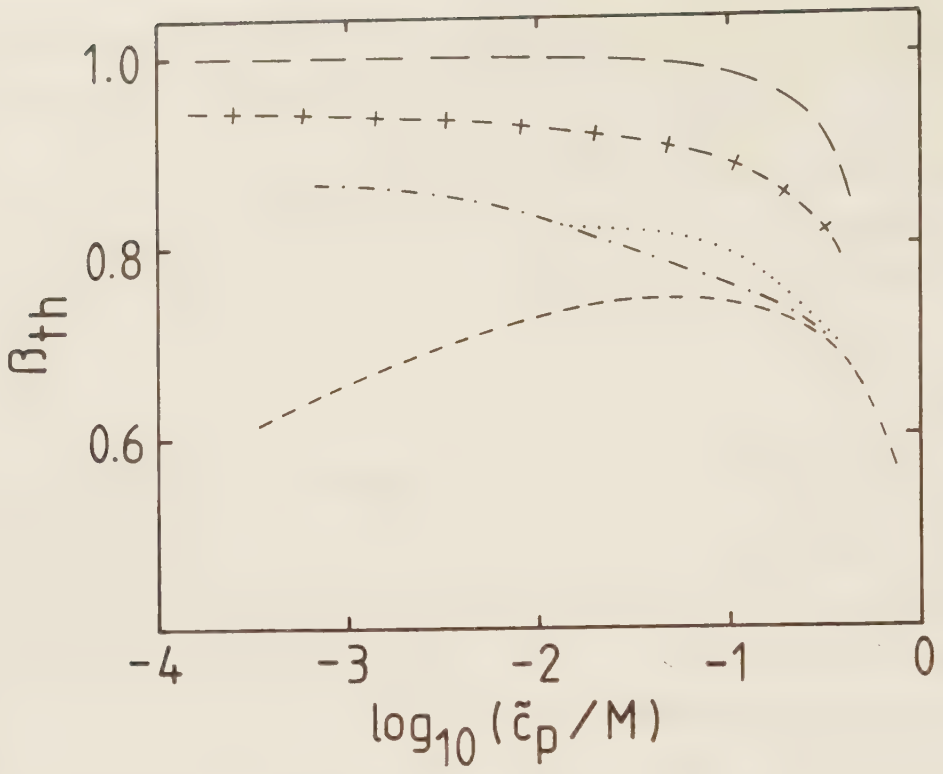

Figure 3.3 The degree of ion association, β_{th}, as a function of the concentration of charged groups in the polyelectrolyte, $\tilde{c}_p$, for spheres in salt free solutions (- - -), spheres in 0.01 M salt solution (•-•-•), spheres in 0.1 M salt solutions (••••••) and planes (— —) and cylinders - + - +) in salt free solutions. The surface charge density is 0.228 Cm^{-2} and the radii of the spheres and cylinders and half the thickness of the plane are 18 Å. The concentration unit used when calculating β_{th} was M.

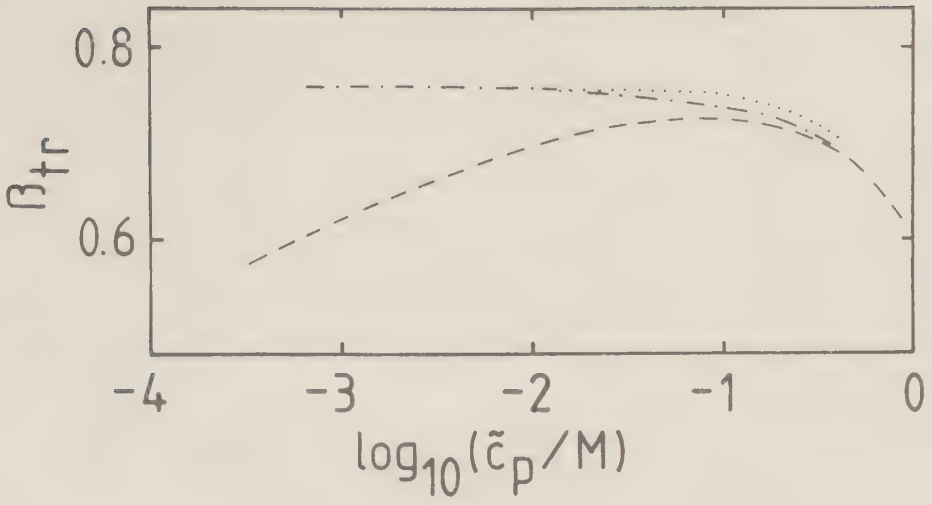

Figure 3.4 The degree of ion association, β_{tr}, as a function of the concentration of charged groups, $\tilde{c}_p$, in a spherical polyelectrolyte in salt free solutions (- -), 0.01 M salt solutions (— • — •) and 0.1 M salt solutions (•••••••). Parameters are as in figure 3.3.

dramatic when the polyion concentration changes by many orders of magnitude. If the salt concentration is kept constant while the concentration of spherical polyelectrolyte is decreased it is on the other hand not possible to dilute the counterions away from the polyelectrolyte. This effect is also demonstrated in figure 3.5 which shows β_{sp} for an infinitely dilute solution of spherical and cylindrical polyelectrolytes at different concentrations of 1:1 salt. It is interesting to see that even at salt concentrations equivalent to that of protons and hydroxyl ions in pure water there is substantial ion binding to the spherical polyelectrolyte in question. Spherical polyions can therefore be assumed to show condensation behaviour, provided that the surface charge density is high enough.

From figures 3.3 - 3.5 we see that the degree of ion association is not very sensitive to the salt concentration whichever definition

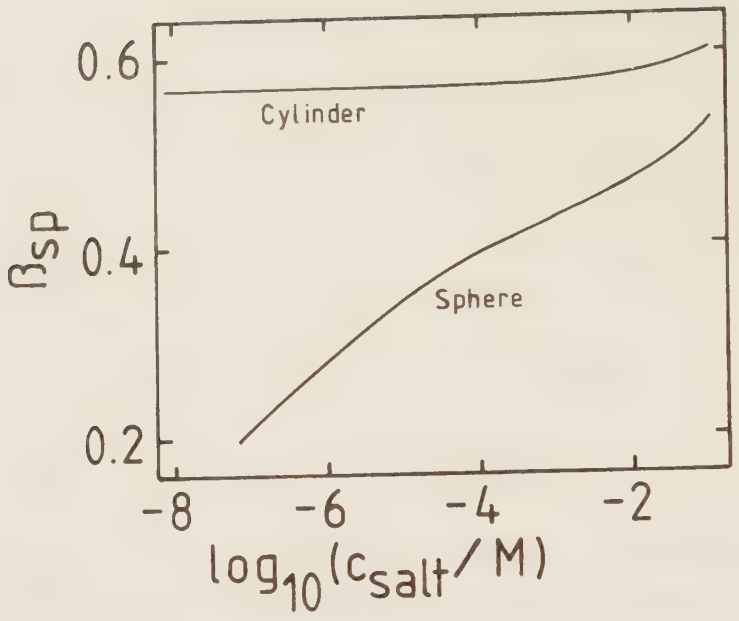

Figure 3.5 The degree of ion association, β_{sp}, (Δ=3 Å), as a function of the total salt concentration for spheres and cylinders under infinite dilution. Parameters are as in figure 3.3.

of β is used. This is also demonstrated in figure 3.6, where the parameters have been chosen so as to represent a cylindrical DNA molecule at a concentration of 15 mM. Figure 3.6 also shows that the behaviour of β_{sp} is not dependent on the choice of Δ.

Figure 8 in paper I and figures 3.3 and 3.4 show that for a given charge density β is smallest for spheres, higher for cylinders and highest for planes. Also one notices that β_{sp} increases with increasing polyelectrolyte and salt concentration, whereas β_{tr} and β_{th} both decrease at high polyelectrolyte and salt concentrations. It follows from geometrical considerations that β_{sp} will increase at high polyelectrolyte concentration since the region within a distance Δ from the surface constitutes larger and larger portions of the solution as the concentration is raised. With increasing polyion concentration

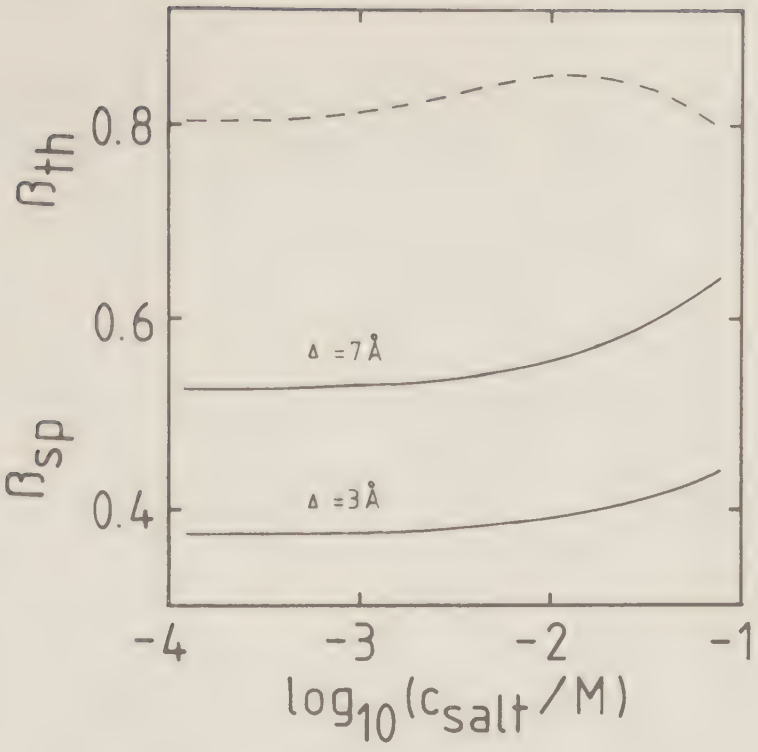

Figure 3.6 The degree of ion association, β_{sp} (------) and β_{th} (- - - -), as a function of the total salt concentration, $\tilde{c}_{salt}$, in a 15 mM DNA solution. The radius of the cylindrical DNA molecules is 10 Å and the distance between charged groups when projected on the cylindrical axis of the molecule is 1.7 Å.

the absolute value of the electrostatic potential at the surface of the polyelectrolyte, $|\phi_A|$, decreases. This can be seen in figure 3.7 which shows $|e\phi_A/kT|$ for different geometries as function of polyion concentration. At sufficiently high polyion concentration $|e\phi_A/kT|$ will decrease below 1. Therefore β_{tr} and β_{th} should also decrease at high polyion concentration. Similarily β_{tr} and β_{th} can decrease at high salt concentration as is shown in figures 3.3, 3.4 and 3.6.

Polyelectrolytes will attract divalent counterions much more effectively than monovalent ones and the extent of this discrimination

between monovalent and divalent ions will depend on polyion concentration due to the fact that $|e\phi_A/kT|$ depends on the polyion concentration, see figure 3.7.

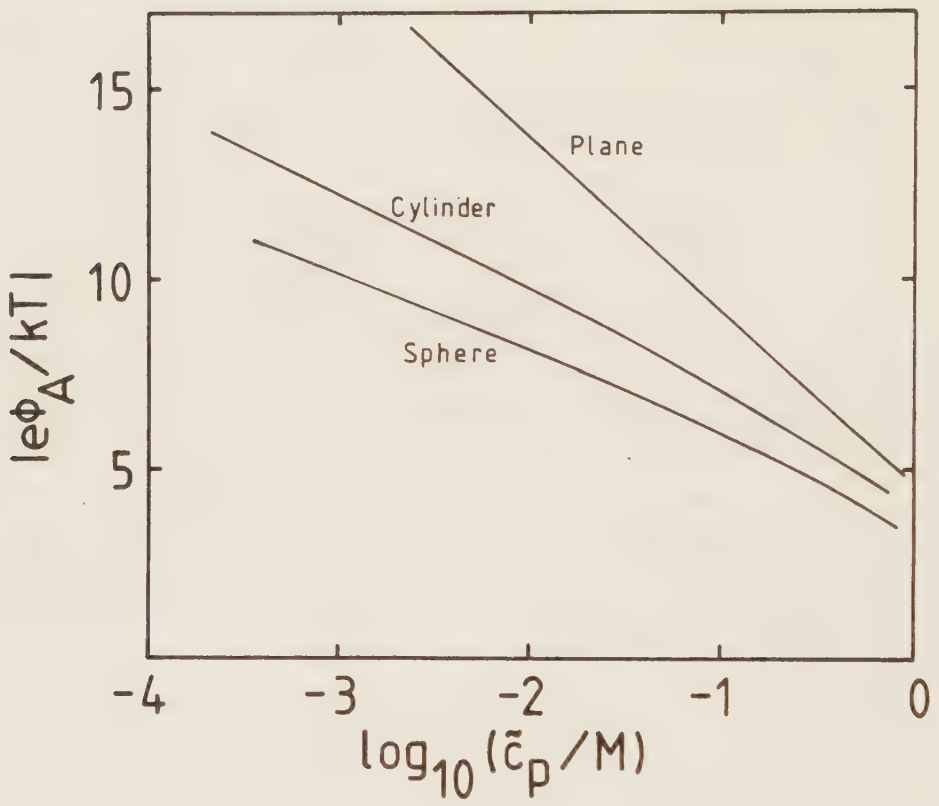

Figure 3.7 The absolute value of the reduced electrostatic potential at the surface of polyelectrolytes, $|e\phi_A/kT|$ for planar, cylindrical and spherical geometries, as a function the concentration of ionic groups in the polyelectrolyte, $\tilde{c}_p$, in salt free solutions. Parameters are as in figure 3.3.

This effect is shown in figure 3.8, where β^+_{sp} for three different DNA concentrations, with $\tilde{c}_+ = \tilde{c}_p$, is plotted as a function of the ratio $2\tilde{c}_{2+}/\tilde{c}_p$. (β^+_{sp} is the degree of ion association for monovalent counterions).

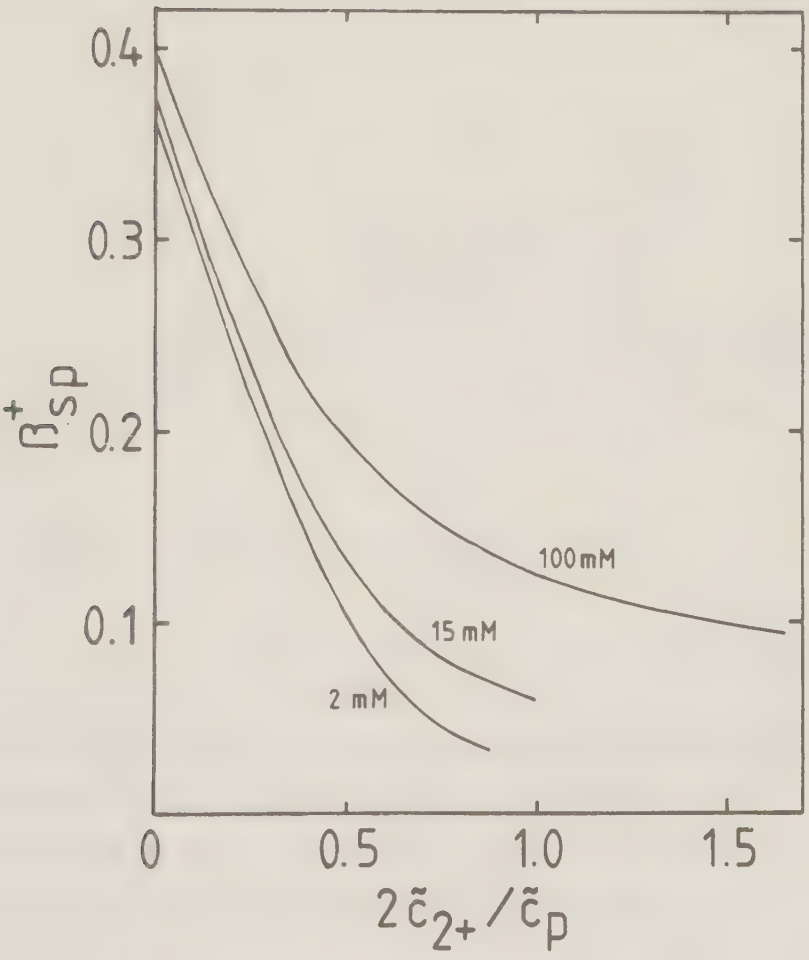

Figure 3.8 The degree of ion association for monovalent counterions β^+_{sp} (Δ = 3Å) as a function of the ratio $2\tilde{c}_{2+}/\tilde{c}_+$ for three different concentrations of originally salt free DNA solutions. The coions are also monovalent. Parameters are as in figure 3.6.

In figure 3.9 the fraction of bound divalent ions, p_b^{2+}, is plotted. p_b^{2+} is defined by

$$p_b = \beta_{sp}^{2+} \tilde{c}_p / \tilde{c}_{2+} \qquad (3.9)$$

where β_{sp}^{2+} is the degree of ion association for divalent counterions. Figures 3.8 and 3.9 show that the polyelectrolyte concentration will have a marked effect on the competition between monovalent and divalent counterions.

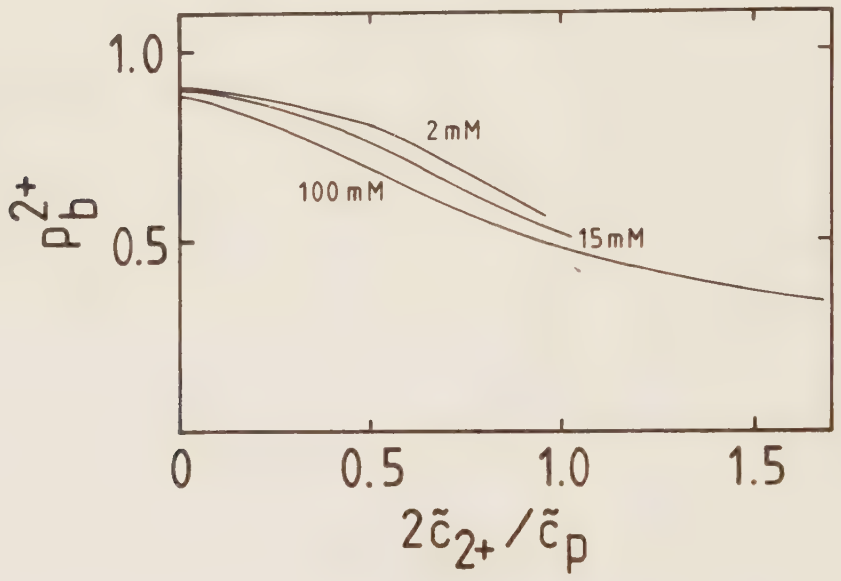

Figure 3.9 The fraction of bound divalent ions, $p_b^{2+}(\Delta = 3\text{Å})$, as a function of the ratio $\tilde{c}_{2+}/\tilde{c}_+$, for three different concentration of an originally salt free DNA solution. The coions are also monovalent. Parameters are as in figure 3.6.

3.3 Comparison between theory and experiments

Ion binding to linear polyelectrolytes in salt free solutions has been studied through measurements of osmotic pressure by many investigators and comparison between theory and experiment has been

made (22, 29). In general the agreement between theory and experiment is satisfactory. It is not necessary to assume any "site binding" of counterions to polyelectrolytes in order to reproduce the main characteristics of the experimental results.

A method used extensively for studies of ion binding in polyelectrolyte systems in NMR (30). In principle one can use any NMR parameter for the counterion, such as relaxation times, quadrupolar splittings and chemical shifts, to probe the binding of counterions, provided that it is different for free and bound counterions. Under fast exchange conditions one will see only one signal which is an average for all counterions. As implied above NMR experiment are often satisfactorily interpreted in a two state model, where there are assumed to be only bound and free counterions. If Q_b is the quantity that would be measured if only bound ions could be observed and Q_f that if only free ions could be observed then the observed signal under fast exchange conditions is given by

$$Q_{obs} = p_b Q_b + p_f Q_f = p_b (Q_b - Q_f) + Q_f \qquad (3.10)$$

where p_b and p_f are the fractions of bound and free counterions respectively. It is possible to get a measure of Q_f from a measurement on a polyelectrolyte free solution. Therefore it is convenient to define the excess quantity, Q_{ex}, by

$$Q_{ex} = Q_{obs} - Q_f = p_b (Q_b - Q_f) \qquad (3.11)$$

where Q_{ex} is thus proportional to p_b and if $Q_b - Q_f$ is independent of parameters such as total polyelectrolyte and salt concentration Q_{ex} can be used to probe changes in p_b. However it is not enough for a determination of p_b, which is given by

$$p_b = \beta'_{sp} \tilde{c}_p / (\tilde{c}_p + \tilde{c}_{salt}) \qquad (3.12)$$

The above approach has been used to interpret NMR measurement of quadrupolar splittings in lamellar liquid crystals of ionic surfactants (32). It is generally found that the theory explains all the main features of the ion binding behaviour in these systems, which can be characterised as infinite planar polyelectrolytes.

In paper II we compare results from ^{23}Na NMR measurements with theoretical ion binding results as obtained from PB theory. The first parameter considered is the change in counterion binding upon titration of poly(acrylic acid) (PA). In calculating the variation in β under a titration experiment it is unrealistic to keep Δ constant since this would mean that the volume, which is integrated over in equation (3.8), varies linearly with the distance between the charged groups. Δ therefore is allowed to vary such that the integrated volume remains constant. When this is done the agreement between theory and experiment is satisfactory. The theory also explains the change in excess relaxation rates when a polyelectrolyte solution is diluted with water as well as the effect of salt containing monovalent or divalent counterions. In all cases it is found that PB theory satisfactory explains the experimental results.

Comparing ion binding results in micellar systems with theory is slightly more complicated than in simple polyelectrolytes. This is bacause of the fact that the size of the aggregates as well as the monomer concentration changes with total surfactant and salt concentration. The comparison between theory and experiments for micellar systems is therefore postponed until the theory for equilibrium in micellar systems has been presented in chapter 5.

4. THERMODYNAMIC FUNCTIONS IN POLYELECTROLYTE SYSTEMS

4.1 Fundamental equations

The presence of a polyelectrolyte will result in ion distributions for the small ion that differ greatly from those that would prevail in a system containing the same number of uncharged species. In one sense the polyelectrolyte orders the small ions in the solution since it attracts counterions and repels coions. The polyions themselves can also form lattice-like structures in the solution (31). The entropy of a polyelectrolyte system is therefore expected to be smaller than in a system where all the particles are neutral.

The ideal entropy of mixing, ΔS_{id}, is

$$\Delta S_{id} = -k \sum_i n_i \ln(X_i) \qquad (4.1)$$

where n_i and X_i are the number and mole fraction of particle i, respectively. Equation 4.1 is strictly valid only if there is no interaction between the molecules, as, for example, in an ideal mixture of ideal gases. This is of course not true for ionic solutions, where one has not only ion-ion correlations but also ion-water correlations (interactions). As pointed out in chapter 2 the PB equation neglects ion-ion correlations and it is therefore consistent with the PB equation to use 4.1 to calculate entropies. The water in the model used here is represented by a dielectric continuum and water-ion interactions are therefore taken into account implicitly.

In a polyelectrolyte solution X_i is dependent on distance from the polyelectrolyte and in order to obtain the entropy it is necessary to express the entropy in differential form and integrate over the water phase. The result is (13)

$$S = -k \sum_{i \neq w} \int c_i(r)\{\ln(c_i(r)V_{H_2O})-1\}dV \qquad (4.2)$$

where the summation does not include water. Here it has been used that there is a large water excess. V_{H_2O} is the molecular volume of water. Concentration are expressed in number of ions per unit volume. $c_i(r)$ varies with distance from the polyelectrolyte.

The entropy of a solution, if all the ions are equally distributed over the aqueous volume, S_o, is (13)

$$S_o = -k \sum_{i \neq w} n_i \{\ln(\tilde{c}_i \, V_{H_2O}) - 1\} \tag{4.3}$$

where $\tilde{c}_i$ and n_i are the average concentration and number of ion i in the water phase, respectively. The excess electrostatic entropy of the ion distribution, S_{ions}, is then given by

$$S_{ions} = S - S_o = -k \sum_{i \neq w} \left| \int c_i(r) \{\ln(c_i(r) - 1\} dV - n_i \ln(\tilde{c}_i) \right| \tag{4.4}$$

The electric field from the polyelectrolyte will also contribute to the excess electrostatic free energy, G_{el}. The energy of the electric field, E_{el}, is given by (13)

$$E_{el} = \varepsilon_o \varepsilon_r / 2 \int (\nabla \phi)^2 \, dV \tag{4.5}$$

The free energy of a polyelectrolyte solution is the sum of equation (4.2) and (4.5). It can be shown that the free energy expressed in this way has a minimum when the ions are distributed according to a Boltzmann distribution law (equation (2.1)) (19). This method of deriving the PB equation therefore shows that the ion-ion correlation are neglected in the PB equation, since they are neglected in equation (4.2).

The excess electrostatic free energy, G_{el}, is obtained from

$$G_{el} = E_{el} - TS_{ions} \tag{4.6}$$

This excess electrostatic free energy can also be calculated in at least two other independent ways (13). They have been shown to be equivalent to equation (4.6), within the approximations of the PB equation (13).

The excess electrostatic free energy per monovalent charged group in the polyelectrolyte, G_{el}/n, can, within the cell model, be expressed as (I)

$$G_{el}/nkT = e\phi_A/kT - E_{el}/nkT + n_+/n \ln(c_{+o}/\tilde{c}_+) + n_-/n \ln(c_{-o}/\tilde{c}_-) \qquad (4.7)$$

when only 1:1 salt is present. In the limit of an infinite cell volume, i.e. when $c_{+o}=c_{-o}=c_o$, this equation can be written as (see appendix I)

$$G_{el}/nkT = e\phi_A/kT - E_{el}/nkT - c_o/n \int (2\cosh(e\phi/kT)-2)dV \qquad (4.8)$$

which is an equation that has often been used in the literature (32-35).

Due to the temperature dependence of ε_r, see figure 4.1, E_{el} is

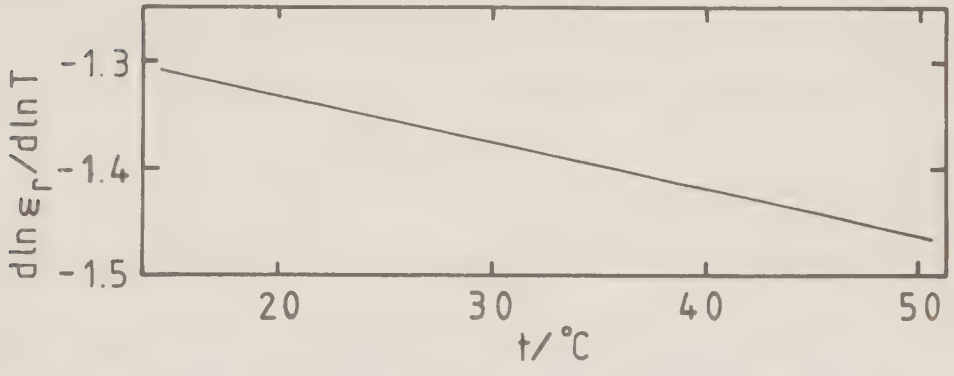

Figure 4.1 The temperature dependence of the dielectric constant of water, ε_r, plotted as d ln ε_r/d ln T vs. t (from ref. 36).

not purely an enthalpy. The enthalpy obtained by applying the Gibbs-Helmholtz equation to equation (4.7) is (III)

$$H_{el} = \left(1 + \frac{d \ln \varepsilon_r}{d \ln T}\right) E_{el} \qquad (4.9)$$

and the excess electrostatic entropy, S_{el}, is accordingly

$$S_{el} = S_{ions} + \frac{1}{\varepsilon_r} \frac{d\varepsilon_r}{dT} E_{el} \tag{4.10}$$

The excess electrostatic free energy can therefore be written as

$$G_{el} = H_{el} - TS_{el} \tag{4.11}$$

In chapter 2 we saw that inspite of the fact that ion-ion correlations are neglected in the PB equation it still describes the ion distribution around the polyelectrolyte very well. This does not necessarily imply, however, that the free energy is correctly described by the PB equation. To test the PB free energies one has to compare them with values obtained from more exact treatments such as MC simulations. Such a comparison between the free energies as obtained from the PB equation and MC simulations was recently performed by Linse et al. (20). One of their figures is reproduced in figure 4.2. The free energy shown in the figure is the free energy per charged group in a sphere, as obtained from equation 4.7 minus the self energy per charged group in the sphere, E_m, which is given by

$$E_m = \frac{1}{8\pi\varepsilon_o\varepsilon_r} \frac{ne^2}{r_b} \tag{4.12}$$

For the case examined in figure 4.2 is E_m = 10.92 kT per charged group. The conclusion that can be drawn from this figure is that there is a small difference between the results of the PB equation and the results of MC calculations. At low salt concentration this difference is almost independent of salt and polyelectrolyte concentration, because the energy from ion-ion correlations is included in the MC energy but not in the PB energy (20). This effect becomes larger for polyelectrolytes with lower charge at high salt concentrations, where the ion-ion correlations are more important in determining the free energy (20).

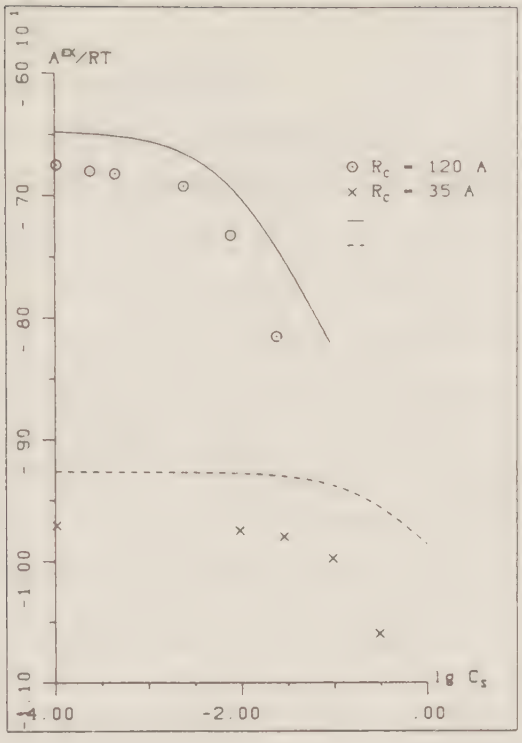

Figure 4.2 The excess electrostatic free energy per charged group in a spherical polyelectrolyte, obtained as described in the text, as a function of the total salt concentration for two different cell radii, r_c. The points are from MC simulations and the curves are from the PB equation. Parameters are as in figure 2.2.

As mentioned in chapter 2 the concentration of counterions near the polyelectrolyte is underestimated with the PB equation, as compared to the results of MC simulations. This means that the polyelectrolyte is less shielded in the PB approach than in the MC approach. The electrostatic energy as obtained from the PB equation should therefore be larger than the electrostatic energy obtained in MC simulations, which is indeed found to be the case (20). For the same reason S_{el} will be more negative when calculated by a MC simulation than when calculated from the PB equation. There is therefore a kind of entropy enthalpy compensation, which partially explains the success of the PB equation in calculating free energies.

4.3 Some numerical examples

For polyelectrolytes at infinite dilution is it found that the excess electrostatic free energy per charged group in a polyelectrolyte depends linearly on the logarithm of the salt concentration, $\tilde{c}_{salt}$, i.e. (I)

$$G_{el}/nkT = a + b \log(\tilde{c}_{salt}) \qquad (4.13)$$

where a and b are constants. This is a good approximation for planes and cylinders when the salt concentration changes by many orders of magnitude. However the range of validity of equation (4.13) is much less for spheres. This can be seen in figure 4.3 where G_{el}/nkT is

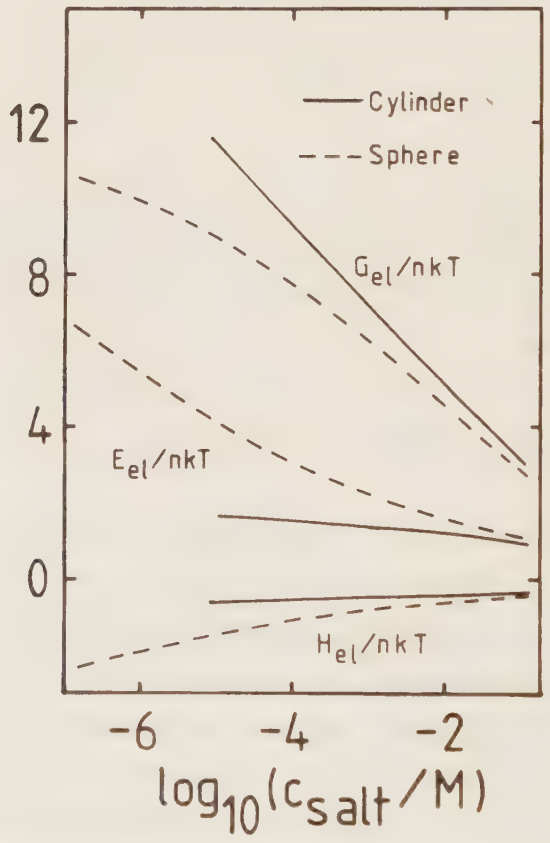

Figure 4.3 The excess electrostatic free energy (G_{el}), enthalpy (H_{el}) and energy (E_{el}) per charged group in spheres and cylinders at infinite dilution as a function of the salt concentration. Parameters are as in figure 3.3.

plotted vs. $\log(\tilde{c}_{salt})$ for spheres and cylinders, and where the parameters have been taken to represent micellar systems.

Figure 4.3 also shows the contributions of H_{el} and E_{el} to G_{el}. A striking difference between the spherical and cylindrical geometries is that E_{el} constitutes an ever larger part of G_{el} as the salt concentration decreases for spheres, while the converse is true for cylinders. It can be seen, for spheres, from the difference between the curves for G_{el} and E_{el}, that $-TS_{ions}$ increases first as the salt concentration decreases whereafter it decreases. For the cylinder however $-TS_{ions}$ increases with decreasing salt concentration. This behaviour is related to the different ion binding properties of spheres and cylinders at low salt concentrations. For spheres it is possible to dilute the counterions away, see chapter 2. E_{el}/nkT for spheres will therefore approach, as the salt concentration increases, the value for a charged sphere without counterions. For the sphere considered in figure 4.3 this value is 11.53 kT. For a sphere $-TS_{ions}$ will approach zero, since the small ions tend to a uniform distribution. For the cylinder however it is not possible to dilute the counterions away and thus $-TS_{ions}$ will increase with decreasing salt concentration. For the same reason a cylinder will be effectively shielded by its counterions. The energy of the electrostatic field will therefore make a small contribution to the free energy of the cylinder.

The value of $(1 + d \ln\varepsilon_r/d \ln T)$ is -0.36 at 25°C, see figure 4.1. Since E_{el} is small and positive the electrostatic enthalpy will be small and negative, except for spheres at low salt concentrations. Figure 4.4 shows the temperature dependence of G_{el}/n, E_{el}/n and of H_{el}/n for a sphere in a salt solution. It is seen that the temperature dependence of G_{el} is not large and that H_{el} only makes a small contribution to G_{el} at the temperatures considered.

In figure 4.5 we show how G_{el}/nkT, E_{el}/nkT and H_{el}/nkT change with total surface charge density for a sphere under infinite dilution in a salt solution. This figure shows the behaviour which

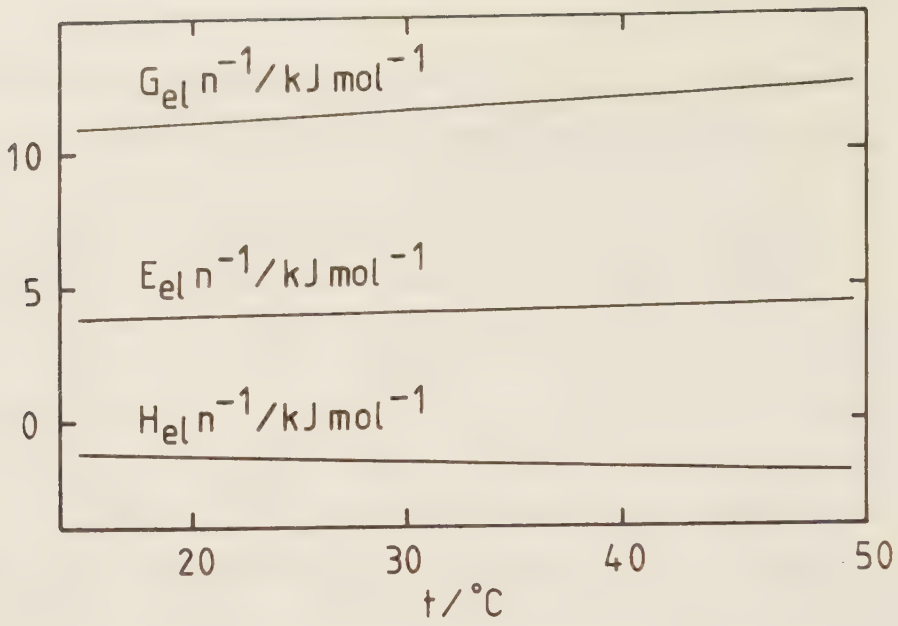

Figure 4.4 The temperature dependence of the excess electrostatic free energy (G_{el}), enthalpy (H_{el}) and energy (E_{el}) per charged group in a spherical polyelectrolyte at infinite dilution in a 10^{-2}M salt solution. Parameters are as in figure 3.3.

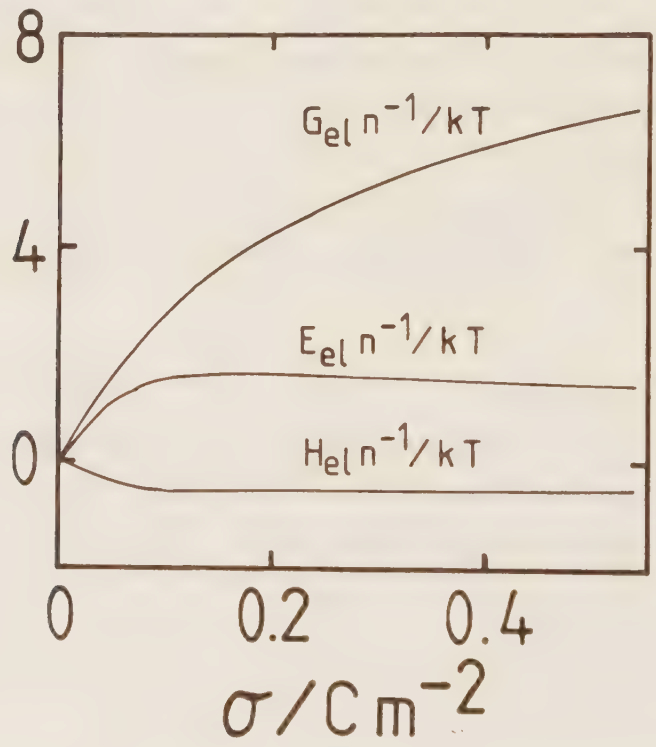

Figure 4.5 The excess electrostatic free energy (G_{el}), enthalpy (H_{el}) and energy (E_{el}) per charged group in a spherical polyelectrolyte of radius 18 Å at infinite dilution in a 10^{-2}M salt solution, as a function the total surface charge density, σ.

can be expected from the ion binding properties of a sphere. $-TS_{ions}$ increases with total surface charge density while E_{el} levels off due to the accumulation of counterions.

Figure 4.3 shows that the excess electrostatic free energy of a cylinder is larger than that of a sphere with the same radius and same surface charge density. This difference is dependent on the radii of the sphere and cylinder and it will approach zero as the radii go to infinity. This is demonstrated in figure 4.6 which shows that a substantial error is introduced if the analytical solution of the PB equation for a plane (infinite radius) is used to calculate the free energies of spheres and cylinders at such low salt concentration. The difference between the three geometries will of course decrease with increasing salt concentration (I).

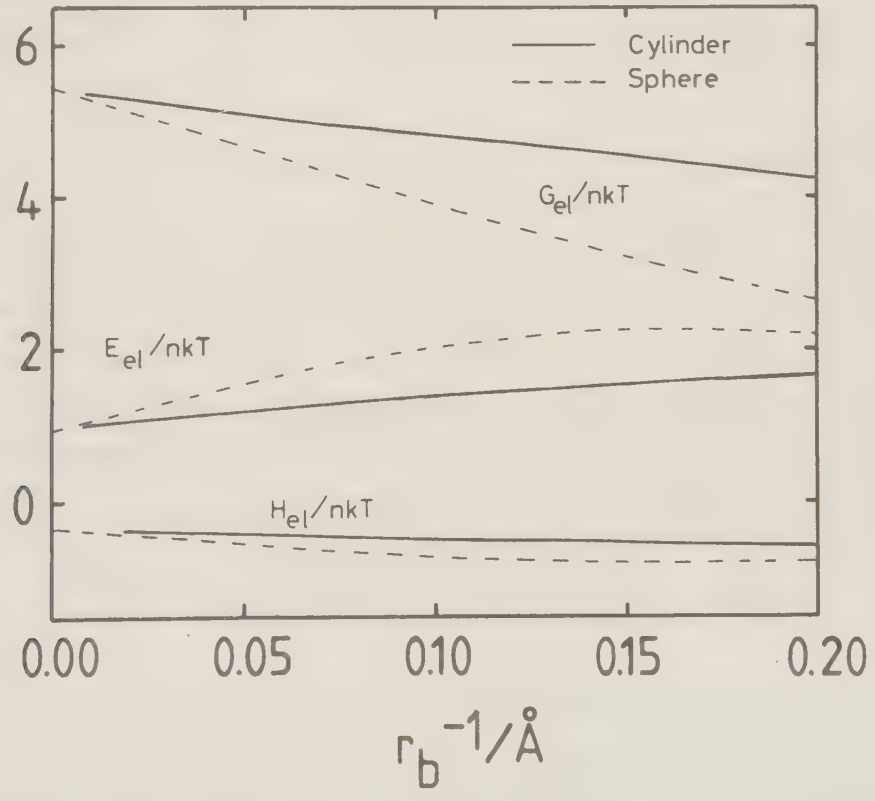

Figure 4.6 The excess electrostatic free energy (G_{el}), enthalpy (H_{el}) and energy (E_{el}) per charged group in spherical and cylindrical polyelectrolytes in a 10^{-2}M salt solution as a function of the inverse or the radius. σ=0.228 cm^{-2}.

4.3 Enthalpies of proton dissociation of polyacrylic acid

Under the titration of a polyacid, for example poly(acrylic acid) (PA), with base the average distance between charged groups increases. This results in an increased degree of counterion binding, as was seen in chapter 3. The charge density will also influence the thermodynamic properties of the poly(acrylic acid)-polyacrylate systems. In particular it will influence the thermodynamics of proton dissociation of PA, since the shorter the distance between the negatively charged groups, the harder it is to create a new negative group by deprotonating an acid group. As the degree of neutralisation, α, increases the acid will therefore become weaker. This is manisfested as an increase in apparent pK_a values with α (37).

The proton dissociation process can be written in simplified form as

$$\frac{1}{n}\{(1-\alpha_2)PAH + \alpha_2 PA^-\}_n + (1-\alpha_2)Cl^- \rightarrow$$

$$\frac{1}{n}\{(1-\alpha_1)PAH + \alpha_1 PA^-\}_n + (1-\alpha_1)Cl^- + (\alpha_2-\alpha_1)HCl(aq) \qquad (4.14)$$

where n is the number of monomer units in the polyelectrolyte. The free energy change in the process can be dividied into two part, one arising from the free energy change in deprotonating an acid group, $\Delta G_a(mon)$, and the other arising from the interaction with other ionic groups on the polyelectrolyte. The free energy change per mol monomer in the macromolecule can be written as

$$\Delta G_a = \Delta G_a(mon) + (G^m_{el}(\alpha_2) - G^m_{el}(\alpha_1))/(\alpha_2 - \alpha_1)$$

$$\cong \Delta G_a(mon) + dG^m_{el}(\alpha)/d\alpha \qquad (4.15)$$

where $G^m_{el}(\alpha)$ is the electrostatic free energy per mol monomer unit, at degree of neutralisation α. Similar expressions can be written for the enthalpy and entropy change (III).

From the discussion in the previous section we know that the relative contributions of H_{el} and $-TS_{ions}$ to the excess free energy

change with charge density. Figure 4.7 shows how $H^m_{el}(\alpha)$, the electrostatic enthalpy per mol monomer at degree of neutralisation α, changes with α. Here the parameters have been chosen so as to

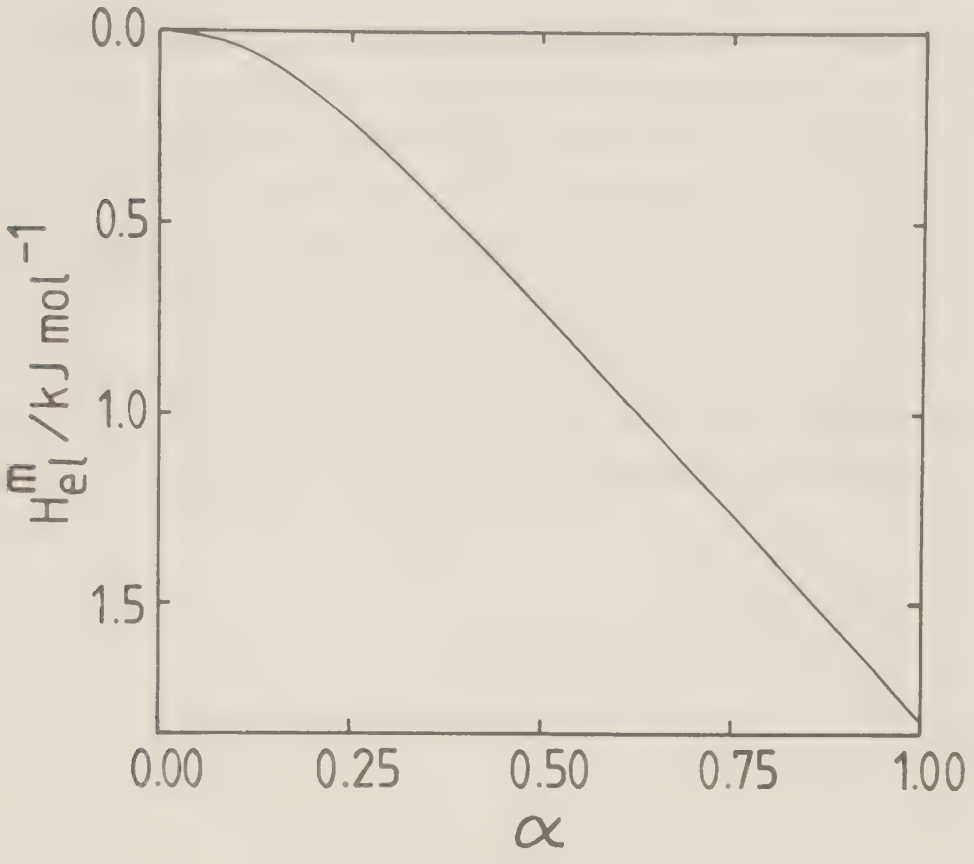

Figure 4.7 The excess electrostatic enthalpy per mol monomer in poly(acrylic acid), $H^m_{el}(\alpha)$, as a function of the degree of neutralisation, α. The radius of the cylinder is 2 Å and the distance between charges, when projected on the central axis of the cylinder, is 2.5 Å.

mimic an experimental condition described in paper III. The electrostatic contribution to the enthalpy of dissociation is obtained from the slope of this curve, $d\,H^m_{el}/d\alpha$. Comparison between experiment and theory shows that the general trend in $d\,H^m_{el}/d\alpha$ with α is reproduced. The theoretical values of $d\,H^m_{el}/d\alpha$ are, however, a factor of 2 too low. In addition the temperature dependence of $d\,H^m_{el}/d\alpha$ is wrong.

The fact that there is a discrepancey between theory and experiments is not strange if it is kept in mind that nearly half of the electrostatic enthalpy has its origin within a distance of 3-4 Å from the surface of the polyelectrolyte (III) and that the model poorly describes the situation near the surface. For example the discrete nature of the charges on the polyelectrolyte is neglected.

Scerjanc has compared experimental and theoretical values for the heat of dilution of PA (38). In order to get agreement between theory and experiment he found it necessary to assume that the distance between the charges is only half of that which can be deduced from the structure of the polyelectrolyte. Thus there are obvious problems in interpreting the results of calorimetric experiments in terms of PB theory. The free energy is however in much better agreement with experiments (37,39).

5. APPLICATIONS TO MICELLES

Ionic surfactants in water solution associate to form various kinds of aggregates, provided that the total concentration is higher than the cmc (6,7,14). The aggregates formed near the cmc, called micelles, are roughly spherical in shape. Spherical micelles can be described as a hydrocarbon core with the ionic groups of the micellised surfactant at the surface, where they are in contact with the water. The radius of the hydrocarbon core of a spherical micelle is approximately equal to the length of an extended hydrocarbon chain, see figure 1.1. The ionic groups do not cover the whole surface of the micelle, thus there still is some contact between the water and the hydrocarbon chains of the micellised surfactants. The contact between the water and the hydrocarbon is unfavourable. This contact in a micelle is, however, much less than if the surfactants were dissolved as monomers in solution. A driving force for micellisation is thus the reduction in total hydrocarbon water contact (14,15). This is a clear manifestation of the hydrophobic effect. If the aggregates formed were infinite planar bilayers, whose thickness was that of two extended hydrocarbon chains, the reduction in hydrocarbon water contact would be maximal. There are however two forces that oppose the formation of infinite bilayers. One is an entropy effect which tends to keep the aggregates small and the other the electrostatic repulsion of the head groups, which tends to maximise the distance between the head groups. Planar bilayers can first form at high surfactant concentration (19).

A theory of micellar solutions must in an expression for the free energy contain contributions from the three above mentioned factors. In papers I and IV we develop such a theory which is based

on the cell model of polyelectrolytes. Paper I contains a description of the theory and application when micellar size distribution is assumed to be monodisperse. In paper IV is the micellar size distribution allowed to be polydisperse.

The electrostatic free energies are calculated from the PB equation and the cell model. The size of the cell depends on concentration of all species as well as the size of the aggregate which it contains. The electrostatic effects vary both with the size of the aggregates and the total concentration of micellised surfactant. The entropy of mixing of the cells and the entropy of mixing within the cells is assumed to be ideal. The energy associated with the hydrophobic effect is modeled in a very simplified way, by assuming that the free energy due to the contact between the water and the hydrocarbon in the micelle, G_s^n, is proportional to the surface area of the hydrocarbon core of the micelle, i.e.

$$G_s^n = \gamma A_n \qquad (5.1)$$

where A_n is the contact area and γ a proportionality constant, which is set equal to $18 \cdot 10^{-3}$ N/m (18,19).

The total free energy of a micellar solution, G, is then obtained by summing over all cells according to

$$G = \sum_n N_n G_n + \sum_n N_n \ln Y_n \qquad (5.2)$$

where G_n is the free energy per cell and N_n the number of cell with aggregates of aggregation number n. Y_n is given by

$$Y_n = N_n / \sum_n N_n \qquad (5.3)$$

If polydispersity is taken into account then we want to calculate all Y_n. For a monodisperse distribution we put $Y_n = 1$ for the allowed aggregation number, n_s and $Y_n = 0$ for all other aggregation numbers.

From the equation for the total free energy it is possible to derive equations for the chemical potentials of each species (I, IV). The expressions for the chemical potentials of the surfactant in the water region, μ_{am}^{w} and in the micelle, μ_{am}^{a}, are (IV)

$$\mu_{am}^{a} = \mu_{am}^{o,a} + G_s^n/n + \mu_{el}^{n} + kT/n \ln X_m^n + kT/n \ln Y_n \qquad (5.4)$$

$$\mu_{am}^{w} = \mu_{am}^{o,w} + kT \ln (c_{amo}^{n} V_{H_2O}) \qquad (5.5)$$

where $\mu_{am}^{o,a}$ and $\mu_{am}^{o,w}$ are standard chemical potentials for the surfactant in the aggregate and water, respectively. X_m^n is the mole fraction of micelle in a cell. c_{amo} is the concentration of the surfactant at the cell boundary and V_{H_2O} the molecular volume of water. μ_{el}^{n} is the electrostatic contribution to the chemical potential of the surfactant, in a micelle of aggregation number n, given by

$$\mu_{el}^{n} = z_{am}\, e\, \phi_A^n - E_{el}^{n} - kT/n(n_+^n + n^n) + kT\, V_1/n\, (c_{+o} + c_{-o}) \qquad (5.6)$$

The chemical potential of the surfactant is the same in the water phase as in the micelle, leading to

$$\mu_{am}^{a} = \mu_{am}^{w} \qquad (5.7)$$

and for the micellar size distribution

$$- kT/n \ln Y_n = -(\mu_{am}^{o,a} - \mu_{am}^{o,w}) - G_s^n/n - \mu_{el}^{n}$$
$$- kT/n \ln X_m^n + kT \ln(c_{amo}^{n} V_{H_2O}) \qquad (5.8)$$

For a monodisperse system near the cmc, which can be approximated by an infinite dilution system (I), one finds that

$$\mu_{el}^{n} = G_{el}^{n}/n \qquad (5.9)$$

see appendix II. This is equivalent to the expression used by Overbeek and Stigter (34) and by Stigter (40).

Much progress can be made by assuming that there is a monodisperse distribution (I). In this case the value of $\mu_{am}^{o,a} - \mu_{am}^{o,w}$ is adjusted to get the right value of the cmc. When this is done for a homologous series of amphiphiles it is found that $\mu_{am}^{o,a} - \mu_{am}^{o,w}$ varies linearly with the number of CH_2 groups, n_c, in the surfactant and that the slope of $\mu_{am}^{o,a} - \mu_{am}^{o,w}$ vs. n_c is comparable with that found in measurements of the free energy of transfer of a homologous series of alkanes from water to a hydrocarbon phase (14). Having fixed the value of $\mu_{am}^{o,a} - \mu_{am}^{o,w}$ for a given surfactant it is possible to calculate a number of properties of surfactant solutions. It is possible to predict the decrease in monomer concentration above the cmc and to calculate how the activities of different ions vary with total surfactant concentration. The cmc values at different salt concentration can also be calculated as well as the change in cmc when the counterion is changed from monovalent to divalent. It is also possible to calculate different degrees of ion association in micellar systems. The theory has been applied to n-alkane sulfate systems and generally it is found that it correctly reproduces the experimental quantities (I).

By restricting the model to a monodisperse distribution of a given aggregation number it is not possible to treat properties of the micelles themselves. Thus the increase in aggregation number and polydispersity with total surfactant and salt concentration is not taken into account. The growth of micelles is restricted by the fact that the head groups have to stay at the surface of the aggregate. After the micelles have reached their maximum spherical size can they either grow as disks or cylinders. Experiments show that they grow to form cylindrical aggregates at high surfactant and salt concentration (41). We therefore make the following assumptions about micell geometries (IV). The micelles are spheres for aggregation numbers lower than that of the maximum spherical micelle. In this

case the hydrocarbon chains are assumed to pack into perfect spheres. For aggregation numbers larger than that of the maximum spherical micelle the micelles are hemisphere capped cylinders with the radius of the hydrocarbon core equal to the length of an extended hydrocarbon chain. A problem with this model is that a solution of the PB equation for the hemisphere capped cylinders is not feasible. We have therefore developed an interpolation scheme which uses the solutions to the PB equation for the spheres and an infinite cylinder.

If equation 5.7 is used it is not possible to obtain maxima in the size distribution. We therefore modified equation 5.7 slightly and introduced a correction factor which made the small micelles more unfavourable. The fact that some kind of a correction factor is needed is not surprising since the macroscopic model used here must be very crude for the small aggregates. Having fixed the form of this correction factor it is however possible to reproduce, at least qualitatively, all the main characteristics of the micellar size distribution for dodecyl sulfate (IV).

REFERENCES

1. "Biological Polyelectrolytes", ed. A.Veis, Dekker, New York, 1970.

2. R.Steiner and D.B.S.Miller, in chapter 2, ref 1.

3. F.A.Bettelheim, in chapter 3, ref 1.

4. F.Oosawa, "Polyelectrolytes", Dekker New York, 1971.

5. G.S.Manning, Accs.Chem.Res., 12, 443 (1979).

6. H.Wennerström and B.Lindman, Phys.Rep., 52, 1 (1979).

7. B.Lindman abd H.Wennerström, Topp.Curr.Chem., 87, 1 (1980).

8. G.Guoy, J.Phys., 9, 457 (1910).

9. D.L.Chapman, Phil.Mag., 25, 475 (1913).

10. B.Jönnson, H.Wennerström and B.Halle, J.Phys.Chem., 84, 2179 (1980).

11. R.Fuoss, A.Katchalsky and S.Lifson, Proc.Natl.Acad.Sci. USA, 37, 579 (1951).

12. T.Alfrey, P.W.Berg and H.Morawetz, J.Polymer Sci., 7, 543 (1951).

13. R.A.Marcus, J.Chem.Phys., 23, 1057 (1955).

14. C.Tanford, "The Hydrophobic Effect", 2nd. ed., Wiley, New York, 1980.

15. A.Ben-Naim, "Hydrophobic Interactions", Plenum, New York, 1980.

16. H.Maeda and F.Oosawa, Biophys.Chem., 12, 215 (1980).

17. S.Engström and H.Wennerström, J,Phys.Chem., 82, 2711 (1978).

18. B.Jönnson and H.Wennerström, Chem.Scr., 15, 40 (1980).

19. B.Jönnson, "The Thermodynamics of Ionic Amphiphile-Water Systems. A Theoretical Analysis", thesis, University of Lund, 1981.

20. P.Linse,G.Gunnarsson and B.Jönsson. Submitted for publication.

21. W.van Megen and I.Snook, J.Chem.Phys., 73, 4656 (1980).

22. A.Katchalsky, Pure Appl.Chem., 26, 327 (1971).

23. L.Kotin and M.Nagasawa, J.Chem.Phys., 36, 873 (1962).

24. U.P.Strauss, in "Polyelectrolytes", ed. E.Sélégny, Reidel, Dordrecht, 1974, p 79.

25. H.P.Gregor, in "Polyelectrolytes", ed. E.Sélégny, Reidel, Dordrecht, 1974, p 87.

26. A.D.MacGillivary, J.Chem.Phys., 56, 80, 83 (1972).

27. H.Wennerström, B.Lindman, G.Lindblom and G.J.T.Tiddy, J.C.S. Faraday Trans. I, 75, 663 (1979).

28. A.Katchalsky, Z.Alexandrowicz and O.Kedem, In "Chemical Physics of Ionic Solutions", eds. B.E.Conway and R.G.Barrads, Wiley, New York, 1966, p 295.

29. D.Dolar, in "Polyelectrolytes", ed. E.Sélégny, Reidel, Dordrecht, 1974, p 97.

30. S.Forsén and B.Lindman, in "Methods of Biochemical Analysis", vol.27, ed. D.Glick, Wiley,New York, 1981, p 289.

31. N.Ise and T.Okubo, Accs.Chem.Res.. 13, 303 (1980).

32. A.L.Loeb, J.Th.G.Overbeek and P.H.Wiersma, "The Electrical Double Layer Around a Spherical Colloid Particle", M.I.T.Press, Cambridge, 1961.

33. E.J.W.Verwey and J.Th.G.Overbeek, "Theory of the Stabilty of Lyophobic Colloids",Elsevier, Amsterdam, 1948.

34. J.Th.G.Overbeek and D.Stigter, Recl.Trav.Chim.Pays-Bas, 75, 1263 (1956).

35. S.L.Brenner and R.E.Roberts, J.Phys.Chem., 77, 2367 (1973).

36. C.G.Malmberg and A.A.Maryott, J.Res.Natl.Bur.Stand. 56, 1 (1956).

37. Y.Kawgushi and M.Nagasawa, J.Phys.Chem., 73, 4382 (1969).

38. I.Kagawa and H.P.Gregor, J.Polymer Sci., 23, 477 (1957).

39. J.Skerjanc, Biophys.Chem.,1, 376 (1974).

40. D.Stigter, J.Colloid interface Sci., 47, 473 (1974).

41. P.J.Missel, N.A.Mazer, G.B.Benedek, C.Y.Young and M.C.Carey, J.Phys.Chen., 84, 1044 (1980).

APPENDIX I.

Proof of that eq. 4.7 reduces to eq. 4.8, when the cell volume approaches infinity.

Eq. 4.7 can be generalised to include many kinds of ions. The resulting equation is

$$G_{el}/nkT = |e\phi_A/kT| - E_{el}/nkT + \sum_{i\neq w} n_i/n \ln(c_{io}/\tilde{c}_i) \qquad \text{AI.1}$$

The behaviour of the first two terms on the right hand side of eq. AI.1 is trivial when V_1, the aqueous volume of the cell approaches infinity. If the salt concentration, $\tilde{c}_i$, is kept constant when V_1 increases we see that $n_i \to \infty$ and $c_{io}/\tilde{c}_i \to 1$ as $V_1 \to \infty$. The last term in eq. AI.1 therefore is a sum of terms , that are products of quantities that approach zero and infinity as $V_1 \to \infty$. By using eq. 2.7 the terms in the sum can now be expressed as

$$n_i/n \ln(c_{io}/\tilde{c}_i) = -n_i/n \ln\left(\int_{V_1} \exp\left(-\frac{z_i e\phi}{kT}\right) dV/V_1 \right) \qquad \text{AI.2}$$

By adding and subbtracting 1 in the logarithm we obtain

$$n_i/n \ln(c_{io}/\tilde{c}_i) = -n_i/n \ln\left(\int_{V_1} \left\{\exp\left(-\frac{z_i e\phi}{kT}\right) - 1\right\} dV/V_1 + 1 \right) \qquad \text{AI.3}$$

For large V_1 we can expand the logarithm

$$n_i/n \ln(c_{io}/\tilde{c}_i) \simeq -n_i/(V_1 n) \int_{V_1} \left\{\exp\left(-\frac{z_i e\phi}{kT}\right) - 1\right\} dV \qquad \text{AI.4}$$

Inserting AI.4 into AI.1 we obtain

$$G_{el}/nkT = |e\phi_A/kT| - E_{el}/nkT + \sum_{i\neq w} \tilde{c}_i/n \int_{V_1} \left\{\exp\left(-\frac{z_i e\phi}{kT}\right) - 1\right\} dV \qquad \text{AI.5}$$

For an infinte cell we have,for only 1:1 salt present, $\tilde{c}_+ = \tilde{c}_- = c_o$. In that case it is easily seen that eq. AI.1 can be written as eq. 4.8. This completes the proof.

APPENDIX II.

Proof of that $\mu_{el} = G_{el}/n$ for an infinte cell.

Dropping the index n in eq. 5.6 and generalising to many kinds of ions can it be written as

$$\mu_{el} = z_{am}e\phi_A - E_{el}/n - kT \sum_{i\neq w} n_i/n + kTV_1 \sum_{i\neq w} c_{io}/n \qquad \text{AII.1}$$

Using eq. 4.7 can eq. AII.1 be rewritten as

$$\mu_{el} = G_{el}/n - kT \sum_{i\neq w} n_i \ln(c_{io}/\tilde{c}_i) - kT \sum_{i\neq w} n_i/n + kTV_1 \sum_{i\neq w} c_{io}/n \qquad \text{AII:2}$$

For large V_1 can we treat the logarithmic term as in appendix I. Eq. AII.2 can then be written as

$$\mu_{el} = G_{el}/n - kT/n \sum_{i\neq w} (c_{io}-\tilde{c}_i) \int_{V_1} \{\exp(-\frac{z_i e\phi}{kT}) - 1\} dV \qquad \text{AII.3}$$

As $V_1 \to \infty$ then $\tilde{c}_i \to c_{io}$, which gives the following equation for an infinte cell volume.

$$\mu_{el} = G_{el}/n \qquad \text{AII.4}$$

This completes the proof.

ACKNOWLEDGEMENTS

Sture, Bengt, Björn, Hans, Jan Erik, Bo, Sven, Per, Eva, Bodil, Eva, Mats, Connie, Lennart, Hans, Pétur, Bertil, Torbjörn, Helene, Norman, Tom, Bill, Gerd and others at the Chemical Centre, who have in any way assisted me during my stay in Lund. Thank you all very much for your collaboration and tolerance.

And last but not least. Special thanks to Håkan.

I

Reprinted from the Journal of Physical Chemistry, 1980, 84, 3114.
Copyright © 1980 by the American Chemical Society and reprinted by permission of the copyright owner.

Surfactant Association into Micelles. An Electrostatic Approach

Gudmundur Gunnarsson,* Bengt Jönsson, and Håkan Wennerström

Division of Physical Chemistry 2, Chemical Center, S-220 07 Lund 7, Sweden *(Received: March 6, 1980)*

The association of ionic amphiphilic molecules to micellar aggregates is analyzed with special emphasis on the electrostatic effects, which are treated by using the Poisson–Boltzmann equation. From a model expression of the free energy of a micellar solution, which in addition to the electrostatic free energy contains contributions from the hydrophobic effect and from the entropy of mixing of the micelles, chemical potentials for the components are derived. Through the use of the cell model the chemical potentials can be expressed in closed form, and the effect of finite micellar concentrations can be studied. The equations obtained are compared with alternative methods for describing the electrostatic effects, and a rationalization of previously used more approximate methods is obtained. It is shown that the theory can describe the dependence of the critical micelle concentration on the salt concentration, the alkyl chain length, and the valency of the counterion. It is found that the theory is in good agreement with recent measurements of single ion activities, which show that the activity of the amphiphilic ion decreases with increasing total amphiphile concentration. Finally the counterion binding is considered, and degrees of ion association, β, are defined, relating to thermodynamic, transport, and spectroscopic measurements. They are found to be of similar magnitude and also in agreement with experimental observations.

Introduction

The association of amphiphilic molecules into micellar aggregates in aqueous solutions leads to a reduction of the energetically unfavorable contact between water and the apolar parts of the amphiphilic molecules while the polar groups are still solvated by the water. For the hydrophobic effect, there exist semiempirical expressions[1] that can be used in a quantitative analysis of the micelle formation process.[2-6] The understanding of the interactions involving the polar groups is less well developed. Even for ionic amphiphiles, where the ion–ion and ion–solvent interactions dominate, the theoretical analysis is still rather incomplete. Already in 1956 Overbeck and Stigter[7] analyzed the electrostatic effects involved in the formation of micelles on the basis of the nonlinearized Poisson–Boltzmann equation, and this work has been further refined by Stigter.[8-11] In spite of the sound work by the Dutch workers,[7-12] there have since appeared several[13-15] less

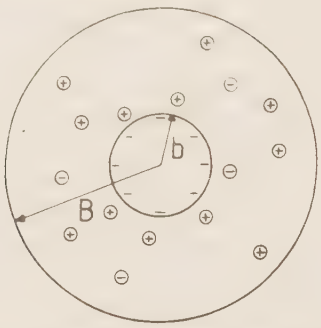

Figure 1. Model of a spherical micelle with radius b in a spherical cell with radius B.

satisfactory treatments of the electrostatic interactions in micellar solutions. It is also symptomatic that in the recent theoretical models for micelle formation[2-6,16,17] rather simplified treatments are used. The reason for this seems to be that the Poisson–Boltzmann equation has to be solved numerically in spherical symmetry.

The work in ref 7–12 is confined to micelles infinitely diluted in an electrolyte solution. This means that the properties of the micelles are determined at fixed chemical potentials of the water and the salt. When considering equilibria this is not always quite satisfactory since the chemical potential of component i is evaluated as a derivative of the free energy at constant amounts of components $j \neq i$. A formally more satisfactory description can be obtained by using the cell model[18] which has been used with success in polyelectrolyte systems[19-24] for the description of electrostatic effects.

In the present paper we show how one can obtain explicit expression for the chemical potentials of all components in the micellar system and that the use of the cell model, in fact, simplifies the description of the electrostatic effects. It becomes possible to describe the effect of micelle concentration on the monomer activity, the variation of the critical micelle concentration (cmc) with alkyl chain length, salt concentration, counterion valency, and also the counterion binding within one and the same formalism and in a conceptually clear way.

Electrostatic Model

In the cell model the total micellar solution is divided into cells, each containing a micellar aggregate and an amount of water and electrolyte giving the relevant concentrations for the particular system. To simplify the calculations the cells and the micelles are assumed spherical (see Figure 1) so that there is a central aggregate solely composed of amphiphile molecules and outside a spherical shell consisting of an aqueous solution. The charges in the system are located in the aqueous region and at the micellar surface, where they are assumed to be uniformly distributed with a surface charge density σ. In the region $b < r \leq B$ we assume the validity of the Poisson–Boltzmann (PB) equation which in spherical symmetry is[23]

$$\epsilon_r\epsilon_0 \frac{1}{r^2}\frac{\mathrm{d}}{\mathrm{d}r}\left(r^2\frac{\mathrm{d}}{\mathrm{d}r}\phi\right) = -\rho = -\sum z_i F c_i = -F\{c_{+0}\exp(-e\phi/kT) - c_{-0}\exp(e\phi/kT)\} \quad (1)$$

assuming that only monovalent ions are present in the solution. (For a summary of symbols used see Appendix 3.) For an electroneutral system the absolute value of the potential is arbitrary, and it has been chosen to be zero at the boundary of the cell, i.e., $\phi(B) = 0$. Then c_{+0} and c_{-0} are the concentrations (mol m^{-3}) of positive and negative ions, respectively, at $r = B$.

The total amount of positive, n_+, and negative, n_-, ions in N cells is determined through the relation

$$n_\pm = Nc_{\pm 0}N_A\int_b^B \exp(\mp e\phi/kT)4\pi r^2\,\mathrm{d}r \quad (2)$$

and the boundary conditions specifying the solution of eq 1 are

$$\left.\frac{\mathrm{d}\phi}{\mathrm{d}r}\right|_B = 0 \quad (3)$$

from the electroneutrality of the cell and

$$\left.\frac{\mathrm{d}\phi}{\mathrm{d}r}\right|_b = -\sigma/\epsilon_r\epsilon_0 \quad (4)$$

using Gauss' law. The cell model combined with the PB equation as in eq 1 has previously been used for micellar systems by Bell and Dunning[24] and Mille and Vanderkooi.[23]

To arrive at the PB equation (eq 1) from first principles, one has to make a series of approximations relating both to the statistical mechanical treatment[25] and to assumptions about the physical model. However, it appears that the PB equation gives a good first-order description of a number of properties related to electrostatic effects in colloidal and polyelectrolyte systems.[7,21,22,25-35]

From a solution of the PB equation the electrostatic free energy can be determined in several equivalent ways.[20] In our opinion, the most direct and conceptually most susceptible method is to separately determine the energy of the direct ion–ion interactions E_{el} and the entropy S_{el} caused by the nonuniform ion distribution. The free energy G_{el} is the sum (the systems are considered to be incompressible and then the Gibbs and Helmholtz free energies are equivalent)

$$G_{el} = E_{el} - TS_{el} \quad (5)$$

The assumption of a Boltzmann distribution of the ions in an effective potential ϕ, which is the basis of eq 1, implies that the correlation between the ions in the solution are neglected.[25] Due to this E_{el} and S_{el} can be calculated from a given solution of eq 1, and there is no need to use a charging process in calculating G_{el} as is usually done.[7,28] Thus per cell[20]

$$E_{el} = \tfrac{1}{2}\int \rho\phi\,\mathrm{d}V = 2\pi\epsilon_r\epsilon_0\int_b^B (r\,\mathrm{d}\phi/\mathrm{d}r)^2\,\mathrm{d}r = 2\pi b^3\sigma^2/\epsilon_0\epsilon_r + 4\pi RT\{B^3(c_{+0} + c_{-0}) - b^3[c_+(b) + c_-(b)]\} - 3kT(n_+ + n_-)/N \quad (6)$$

The last equality is obtained by using eq 1 as shown in Appendix 1.

Because of the presence of the charged micellar aggregate, the ions are nonuniformly distributed, leading to a decrease in entropy relative to the entropy S_{id} of the uncharged system and[20]

$$TS_{el} = T(S - S_{id}) = -RT\sum_i\left\{\int c_i(\ln c_i - 1)\,\mathrm{d}V - n_i/N(\ln \bar{c}_i - 1)\right\} \quad (7)$$

where $\bar{c}_i$ is the mean concentration of ion i. It is a characteristic feature of polyelectrolyte systems that the entropy term TS_{el} provides a substantial contribution to G_{el}.

The integral in eq 7 reduces to the same type of integral as the one in eq 6, and the expression for G_{el} per cell can be written as (see Appendix 2)

$$G_{el} - TS_{id} = \{z_{am}n_{am}{}^a e\phi_A - NE_{el} - kT(n_+ + n_-) + kT(n_+\ln c_{+0} + n_-\ln c_{-0})\}/N \quad (8)$$

which is in a form suitable for the determination of

chemical potentials. Here $n_{am}{}^{a}$ is the total amount of amphiphilic ions in the aggregates and $z_{am}e$ their charge and ϕ_A the potential at the aggregate surface.

Chemical Potentials

The equilibrium between the amphiphile in the monomeric state and in the micelles is most conveniently described in terms of the chemical potential which is equal for the two states at equilibrium. Similarly the thermodynamic description of counterion binding is also related to the chemical potential.

To arrive at expressions for the chemical potential the electrostatic model in the previous section has to be extended to include also the nonelectrostatic effects which are responsible for the formation of the aggregates. In a micellar solution there is a distribution of aggregate sizes, but in the absence of added electrolyte the polydispersity is generally small.[36,37] It is then a reasonable first approximation to consider only a single type of aggregate. Experimental evidence indicates[37] that the preferred aggregate size corresponds approximately to spheres with radii equal to the length of an extended amphiphile molecule.

With the constraint of a single micelle aggregation number, n, the total free energy, G, of a micellar solution with N micelles is

$$G = NG_0 + G_{mix} \tag{9}$$

where G_0 is the free energy per cell including the micelle and the corresponding amount of solution. G_{mix} is the free energy of mixing for the micelles in the solution, which under the assumption of ideal mixing within the cells is

$$G_{mix} = kTN(\ln c_m - 1) \tag{10}$$

At low concentrations of micelles, c_m, G_0 contains the free energy contribution of eq 8, the standard chemical potentials, μ^θ, of the components, and a contribution G_s due to the interface between the micelles and the aqueous region. It is G_s that accounts for the cooperativity of the micelle formation. Thus

$$G_0 = n\mu_{am}{}^{\theta,a} + \frac{1}{N}\sum_i n_i{}^{w}\mu_i{}^{\theta,w} + G_{el} - TS_{id} + G_s \tag{11}$$

Here the superscripts a and w refer to the aggregate and the aqueous part, respectively. The subscript am refers to the amphiphile and the sum is over components i in the aqueous region. In some of the applications discussed below it is necessary to have an explicit expression for the contribution G_s. In the limit of a macroscopic particle G_s is a surface free energy, and we assume that also for the micelles it is proportional to the area

$$G_s = \gamma A \tag{12}$$

where γ is the constant of proportionality. Surprisingly, this expression has been shown to describe accurately the phase equilibria involving liquid crystals at higher amphiphile concentrations.[29,38] For carboxylic soaps γ is approximately 18 mJ/m^2 within the present model.[29,38]

In calculating the chemical potentials from the expression for the free energy, it is the contribution from the electrostatic effects that gives the largest computational problem. However, Marcus[20] has elegantly derived analytical expressions for the mobile ions so that

$$\mu_\pm{}^{w} = \mu_\pm{}^{\theta,w} + kT \ln c_{\pm 0} \tag{13}$$

Following Marcus[20] one obtains for the water

$$\mu_{H_2O} = \mu_{H_2O}{}^{\theta} - RT(c_{+0} + c_{-0} + c_m)v_{H_2O} \tag{14}$$

where the last term in the parentheses is due to G_{mix}, and v_{H_2O} is the molecular volume of water. In eq 13 and 14 it is assumed that the volume of the aqueous region is determined by the amount of water available. For amphiphiles with a high aqueous solubility, this assumption might no longer be justified. An interpretation of eq 13 and 14 is that at the border of the cell where the electrostatic force on the ions is zero the solution behaves as an ideal system. For the amphiphiles in the aggregates the chemical potential can now be determined through the relation

$$G = \sum_j n_j\mu_j \tag{15}$$

Combining eq 8–15

$$\mu_{am}{}^{a} = \mu_{am}{}^{\theta,a} + z_{am}e\phi_A + \frac{1}{n}\left\{\gamma A - E_{el} - \frac{kT}{N}(n_+ + n_-) + RTV_1(c_{+0} + c_{-0}) + kT \ln c_m\right\} \tag{16}$$

where V_1 is the aqueous volume in a cell. Equation 16 can also be obtained by explicitly calculating the derivative $\partial G/\partial n_{am}{}^{a}$ from eq 9.[38]

In his treatment of micellar equilibria, Stigter[8] associates the electrostatic effects solely with the amphiphile and writes

$$\mu_{am}{}^{a}(el) = G_{el}/n \tag{17}$$

while in the present case the chemical potentials of the mobile ions and the water also include an electrostatic term. However, in the limit of infinite dilution considered by Stigter, eq 16 and 17 can be shown to be equivalent. The advantage with the cell model is that in addition to the cmc effects, one can discuss counterion and water activity, and the effect of increased micellar concentration on the monomer activity.

Some treatments of micellar equilibria[13–15] have included only the first two terms of the right-hand side of eq 16 for the expression of the $\mu_{am}{}^{a}$. As pointed out by Stigter,[8] this assumes that one can add a monomer to the micelle without changing its properties. This is true for bulk phases, but in the present model of a single aggregation number addition of monomers to the system can only lead to the formation of new micelles.

Computation Procedure

Equation 1 was solved by Hoskin[39] for infinite dilution in a salt medium, and his results were later extended by Loeb et al.[12] For finite micelle concentrations, solutions have been obtained both with counterions alone and with added salt by Bell and Dunning[24] and recently by Mille and Vanderkooi.[23] At infinite dilution, a numerical solution of eq 1 is straightforward, but at finite concentrations the constants c_{+0} and c_{-0} have to be fitted to eq 4. In addition, an extra constraint is usually imposed such as a given salt or monomer concentration or an equilibrium between amphiphile molecules in micelles and in aqueous solution. By initially guessing c_{+0} and c_{-0} we solved eq 1 by a fourth-order Runge–Kutta method. The solution was then checked against the additional conditions. If the calculated and given boundary conditions differed more than 1 ppm from each other, new values of c_{+0} and c_{-0} were guessed with an algorithm based on the Newton–Raphson method until convergence was reached.

A problem with this scheme is that rather good guesses of the initial values of c_{+0} and c_{-0} are required to avoid divergence. Thus eq 1 was first solved for the case of counterions only, and then a solution could be obtained for increasing salt concentrations by using the previously

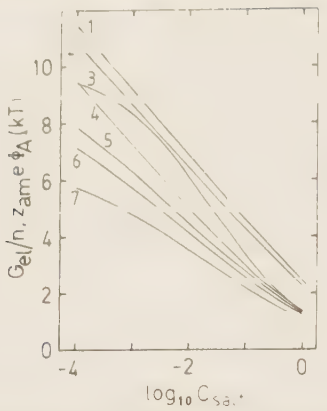

Figure 2. Comparison of different methods of estimating the electrical part of the chemical potential of an amphiphile in a micelle at infinite dilution in an electrolyte solution: (1) $z_{am}e\phi_A$ and (4) G_{el}/n (eq 5) for an infinite plane with $\sigma = 0.183$ C m^{-2}, (2) $z_{am}e\phi_A$, (3) G_{el}/n (Debye–Hückel), and (6) G_{el}/n (eq 5) for spheres representing dodecyl sulfate micelles, $\sigma = 0.183$ C m^{-2}, $b = 19.7$ Å, (5) G_{el}/n (eq 5) for spheres representing hexadecyl sulfate micelles, $\sigma = 0.196$ C m^{-2}, $b = 24.7$ Å, (7) G_{el}/n (eq 5) for spheres representing octyl sulfate micelles, $\sigma = 0.162$ C m^{-2}, $b = 14.6$ Å. ($t = 21$ °C; $\epsilon_r = 79.7$.)

calculated values of c_{+0} and c_{-0} for extrapolating to new initial values of c_{+0} and c_{-0}. A similar extrapolation procedure was used when the micelle concentration was changed. For several choices of parameters, it was checked that the solutions were identical, within the numerical limits, to the ones previously obtained by Mille.[40] The micelles are assumed to be spherical with the maximum possible radius; i.e., the radius of the hydrophobic core equals the length of a fully extended hydrocarbon chain (eq 9–2 in ref 1). The aggregation numbers are calculated from eq 9–1 in ref 1. The ionic head groups are assumed to stick straight out from the hydrophobic core,[9] and it is assumed that the ionic charges reside at the terminal oxygen atoms in the *n*-alkyl sulfates and *n*-alkyl carboxylates considered. This results in a decrease in surface charge density from $\sigma = 0.183$ C m^{-2} for dodecyl sulfate micelles to $\sigma = 0.162$ C m^{-2} for octyl sulfate micelles. The relative permittivity is assumed to be that of pure water.

Comparison with Other Models of Micelle Formation

To illustrate the differences and the similarities with other models for treating the electrostatic effects, let us consider the aggregate–monomer equilibrium at varying salt concentrations. At equilibrium the chemical potentials of the amphiphile in the two states are equal, and at small micellar concentrations the infinite dilution approximation, eq 17, can be used. Then (cf. ref 8)

$$\mu_{am}{}^{a} = \mu_{am}{}^{\theta,a} + (1/n)(G_s + G_{el} + kT \ln c_m) = \mu_{am}{}^{\theta,w} + kT \ln c_{am}{}^{w} = \mu_{am}{}^{w} \quad (18)$$

The accuracy of different methods of estimating the electrical contribution G_{el}/n can be seen in Figure 2. It can be noted that all these methods are based on the same physical model. If one includes only the surface potential in G_{el}/n,[13–15] the electrostatic effect is overestimated by $\sim 2\ kT$ in $\mu_{am}{}^{a}$. The Debye–Huckel approximation obtained by linearizing eq 1 gives approximately the same error in G_{el}/n.[4,5] It is a better approximation to use the Gouy–Chapman equation for a plane.[16,17] In that case the error is rather small above a salt concentration of 0.1 M becoming increasingly larger as the salt concentration is decreased.

In the salt concentration region 10^{-3}–10^{-1} M, G_{el}/n can be written approximately as a linear function of ln c_{salt} (eq 19) for the three sphere radii considered. Equation 19

$$\mu_{am}{}^{a}(el) = G_{el}/n = -\alpha kT \ln (c_{salt}) + \delta \quad (19)$$

provides a rationalization of Shinoda's method[15] of describing the electrostatic effects. In calculating the electrostatic contribution to the chemical potential $\mu_{am}{}^{a}$(el) he only includes the surface potential which is calculated by using the Gouy–Chapman theory for planar surfaces but includes an empirical constant K_g so that

$$\mu_{am}{}^{a}(el) = K_g z_{am} e\phi_A \quad (16')$$

Since $|e\phi_A/(kT)|$ is a linear function of ln c_{salt} (cf. Figure 2, curve 1), eq 16′ and 19 are identical with the "empirical" constant K_g identified as the linearization coefficient α of eq 19. The values of α for the sphere sizes corresponding to C_8, C_{10}, and C_{12} alkyl sulfates are respectively 0.58, 0.67, and 0.77, in reasonable agreement with the empirical values of K_g which are usually in the range 0.40–0.70.[15,41]

An alternative to the description of the electrostatic effects in terms of the PB equation is to treat the ion binding to micelles as ordinary chemical equilibrium with defined species.[42] With a single micelle aggregation number

$$nA^- + kP^+ \rightleftarrows (A_nP_k)^{(n-k)-} \quad (20)$$

There are fundamental difficulties associated with such a description, mainly due to the fact that the electrostatic interactions are of a long-range character. It has been shown for polyelectrolyte systems[43,44] that it is not convenient to describe the ion binding properties by using the mass action law based on eq 20, and the same holds for micellar systems. However, if one uses eq 19, the condition that $\mu_{am}{}^{a} = \mu_{am}{}^{w}$ leads to eq 21, which also could be derived

$$\frac{c_m}{c_{am}{}^{n}(c_{am} + c_{salt})^{\alpha n}} = K \quad (21)$$

from eq 20 if k is identified as αn. Thus the equilibrium model can be used to describe variations in the cmc, but the motivation for using a single specific formal degree of ion binding of α is found from the PB equation.

Dependence of the Cmc on Hydrocarbon Chain Length, Salt Concentration, and Valency of the Counterion

The hydrophobic interaction causes the aggregation of the amphiphilic molecules, and it thus gives the major contribution to the difference in the standard chemical potentials $\mu_{am}{}^{\theta,a} - \mu_{am}{}^{\theta,w}$ for the amphiphile in the two environments. In a homologous series the hydrophobic interaction usually increases linearly with alkyl chain length[1] and

$$\mu_{am}{}^{\theta,a} - \mu_{am}{}^{\theta,w} = kT(u - vn_c) \quad (22)$$

where n_c is the number of carbon atoms and u and v are adjustable constants. For nonionic amphiphiles one usually observes a linear dependence of the ln (cmc) on n_c, and the constant v is ~ 1.2.[1] For ionic amphiphiles the cmc dependence on n_c is more complex because of the electrostatic effects. In the absence of added electrolyte, the monomeric amphiphile and its counterion provide the electrolyte concentration, and the electrostatic contribution $\mu_{am}{}^{a}$ at low micelle concentrations is easily calculated from eq 17 by using the experimental cmc values. Then one can calculate values for $\mu_{am}{}^{\theta,a} - \mu_{am}{}^{\theta,w} + \gamma A/n$ from eq 18 assuming that 2% of the amphiphiles are in micelles at the cmc (vide infra). The results for a series of alkyl sulfates[45] are shown in Figure 3, and it is seen that relation 22 holds

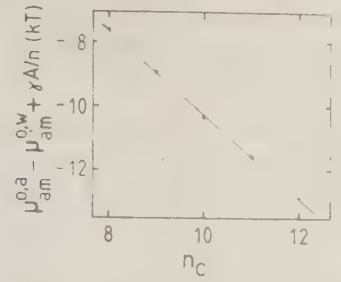

Figure 3. $\mu_{am}^{0,a} - \mu_{am}^{0,w} + \gamma A/n$ calculated from eq 18 and experimental cmc values (from ref 45) for *n*-alkyl sulfates plotted vs. alkyl chain length. The straight line is a least-squares fit to the calculated points with the slope −1.31 and the intercept +2.87. For the micelle concentration mole fraction units have been used. (t = 21 °C; ϵ_r = 79.7.)

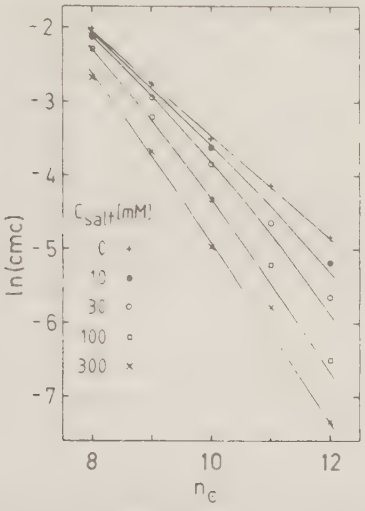

Figure 4. ln (cmc) vs. alkyl chain length for *n*-alkyl sulfates at different salt concentrations. The solid lines are calculated from eq 18, and the experimental points are from ref 45. (t = 21 °C; ϵ_r = 79.7.)

with v = 1.31 or v = 1.21 when the aggregate area in eq 12 coincides with the hydrophobic core or with the surface of charges, respectively. These values of v are in good agreement with those found for nonionics.[1]

When salt is added to the solution, the difference between ionic and nonionic amphiphiles becomes less pronounced. This effect is illustrated in Figure 4, which shows the cmc for C_8–C_{12} alkyl sulfates in sodium chloride solutions from 0 to 300 nM.[45] The calculated points have been determined by using the slope and intercept obtained from Figure 3, and no additional adjustable parameters are added. The agreement with experiments is satisfactory. Very similar results were recently obtained by Funasaki[41] using the theory of Shinoda, and this illustrates once more that the "empirical" constant K_g can be accounted for theoretically within the same physical model.

The cmc values presented in Figures 3 and 4 refer to systems with monovalent counterions. For divalent counterions the cmc is reduced. The dependence on the counterion valency is due mainly to the entropy contribution to G_{el} (eq 7). Since each ion carries two charges, the entropy decrease on ion binding to the micelle is smaller, counted per charge, for the divalent ions. Equation 8 for G_{el} is equally valid for divalent counterions if n_+ and c_{+0} are exchanged for the equivalent parameters n_{2+} and c_{2+0}, and in the PB equation (eq 1) the term c_{+0} $\exp[e\phi/(kT)]$ is exchanged for $2c_{2+0}$ $\exp[-2e\phi/(kT)]$. It is thus straightforward to calculate the cmc for solutions with only divalent counterions by using the same procedure as for the monovalent ions. Experimental determinations of the cmc for soaps with divalent counterions are scarce because of the usually high Krafft points, but for dodecyl sulfate several determinations have been made.[46] Using the value of $\mu_{am}^{\theta,a} - \mu_{am}^{\theta,w} + \gamma A/n$ determined from Figure 3, we have calculated the cmc, and as seen in Table I the agreement between theory and experiment is reasonable. One can conclude that the effect of counterion valency on the cmc is mainly of an electrostatic origin and that specific binding is of secondary importance. Thus if specific binding occurs, it only affects the free energy of micellization to a minor extent.

TABLE I: Comparison between Experimental and Theoretical Cmc Values for Dodecyl Sulfate (DS) with Monovalent and Divalent Counterions

compd	cmc, mM: exptl,[a] t = 25 °C, ϵ_r = 78.3	cmc, mM: theoretical, t = 21 °C, ϵ_r = 79.7
NaDS	7.4	7.83
$Mg(DS)_2 \cdot 6H_2O$	0.88	1.22
$Mn(DS)_2$	1.1	
$Co(DS)_2 \cdot 6H_2O$	0.83	
$Cu(DS)_2 \cdot 1H_2O$	1.0	

[a] From ref 46.

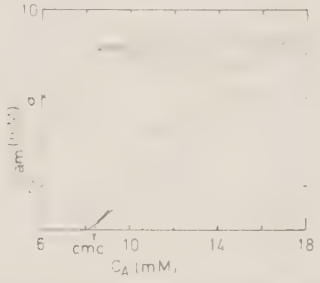

Figure 5. The concentration of monomeric amphiphile, c_{am}^{w} and $c_{am}^{w\infty}$, and of micellized amphiphile, c_{am}^{a} and $c_{am}^{a\infty}$, as a function of the total amphiphile concentration for dodecyl sulfate. The values are calculated from the cell model using eq 16 and in the infinite dilution approximation (superscript ∞) using eq 17 for μ_{am}^{a}. The curves for c_{am}^{a} are extrapolated linearly to $c_{am}^{a} = 0$. In the phase-separation model the intercept represents the cmc as indicated in the figure. (t = 25 °C; ϵ_r = 78.3.)

Monomer Activity above the Cmc

For the description of the micellar aggregation around the cmc, one can use the expressions valid at infinite dilution for the electrostatic effects. However, as the amphiphile concentration is increased, intermicellar interactions soon become important, and it is necessary to use a more refined model as, for example, the cell model developed above.

Two related properties which are clearly influenced by the finite micellar concentration are the monomer concentration and activity. It is usually stated in textbooks that above the cmc the monomer concentration stays constant or increases slightly. However, recent experimental studies[36,47,48] show that there is a decrease in the monomer concentration and the amphiphile ion activity above the cmc.

The nonassociated amphiphile monomer will act as a co-ion, and its chemical potential, μ_{am}^{w}, can be calculated from eq 13. Using the condition $\mu_{am}^{a} = \mu_{am}^{w}$, where the left-hand side is given (eq 16), it is possible to calculate how the monomer and micelle concentrations vary with total amphiphile concentration. The results of such a calculation for sodium dodecyl sulfate are shown in Figure 5, together with results using the infinite dilution approach, i.e., eq 18. It is clearly seen that the cell model predicts a decrease in monomer concentration above the cmc,

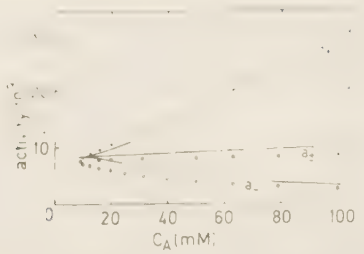

Figure 6. Single ion a_+ (●) and a_- (○) and mean ion $a_\pm$ (□) activities in sodium dodecyl sulfate solutions as a function of the total amphiphile concentration c_A. The experimental values for a_+ and a_- are taken from Table I of ref 47, and $a_\pm$ is estimated from Figure 2 of this reference. The solid lines are calculated from eq 13 and 16. (t = 25 °C; ϵ_r = 78.3.)

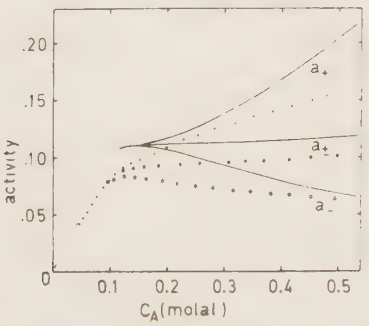

Figure 7. Single ion a_+ (●) and a_- (○) and mean ion $a_\pm$ (□) activities in sodium decanoate solutions as a function of the total amphiphile concentration c_A. Experimental points deduced from Figure 3 of ref 48. The solid lines are calculated from eq 13 and 16. (t = 25 °C; ϵ_r = 78.3.)

whereas eq 18 predicts a slightly increasing monomer concentration above the cmc. However, the two models give approximately the same cmc if it is defined as in Figure 5. It can also be seen that ca. 2% of the amphiphile is in micellar form at the cmc. Approximately the same fraction was found to be in micellar form at the cmc for octyl sulfate, justifying the assumption made in the calculations related to Figures 3 and 4.

The ion activities are also obtained from the cell model using eq 13 and 16. The results for sodium dodecyl sulfate (NaDS) and sodium decanoate are shown in Figures 6 and 7. For these two systems experiments have been performed[47,48] with ion selective electrodes for both amphiphile and counterion. It is seen that eq 16 predicts a clear decrease in monomer activity. For NaDS in Figure 6 the agreement between theory and experiment is very good while it is somewhat less satisfactory for the decanoate system. It can be noted that the interpretation of the experimental data in terms of single ion activities is not clear-cut, because of the possible perturbations from liquid junction potentials. For the two systems both theory and experiment show that the activity of the neutral system consisting of amphiphilic ion plus its counterion stays approximately constant above the cmc.

Figure 7 illustrates a difficulty with the PB equation for polyelectrolyte systems. In the limit of infinite dilution, the ion activities are those of an ideal solution, and the electrolyte solution activity coefficients as in the Debye–Hückel theory do not appear. The reason is that in arriving at the PB equation from first principles one assumes that the positions of the ions in the aqueous medium are uncorrelated,[25] but it is precisely this correlation that gives rise to the Debye–Hückel and higher-order activity corrections. It seems that lacking a description that goes beyond the PB equation, it is most consistent to neglect ion correlations altogether. However, a discrepancy then appears when one compares measured and calculated activities as clearly seen at the cmc in Figure 7.

Counterion Binding

The charged micellar aggregates attract counterions, which leads to changes in the physical properties of these ions relative to an ordinary electrolyte solution. The binding is due to the long-range electrostatic forces, and there is a gradual change in the counterion–micelle interaction as the micelle surface is approached. Depending on the experimental technique used, different aspects of the counterion–micelle interaction are probed.[37] One can distinguish three different classes of experimental methods for studying the degree of ion binding, β, and it is possible to identify a theoretical expression that corresponds to the different experimental methods.

One can perform thermodynamic measurements by using ion specific electrodes or the determination of osmotic pressure. In the former case one has a measure of the total ion activity which can be obtained theoretically from eq 13. To arrive at a measure of the degree of ion binding to the micelles, one must, both in theoretical calculations and in the analysis of experimental data, correct for the effect due to the salt that is present, due, for example, to the dissolved monomeric amphiphile. The thermodynamic degree of ion association β_{th} can then be defined through eq 23, where $\bar{c}_c$ is the mean concentration

$$\beta_{th} = 1 - [(\text{total counterion activity} - \text{activity due to the salt})/(\text{total counterion concentration} - \text{salt concentration})] = (c_{salt} + \bar{c}_c - c_{+0})/\bar{c}_c \quad (23)$$

of counterions due to the micellized amphiphile. In accordance with the remark made in the previous section, the activity coefficient for the salt is taken as unity. In the limit of large dilution, both the numerator and the denominator approach zero while the quotient remains finite.

When β is measured through a transport property, as in a conductivity or diffusion experiment, a quantitative analysis of the particular experiment can be made,[24,49,50] but as a first approximation one can consider the counterions within a region $r \leq r_{tr}$ such that $|e\phi(r)/(kT)| \geq 1$ as moving with the polyion[21] so that

$$\beta_{tr} = \frac{1}{n}\int_b^{r_{tr}} c_+ 4\pi r^2 \, dr \quad (24)$$

Finally in spectroscopic measurements[51,52] and in micellar catalysis,[53] it is often only the counterions in the direct vicinity of the aggregate surface that contribute to the measured property. In that case

$$\beta_{sp} = \frac{1}{n}\int_b^{b+\Delta} c_+ 4\pi r^2 \, dr \quad (25)$$

where the distance Δ should be of the order of a counterion dimension. In the calculations discussed below we have chosen Δ as 3 Å.[30]

From their definitions it seems a possibility that the three β values can be very different. However, as shown in Table II, they are of the same order of magnitude for typical micellar systems. The dependence on the type of amphiphile and its concentration is also rather weak. These findings are in good agreement with experimental estimates[37,54-56] of β, which generally fall in the range 0.5–0.8.

In the same way that eq 20 is unsuitable for describing the micelle association, it also gives a deficient account of

TABLE II: Theoretically Calculated Degrees of Ion Binding, β_{sp}, β_{th}, and β_{tr}, for Three Different Amphiphiles[b]

amphiphile[a]	$c_A{}^{xc}$	β_{th}	β_{tr}	β_{sp}
octyl sulfate	2	0.67	0.59	0.43
(130 mM)	5	0.53	0.48	0.48
dodecyl sulfate	2	0.80	0.72	0.41
(8.2 mM)	5	0.74	0.71	0.41
decanoate	2	0.74	0.67	0.47
(109 mM)	5	0.64	0.61	0.49

[a] Cmc values in parentheses. [b] $t = 25$ °C, $\epsilon_r = 78.3$ monovalent counterions. [c] $c_A{}^x$ = total amphiphile concentration in multiples of the cmc.

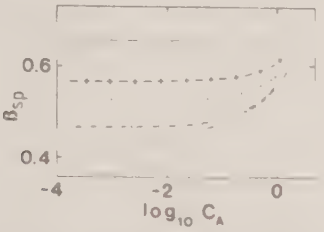

Figure 8. The fraction of bound ions, β_{sp}, as a function of the amphiphile concentration, c_A (M), for spheres in salt-free solutions (- - -), spheres in 0.01 M salt solutions (- · -), spheres in 0.1 M salt solutions (· · ·), and lamellae (——) and cylinders (– + –) in salt-free solutions. The surface charge density is 0.228 C m^{-2} and the radii of the spheres and the cylinders are 18 Å. ($t = 25$ °C; $\epsilon_r = 78.3$.)

the ion binding properties. It follows from the electrostatic theories of polyelectrolyte systems that the counterion concentration close to the polyion is determined mainly by the surface charge density, while it is independent of the salt and polyion concentration over large regions of these parameters.[26,30,43,57-59] This qualitative behavior of the ion binding has been demonstrated for many types of polyelectrolyte systems.[21,31,43,44,59,60] It has been found experimentally in micellar solutions both in micellar catalysis and in nuclear magnetic resonance experiments.[51,53,61,62] To illustrate the similarity between different aggregate geometries Figure 8 shows calculated values of β_{sp} for spherical cylindrical and planar aggregates with the same surface charge. With the exception of the spheres having a finite charge in a salt-free solution where β_{sp} goes toward zero at infinite dilution, the qualitative behavior of β_{sp} is the same. Note that β_{sp} remains constant for the planes and the cylinders and changes only moderately for the spheres while the counterion activity is varied over several orders of magnitude.

Conclusions

It has been demonstrated how within the cell model of micellar solutions one can describe electrostatic effects on the basis of the nonlinearized Poisson–Boltzmann equation for a spherically symmetrical system. All the components in the system contribute to the electrostatic free energy, and closed-form expressions for the chemical potentials have been derived. These expressions have then been used to calculate the dependence of the cmc on the electrolyte concentration, the alkyl chain length, and the counterion valency. It has been demonstrated that the amphiphile activity decreases above the cmc, and counterion association has also been discussed. It is consistently found that, in spite of the clear deficiencies in the model, it gives predictions that are in good agreement with experimental findings. This indicates that for inorganic cations the major part of the micelle–ion interactions is of a nonspecific nature and that specific ion-binding effects are of secondary importance for the energetics.

Acknowledgment. We are indebted to Gordon J. T. Tiddy and B. Lindman for scientific as well as linguistic criticism of the manuscript.

Appendix 1.

Derivation of the Second Equality in Eq 6. Multiply eq 1 by $r^3\, d\phi/dr$ and integrate. This gives eq A1.

$$\tfrac{1}{2}\int_b^B \frac{1}{r}\frac{d}{dr}\left(r^2\frac{d\phi}{dr}\right)^2 dr = -\frac{F}{\epsilon_r\epsilon_0}\int_b^B r^3\frac{d\phi}{dr}\{c_{+0}\exp(-e\phi/kT) - c_{-0}\exp(e\phi/kT)\}\, dr \quad (A1)$$

Equation (A1) can be integrated by parts, which results in one term containing the desired integral defining E_{el} and

$$-\tfrac{1}{2}b^3(\sigma/\epsilon_r\epsilon_0)^2 + \frac{1}{4\pi\epsilon_0\epsilon_r}E_{el} = \frac{RT}{\epsilon_r\epsilon_0}\{B^3(c_{+0}+c_{-0}) - b^3[c_+(b)+c_-(b)]\} - 3kT(n_+ + n_-)/(N4\pi\epsilon_0\epsilon_r) \quad (A2)$$

which after rearrangement results in eq 6.

Appendix 2

Derivation of Eq 8 from Eq 5–7.

$$G_{el} - TS_{id} = \tfrac{1}{2}\int \rho\phi\, dV + RT\left\{\int c_+ \ln c_+\, dV + \int c_- \ln c_-\, dV\right\} - kT(n_+ + n_-)/N \quad (A3)$$

In the first integral the charge distribution can be divided into the charges on the micellar surface and the charges ρ_{ion} due to the mobile ions. The two other integrals can be rewritten by using the last equality of eq 1 and

$$G_{el} - TS_{id} = \tfrac{1}{2}nz_{am}e\phi_A - \tfrac{1}{2}\int \rho_{ion}\phi\, dV + kT(n_+ \ln c_{+0} + n_- \ln c_{-0})/N - kT(n_+ + n_-)/N = nz_{am}e\phi_A - \tfrac{1}{2}\int \rho\phi\, dV - kT(n_+ + n_-)/N + kT(n_+ \ln c_{+0} + n_- \ln c_{-0})/N \quad (A4)$$

When one uses eq 6, this expression reduces to eq 8.

Appendix 3

A	area of the micelles
B	radius of the spherical cell
E_{el}	electrostatic energy due to the ion–ion interactions
F	Faraday's constant
G	total free energy
G_{el}	electrostatic free energy
G_0	free energy per cell
G_{mix}	free energy due to the mixing of micelles
G_s	free energy contribution due to the interface between micelles and water
K_g	"empirical" constant introduced by Shinoda
N	number of cells
N_A	Avogadros number
S_{el}	electrostatic contribution due to the entropy of the ion distribution
S_{id}	entropy contribution due to the ideal mixing of the uncharged ions with water
V_1	volume of the aqueous region in a cell
b	micellar radius
c_i	concentration of species i
$\bar{c}_i$	mean concentration of species i
c_{i0}	concentration of species i at the cell boundary
c_m	concentration of micelles
e	elementary charge
k	Boltzmann's constant

n_i total amount of species i
n micelle aggregation number
n_c number of carbon atoms in a chain
v_{H_2O} molecular volume of water
z_i valency of charged species i
ϕ electrostatic potential
ϕ_A electrostatic potential at the micellar surface
α coefficient of linearization in eq 19
β degree of ion binding, subscript th = thermodynamic, tr = transport, and sp = spectroscopic
γ proportionality constant relating G_s and A
ϵ_0 permittivity of vacuum
ϵ_r relative permittivity
$\mu_i^{\theta,x}$ standard chemical potential of species i in the environment x
μ_i^x chemical potential of species i in the environment x
$\mu_{am}^{\partial}(el)$ electrostatic contribution to the chemical potential of the amphiphile in the aggregate
ρ charge density
σ surface charge density

References and Notes

(1) Tanford, C. "The Hydrophobic Effect"; Wiley: New York, 1973.
(2) Tanford, C. *J. Phys. Chem.* **1974**, *84*, 2469.
(3) Tanford, C. *Micellization, Solubilization, Microemulsions* [*Proc. Int. Symp.*] **1977**, *1*, 119.
(4) Nagarajan, R.; Ruckenstein, E. *J. Colloid Interface Sci.* **1979**, *71*, 580.
(5) Ruckenstein, E.; Nagarajan, R. *Micellization, Solubilization, Microemulsions* [*Proc. Int. Symp.*] **1977**, *1*, 133.
(6) Israelachvili, J. N.; Mitchell, D. J.; Ninham, B. N. *J. Chem. Soc. Faraday Trans. 2* **1976**, *72*, 1525.
(7) Overbeek, J. Th. G.; Stigter, D. *Recl. Trav. Chim. Pays-Bas* **1956**, *75*, 1263.
(8) Stigter, D. *J. Colloid Interface Sci.* **1974**, *47*, 473.
(9) Stigter, D. *J. Phys. Chem.* **1974**, *78*, 2480.
(10) Stigter, D. *J. Phys. Chem.* **1975**, *79*, 1008.
(11) Stigter, D. *J. Phys. Chem.* **1975**, *79*, 1015.
(12) Loeb, A. L.; Overbeek, J. Th. G.; Wiersema, P. H. "The Electrical Double Layer around a Spherical Colloid Particle"; M.I.T. Press: Cambridge, MA, 1961.
(13) Emerson, M. F.; Holtzer, A. *J. Phys. Chem.* **1965**, *69*, 3718.
(14) Emerson, M. F.; Holtzer, A. *J. Phys. Chem.* **1967**, *71*, 1898.
(15) Shinoda, K. In "Colloidal Surfactants"; Shinoda, K., Nakagawa, T., Tamamushi, B. I., Isemura, T., Eds.; Academic Press: New York, 1963; p 1.
(16) Mazer, N. A.; Carey, M. C.; Benedek, G. B. *Micellization, Solubilization, Microemulsions* [*Proc. Int. Symp.*] **1977**, *1*, 359.
(17) Missel, P. J.; Mazer, N. A.; Benedek, G. B.; Young, C. Y., *J. Phys. Chem.* **1980**, *84*, 1044.
(18) Hill, T. L. "Statistical Mechanics"; Addison-Wesley: Reading, MA, 1960.
(19) Fouss, R. M.; Katchalsky, A.; Lifson, S. *Proc. Natl. Acad. Sci. U.S.A.* **1951**, *37*, 579.
(20) Marcus, R. A. *J. Chem. Phys.* **1955**, *23*, 1057.
(21) Katchalsky, A.; Alexandrowicz, Z.; Kedem, O. In "Chemical Physics of Ionic Solutions"; Conway, B. E., Barrads, R. G., Eds.; Wiley: New York, 1966; p 295
(22) Gunnarsson, G.; Olofsson, G.; Wennerström, H.; Zacharov, A. *J. Chem. Soc., Faraday Trans. 1* **1980**, *76*, 1287.
(23) Mille, M.; Vanderkooi, G. *J. Colloid Interface Sci.* **1977**, *59*, 211.
(24) Bell, G. M.; Dunning, A. J. *Trans. Faraday Soc.* **1970**, *66*, 500.
(25) Jönsson, B.; Wennerström, H.; Halle, B. *J. Phys. Chem.* **1980**, *84*, 2179.
(26) Guéron, M.; Weisbuch, G. *J. Phys. Chem.* **1979**, *83*, 1991.
(27) Stigter, D. *J. Phys. Chem.* **1978**, *82*, 1603.
(28) Verwey, E. J. W.; Overbeek, J. Th. G. "Theory of the Stability of Lyophobic Colloids"; Elsevier: Amsterdam, 1948.
(29) Parsegian, V. A. *Trans. Faraday Soc.* **1968**, *62*, 848.
(30) Engström, S.; Wennerström, H. *J. Phys. Chem.* **1978**, *82*, 2711.
(31) Wennerström, H.; Lindman, B.; Lindblom, G.; Tiddy, G. J. T. *J. Chem. Soc., Faraday Trans. 1* **1979**, *75*, 663.
(32) Dolar, D.; Škerjanc, J. *J. Chem. Phys.* **1974**, *61*, 4106.
(33) Träuble, H.; Teubner, M.; Wolley, P.; Eibl, H. *Biophys. Chem.* **1976**, *4*, 319.
(34) Jähnig, F. *Biophys. Chem.* **1975**, *4*, 309.
(35) McLaughlin, S. A.; Szabo, G.; Eisenmann, G. *J. Gen. Physiol.* **1971**, *58*, 667.
(36) Aniansson, E. A. G.; Wall, S. N.; Almgren, M.; Hoffman, H.; Kielman, I.; Ulbricht, W.; Zana, R.; Lang, J.; Tondre, C. *J. Phys. Chem.* **1976**, *80*, 905.
(37) Lindman, B.; Wennerström, H. *Top. Curr. Chem.* **1980**, *87*, 1.
(38) Jönsson, B.; Wennerström, H. *J. Colloid Interface Sci.*, in press.
(39) Hoskin, N. E. *Trans. Faraday Soc.* **1953**, *49*, 1471.
(40) Mille, M. Ph.D. Thesis, University of Wisconsin-Madison, Madison, WI, 1976, Microfilm 76-23333.
(41) Funasaki, N. *J. Colloid Interface Sci.* **1978**, *67*, 384.
(42) Phillips, J. N. *Trans. Faraday Soc.* **1955**, *51*, 561.
(43) Manning, G. S. *Q. Rev. Biophys.* **1978**, *11*, 179.
(44) Record, M. T.; Anderson, C. F.; Lohman, T. M. *Q. Rev. Biophys.* **1978**, *11*, 103.
(45) Experimental points from Huisman, H. F. *Proc. K. Ned. Akad. Wet., Ser. B: Phys. Sci.* **1964**, *67*, 367.
(46) Miyamoto, S. *Bull. Chem. Soc. Jpn.* **1960**, *33*, 375.
(47) Cutler, S. G.; Mears, P.; Hall, D. G. *J. Chem. Soc., Faraday Trans. 1*, **1978**, *74*, 1758.
(48) Vikingstad, E. *J. Colloid Interface Sci.* **1979**, *72*, 68.
(49) Bell, G. M. *Trans. Faraday Soc.* **1964**, *60*, 1952.
(50) Yoshida, N. *J. Chem. Phys.* **1978**, *64*, 4861.
(51) Lindman, B.; Lindblom, G.; Wennerström, H.; Gustavsson, H. *Micellization, Solubilization, Microemulsions* [*Proc. Int. Symp.*] **1977**, *1*, 795.
(52) Thomas, J. K.; Grieser, F.; Wong, M. *Ber. Bunsenges. Phys. Chem.* **1978**, *82*, 937.
(53) Romsted, L. S. *Micellization, Solubilization, Microemulsions* [*Proc. Int. Symp.*] **1977**, *2*, 509.
(54) Brun, T. S.; Høiland, H.; Vikingstad, E. *J. Colloid Interface Sci.* **1978**, *63*, 590.
(55) Lindman, B.; Brun, B. *J. Colloid Interface Sci.* **1973**, *42*, 388.
(56) Zana, R., presented at the 3rd International Conference on Surface and Colloid Science, Stockholm, Sweden, Aug 20–25, 1979.
(57) Stigter, D. *Prog. Colloid Polym. Sci.* **1978**, *65*, 45.
(58) Jönsson, B.; Wennerström, H. *Chem. Scr.* **1980**, *15*, 40.
(59) Guéron, M.; Weisbuch, G. *Biopolymers* **1980**, *19*, 353.
(60) Manning, G. S. *J. Chem. Phys.* **1975**, *62*, 748.
(61) Gustavsson, H.; Lindman, B. *J. Am. Chem. Soc.* **1978**, *100*, 4642.
(62) Rosenholm, J. B.; Lindman, B. *J. Colloid Interface Sci.* **1976**, *57*, 362.

II

Ion binding to polyelectrolytes as described by the Poisson-Boltzmann equation. Comparison with ^{23}Na NMR relaxation experiments

by
GUDMUNDUR GUNNARSSON and HANS GUSTAVSSON
Division of Physical Chemistry 2 and 1
Chemical Centre
P.O.B. 740
S-220 07 Lund 7
Sweden

Abstract

Experimental data on ^{23}Na NMR transverse relaxation rates in aqueous solutions of the sodium salts of poly(acrylic acid) and chondroitin-4-sulfate, at different polymer concentrations, are presented as well as experimental data on ^{23}Na NMR, longitudinal and transverse relaxation rates for poly(acrylic acid) at various degrees of neutralisation. The data are compared with a theory based on the PB equation. The theory is also compared with literature data on ^{23}Na NMR linewidths in Na^{+}-DNA solutions as a function of the concentration of salt containing monovalent or divalent counterions. The comparison between the theory and experiments reveals that the PB theory in all cases satisfactory accounts for the experimental results.

INTRODUCTION

To find an appropriate general description of the interactions between simple ions and polyions is not of great interest, among both chemists and biophysicists. One attempt in this direction is the theory of Manning, which accounts reasonably well for many experimental observations (1). A disadvantage with the theory of Manning is that it assumes that the salt concentration is much higher than the concentration of ionic groups on the polyelectrolyte. The theory of Manning is furthermore limited to linear polyelectrolytes. An alternative theory, not suffering from these limitations, is the Poisson-Boltzmann (PB) equation, first used by Guoy (2) and Chapman (3). In the PB equation one can allow for the dimensions and geometry of the polyelectrolyte and the concentration of the polyelectrolyte can be taken into account through the cell model (4,5). It is interesting to note that the main results of the theory of Manning can be derived from the PB equation in the limit of a line charge at infinite dilution (6,7).

The binding of counterions to polyelectrolytes can be probed by many experimental methods. One such method is NMR where, in favourable cases, the various parameters are sensitive to short range counterion polyelectrolyte interactions (8). In this paper we shall present ^{23}Na NMR relaxation rates for aqueous solutions of poly(acrylic acid) (PA) and chondroitin-4-sulfate (CS). The experimental results at various degrees of neutralisation and polyelectrolyte concentrations are compared with theoretical results from the PB theory. Comparisons are also made between the theory and literature values on Na DNA interactions as measured by ^{23}Na NMR at different concentrations of monovalent and divalent counterions (9).

MATERIALS AND METHODS

The poly(acrylic acid) was used as obtained from the British Drug Houses Ltd., and pure (protein free) chondroitin-4-sulfate was a kind gift from prof. L.A. Fransson, Lund.

The degree of neutralisation, α, is defined as the stochiometric ratio of added NaOH (or HCl) to polyelectrolyte ionizeable groups.

The NMR measurements were performed as described elsewhere (10) on a homebuilt FT spectrometer with a wide-bore Oxford instrument magnet operating at 67.4 MHz and a modified Varian XL-100 spectrometer operating at 26.4 MHz. The excess transverse relaxation rates $R_{2,ex}$ were obtained from high resolution absorption spectra according to

$$R_{2,ex} = \pi(\Delta\nu_{\frac{1}{2},s} - \Delta\nu_{\frac{1}{2},ref}) \qquad (1)$$

where $\Delta\nu_{\frac{1}{2},s}$ and $\Delta\nu_{\frac{1}{2},ref}$ are the line-widths at half height for the sample and the reference, respectively. Longitudinal relaxation rates, R_1, were obtained with the conventional inversion-recovery technique. The reference was an aqueous 0.2 m NaCl solution with the experimentally observed relaxation values $R_{1,ref} = 16.8\ s^{-1}$ and $\Delta\nu_{\frac{1}{2},ref} = 5.9$ Hz.

NMR THEORY AND ION BINDING

In the systems under consideration here the usual fast exchange condition (11) for sodium relaxation is fulfilled (10) and the observed relaxation rate, $R_{i,obsd}$ is therefore given by

$$R_{i,obsd} = p_f R_{i,f} + p_b R_{i,b} \qquad (2)$$

where only the two states of bund and free counterions are considered. p_f and p_b are the fractions of free and bound ions respectively. The intrinsic relaxation rates, R_i, for quadrupolar relaxation of nuclei with spin quantum number I = 3/2 are

$$R_i = \frac{2\pi^2}{5} \chi^2 \tau_c f_i(\omega\tau_c)$$

where the quadrupolar coupling constant, χ, is a measure of the intensity of the interaction, τ_c is the correlation time determined by the dynamics of the interaction. The form of the function, f_i, is determined by whether the equation is for the longitudinal (i = 1) or the transverse relaxation rate (i = 2). The excess relaxation rate, $R_{i,ex}$ is given by

$$R_{i,ex} = R_{i,obsd} - R_{i,f} = p_b(R_{i,b} - R_{i,F}) \qquad (4)$$

Often $R_{i,b}$ is independent of parameters such as polyion and salt concentration and in such cases are changes in $R_{i,ex}$ proportional to changes in p_b. Determination of $R_{i,ex}$ does not however allow for a determination of p_b since $R_{i,b}$ is generally unknown (10).

ION BINDING TO POLYELECTROLYTES AS DESCRIBED BY THE POISSON-BOLTZMANN EQUATION

The polyelectrolytes in this study are modeled as infinite cylinders of radius, r_b, with a smeared out surface charge density, τ. To take the concentration of the polyelectrolyte into account we apply the cell model (4,5) and assign to each polyelectrolyte an electroneutral cylinder of radius r_c containing the counter-ions, added salt and water. The water is modeled as a dielectric continuum of dielectric constant ε_r. The monomer concentration of the polyelectrolyte, c_p is thus

$$c_p = 1/(\pi\, r_c^2\, b_{min}) \qquad (5)$$

where b_{min} is the distance between charges in the fully charged polyelectrolyte. The degree of neutralisation, α, is

$$\alpha = b_{min}/b \qquad (6)$$

where b is the average distance between charges.

A description of the ion distribution around the polyelectrolyte is obtained from a solution of the PB equation. In spite of the approximations inherent in the PB equation it has been shown to give a good description of the ion distribution around polyelectrolytes (13,14,15). In cylindrical symmetry the PB equation is

$$\frac{1}{r}\frac{d}{dr}\left(r\frac{d\psi}{dr}\right) = -\frac{e_o}{\varepsilon_o\varepsilon_r}\sum_i z_i\, c_{io}\, \exp\left(-\frac{z_i e\psi}{KT}\right) \qquad (7)$$

where z_i is the valence of ion i and c_{io} the concentration of ion i at r_c. Here we have assumed that $\psi(r_c) = 0$, which can be done since the absolute value of the electrostatic potential is arbitrary. From the electroneutrality of the cell we have

$$\left.\frac{d\psi}{dr}\right|_{r_c} = 0 \qquad (8)$$

Equation (5) can be solved analytically for an infinite cylindrical polyelectrolyte with counterions only, but without added electrolyte (4, 5). To obtain a solution with added salt one has to resort to numerical methods. The numerical procedure used here is described in ref. (16).

It is not a simple matter to relate the ion distribution, which is obtained from the PB equation, to degrees of ion binding found in experiments. The definition of the degree of ion binding depends on the experimental technique used to probe the ion binding (16). For spectroscopic measurements like ^{23}Na NMR it may be assumed that only ions close to polyelectrolyte charged groups have spectroscopic properties different from those of the bulk solution (17). One can thus define bound ions as those ions which are within a distance Δ from the polyelectrolyte surface, where is typically of the order of 1-5 Å. An alternative definition is to consider ions that are within a given volume, V_b, from each monomer unit is bound. Δ and V_b are related by

$$\Delta = (V_b/\pi b + r_c^2)^{\frac{1}{2}} - r_c \qquad (9)$$

These definitions are of course somewhat ambiguous, but they can be expected to reproduce the trends in ion association, studied by spectroscopic methods, when parameters like polyelectrolyte and salt concentration are varied.

We shall therefore use the following definition of the degree of ion association, β_{sp}, (18).

$$\beta_{sp} = b \int_{r_b}^{r_b+\Delta} C_{+0} \exp(-\frac{e\psi}{KT}) 2\pi r dr \qquad (10)$$

The fraction of bound sodium ions as obtained from the PB equation, p_b^{BP} is therefore

$$p_b^{PB} = \beta_{sp} \alpha \frac{C_p}{c_{Na}} \qquad (11)$$

where c_{Na} is the total Na concentration.

RESULTS AND DISCUSSION

As examples of polyions with variable charge density one may choose polyelectrolytes where the ionizeable group is a rather weakly acidic one, for example as in PA. Here is it necessary to consider H^+ binding to the polyelectrolyte carbocylates as "site-bindning", or phrased differently the protons must bind much stronger to the ionizable groups on the polyelectrolyte than the counterions we want to study, in order to avoid competition effects. Thus with "site binding" of H^+ the charge density can be considered to vary linearly with the degree of neutralisation.

The points in figure 1 show the results of ^{23}Na transverse relaxation rate measurements on the titration of PA with NaOH and of the back-titration of the resulting solution with HCl. Also shown is a theoretical curve obtained from PB theory (eqs. (11) and (4)). In calculating p_b from the PB equation we have assumed that ions within a volume of V_b = 200 $Å^3$ from each monomer unit are bound. To relate the theoretical p_b values to experimentally observed relaxation rates we assume that $R_{i,b}$ in equation (4) is independent of α and multiply the theoretical values with a constant to get the observed relaxation rate at α=1. In figure 2 we show the results from longitudinal relaxation rate measurements on the titration of PA with NaOH. Also shown is a theoretical curve obtained from PB theory in a way similar to that described above. The experimental ratio $R_{1,ex}/R_{2,ex}$ increases slightly at low α indicating an increases in τ_c. It is reasonable to assume that the increase in τ_c has the same origin here as in the case of poly (methacrylic acid) (PM) extensively discussed elsewhere (10). Thus the implication is that a slight coiling

of PA occurs at low charge density. Of course to a much lesser extent than in PM, with its strongly hydrophobic methyl groups. Depending on the degree of coiling, there is a certain risk that neither the model of an extended cylinder (for the PB solutions) nor the line charge model (Manning) apply. Although the small increase in τ_c with decreasing α for PA implies that p_b decrease somewhat faster than $R_{1,ex}$ and $R_{2,ex}$ at low α it certainly can not account for the total excess relaxation in figures 1 and 2 for low α. Therefore the experiments clearly indicate that there is some extent of ion binding to the polymer for low α and that there is no true discontinuity.
The results of PB theory are in agreement with this. This is at variance with a recent conclusion of Manning (19), who states there is no binding of counterions to the polyion for $\alpha < 0.35$.

In figure 3 we show the results fo ^{23}Na transverse relaxation rate experiments on the dilution of PA of three different molecular weights at $\alpha = 1$. Also shown are the results of PB theory obtained as in figure 1. It is seen that the theoretical curve parallels the experimental curves for the lower molecular weight samples whereas a deviation is obtained at low concentration for the high molecular weight sample. The increase in $R_{2,ex}$ at low concentration for the highest molecular weight sample is mainly due to a change in polyion counterion interaction dynamics (a τ_c effect). Similar effects are observed for poly(methacrylic acid) for which τ_c is much more easily determined (10).

In figure 4 we show how $R_{2,ex}$ for ^{23}Na varies with the concentration of chondroitin-4-sulfate (CS). The initial solution was 0.175m in charged groups of CS (α=1) and 0.275 m in Na^+. Theoretical estimates from PB theory are also shown.

From the results in figures 3 and 4 we see that the theory based on the PB equation surprisingly well describes the decrease in β with polyelectrolyte concentration. When comparing experimental values with the theory of Manning it is often assumed that the degree of ion binding is independent of polyelectrolyte concentration. For infinite cylinders one finds from PB theory that β is independent of concentration only at low polyelectrolyte concentrations (16). Comparison between figures 3 and 4 reveals that the relative decrease in $R_{2,ex}$ is larger for CS than that for PA. This is a manifestation of the much lower surface charge density of CS.

Mannings limiting law predicts that β is independent of salt concentration (1). Measurements of $R_{2,ex}$ as a function of c_p/c_{Na} should therefore give a straight line, provided that $R_{2,b}$ is independent of salt concentration. This is indeed found to be the case in many e periments as for example those of Bleam et al. (9) on ^{23}Na NMR linewiths in DNA solutions. To check whether the results from PB theory are consistent with these experiments we calculated p_b as a function of c_p/c_{Na} for DNA at two different concentrations. The results are shown in figure 5 for two different values of Δ, Δ =3Å and Δ = 7Å. The experiments of Bleam et al. were performed in the range $0 < c_p/c_{Na} < 0.6$. The deviation of the theoretical curves from a straight line is not large in this range, whichever value of Δ is chosen, and probably not large enough to be observable in experiments. The difference between the curves for different DNA concentrations is likevise not large enough to be obserable in experiments. We see thus that theoretical calculations based on the PB equation are also consistent with the experiments of Bleam et al. (9).

Bleam et al. (9) have also with ^{23}Na NMR performed masurements on the competition between Na^+ and Mg^{2+}.

In figure 6 we plot the experimental results of Bleam et al. (9) and calculated curves that follow from PB theory, one with $\Delta = 3$ Å and the other with $\Delta = 7$ Å. All the theoretical curves have been made to coincide with the experimental ones at zero Mg^{2+} concentration. It is seen that PB theory satisfactory accounts for the experimental results and that the results are not very sensitive to the value of Δ.

Rose et al. (20) have from ^{25}Mg NMR measurements in DNA solutions drawn the conclusion that site binding of Mg^{2+} dominates the appearance of the spectrum. On the other hand is it possible to rationalize the experimental data in figure 6 without any assumption about site binding.

CONCLUSIONS

Comparison between the results of ^{23}Na NMR measurements and the theory based on the PB equation shows that PB theory in all cases is in satisfactory agreement with experiments. The work reported in this paper thus supports the conclusion of Stigter (21) that the PB equation can be viewed as a second member in a hierarchy of theories where the theory of Manning is the first and the more approximative one.

It is interesting to see that it is not necessary to introduce any site binding effects in order to explain the results of the experiments considered above. The overall ion binding behaviour in these systems is thus determined by long range electrostatic effects and site binding is thus only a secondary effect.

REFERENCES

1) G.S. Manning, Accs.Chem.Res., 12, 443, 1979.

2) G. Gouy, J.Phys.Radium, 9, 457, 1910.

3) D.L. Chapman, Phil.Mag., 25, 475, 1913.

4) R. Fuoss, A. Katchalsky and S. Lifson, Proc.Natl.Acad.Sci., U.S.A., 37, 579, 1951.

5) T. Alfrey, P.W. Berg and H. Morawetz, J.Polymer Sci., 7, 543, 1951.

6) A.D. MacGillivray, J.Chem.Phys., 56, 83, 1972.

7) R.W. Wilson, D.C. Rau and V.A. Bloomfield, Biophys.J., 30, 317, 1980.

8) S. Forsén and B. Lindman, in "Methods of Biochemical Analysis", vol.27, p. 289, 1981, ed. D. Glick, John Wiley, New York.

9) M.L. Bleam, C.F. Andersson and M.T. Record, Jr., Proc.Natl.Acad.Sci. U.S.A., 77, 3085, 1980.

10) H. Gustavsson, B. Lindman and T. Bull, J.Amer.Chem.Soc., 100, 4655, 1978.

11) T. Bull, J.Magn. Res., 8, 344, 1972.

12) A. Abragam, "The Principles of Nuclear Magnetism", Oxford University Press, Oxford, 1961.

13) B. Jönsson, H. Wennerström and B. Halle, J.Phys.Chem., 84, 2179, 1980.

14) W. van Megen and I. Snook, J.Chem.Phys., 73, 4656, 1980.

15) P. Linse, G. Gunnarsson and B. Jönsson, to be published.

16) G. Gunnarsson, B. Jönsson and H. Wennerström, J.Phys.Chem., 84, 3114, 198

17) H. Wennerström, B. Lindman, G. Lindblom and G.J.T. Tiddy, J.Chem.Soc., Faraday Trans I, 75, 663, 1979.

18) S. Engström and H. Wennerström, J.Phys.Chem., 82, 2711, 1978.

19) G.S. Manning, J.Phys.Chem., 85, 870, 1981.

20) D.M. Rose, M.L. Bleam, M.T. Record, Jr. and R.G. Bryant, Proc. Natl.Acad.Sci., U.S.A., 77, 6289, 1980.

21) D. Stigter, J.Phys.Chem., 82, 1603, 1978 ; G.S. Manning has commented on this ref. in J.Phys.Chem., 82, 2349, 1978.

FIGURE CAPTIONS

Figure 1. ^{23}Na excess transvers relaxation rates, $R_{2,ex}$, at 67.4 MHz, as a function of the stochiometric degree of neutralisation, α. The circles were obtained from measurements in which 0.095 M aqueous polyacrylic acid was titrated with 1.0M NaOH and the filled points were obtained from measurements in which the solution that was obtained in the above mentioned experiment was titrated with 1 M HCl. The theoretical curves were obtained from eqs. (11) and (4) by using $R_{2,b} - R_{2,F} = 165.3\ s^{-1}$ $V_b = 200\ Å^3$, $R_b = 3$ Å, $b_{min} = 2.5$ Å. $\varepsilon = 78.3$, $t = 25^oC$, $M_w = 250\ 000$.

Figure 2. ^{23}Na excess longitudinal relaxation rates, $R_{1,ex}$, at 67.4 MHz, as a function of the stochiometric degree of neutralisation, α. The circlus were obtained from experimetns as described in Figure 1. The theoretical curve from P-B theory was obtained by letting the theoretical and experimental curves coincide at $\alpha = 1$. Parameters as in Figure 1.

Figure 3. ^{23}Na excess transverse relaxation rates, R_{2ex}, at 67.4 Hz as a function of the concentration of monomer units in polyacrylic acid, cp, for polymers of three different molecular weights. The points are from experiments and the curve is a theoretical one obtained from eq. (4) and (11). Parameters as in Figure 1. $\alpha = 1$.

Figure 4. ^{23}Na excess transverse relaxation rates, $R_{2,ex}$, at 26.5 MHz, as a function of the total concentration of ionic charges in chondroitin-4-sulfate, c_p.The points are from experiments and the curve is a theoretical one obtained from eqs. (11) and (4) using $R_{2,b} - R_{2,f} = 259\ s^{-1}$. $R_b = 5$ Å, $\Delta = 1$ Å, $c_p/c_{Na} = 0.64$, $t = 25^oC$.

Figure 5. Theoretical values of the fraction of bound counterions as obtained from PB theory, P_b^{PB}, vs. c_p/c_{Na} at two different DNA concentrations, 2mM (- - -) and 15 mM (———). R_b = 10 Å, b_{min} = 1.7 Å t = 25°C.

Figure 6. ^{23}Na excess linewidths, $\Delta\nu_{ex} = R_{2ex}/\pi$, at 24.5 MHz as a function of the Mg^{2+} concentration for a 15 mM NaDNA solution. The total concentration of Na^+ is 23.8 mM. The circles are from the experiments of Bleam et al. (9).

The curves are obtained from eqs. (11) and (4) using $\Delta\nu_b - \Delta\nu_f = 121.5\ s^{-1}$.

For Δ = 3Å (———) and $\Delta\nu_b - \Delta\nu_f = 86.3\ s^{-1}$

For Δ = 7Å. Parameters as in Figure 5.

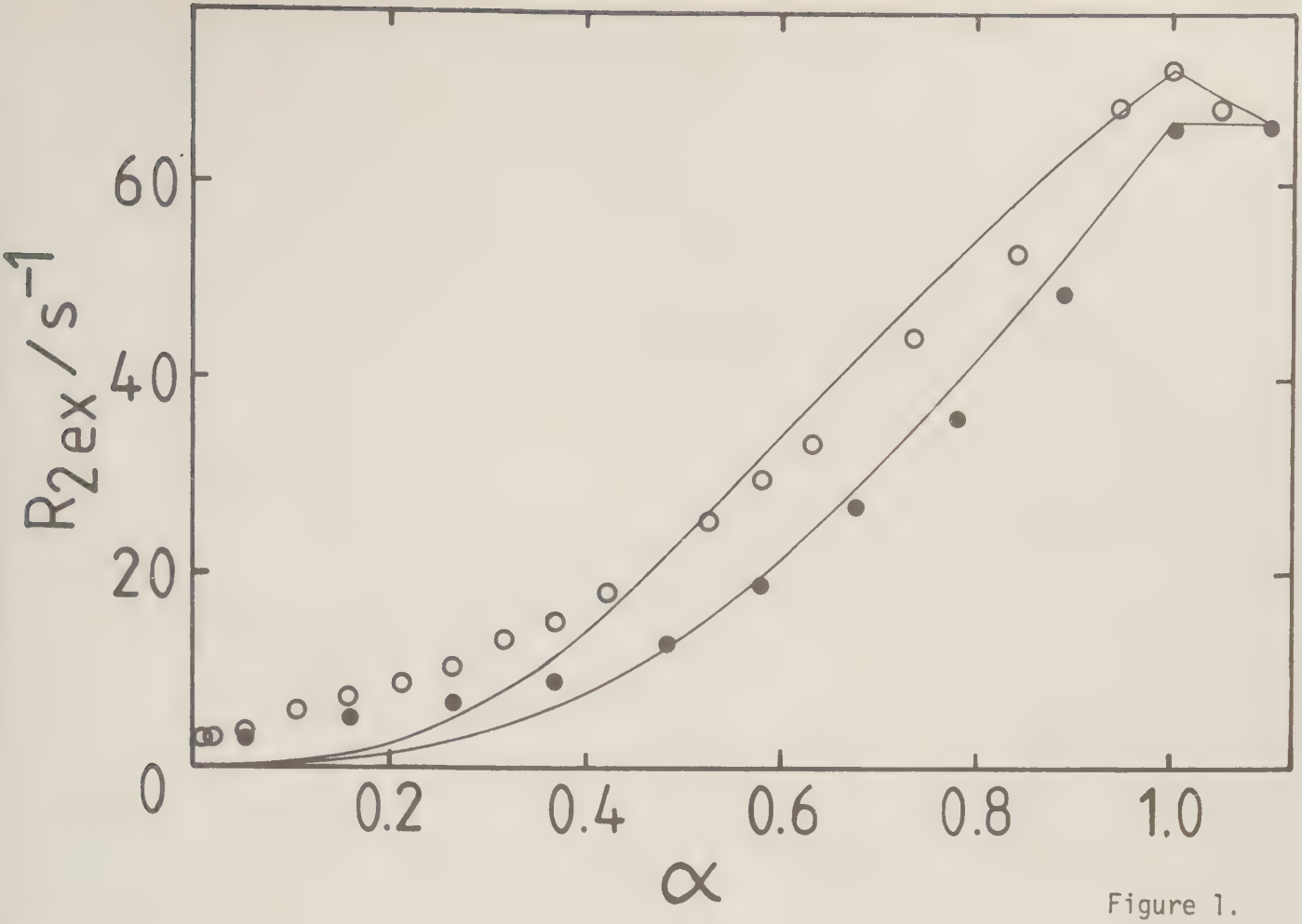

Figure 1.

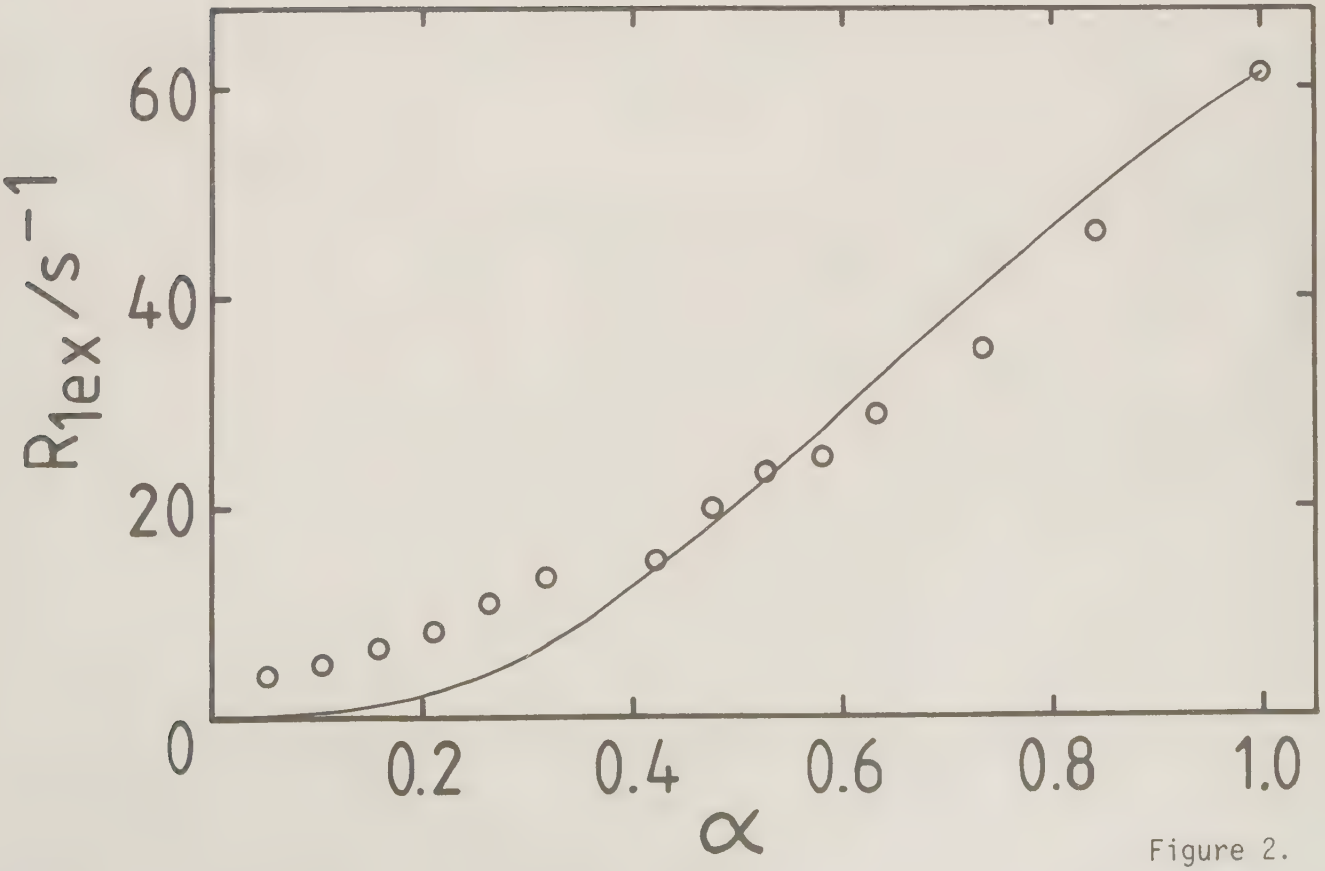

Figure 2.

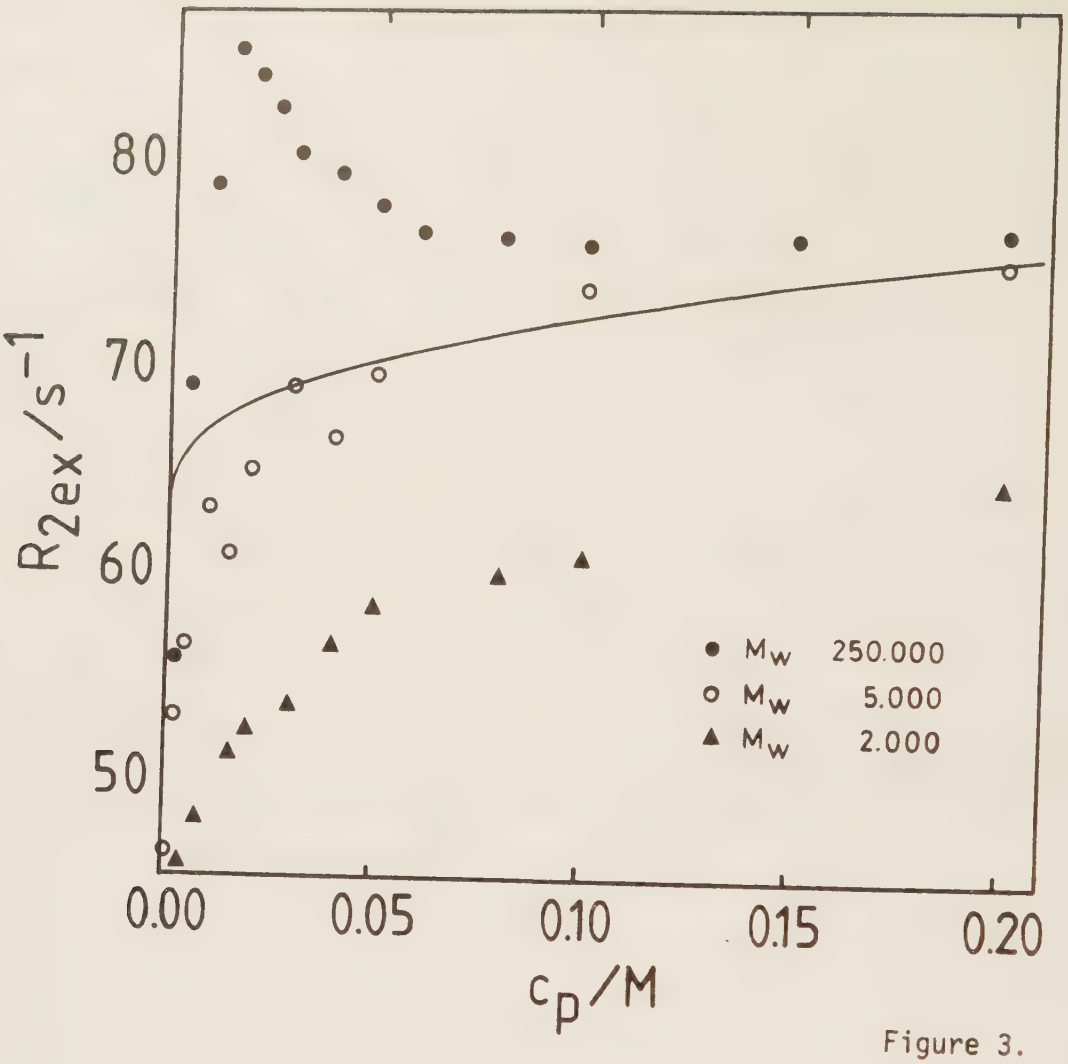

Figure 3.

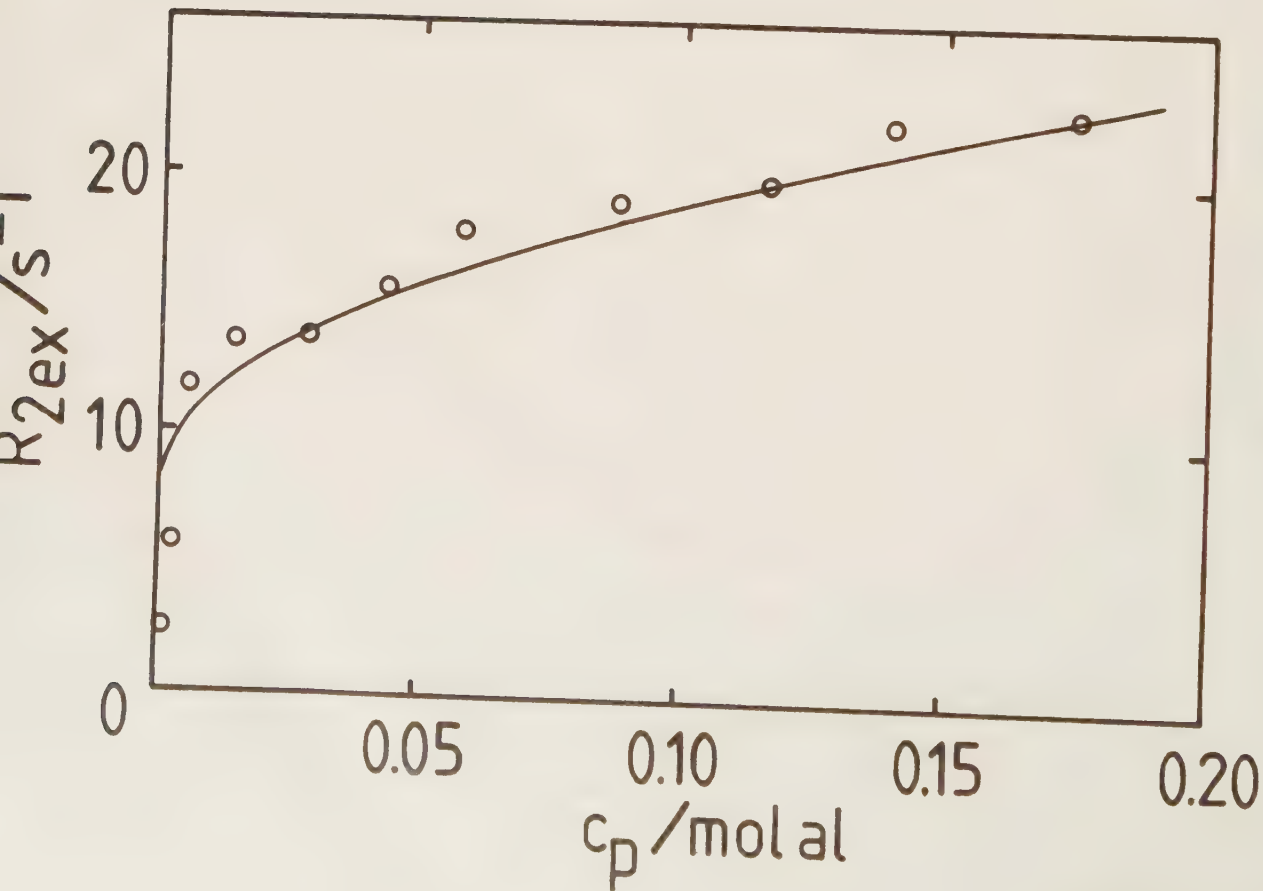

Figure 4.

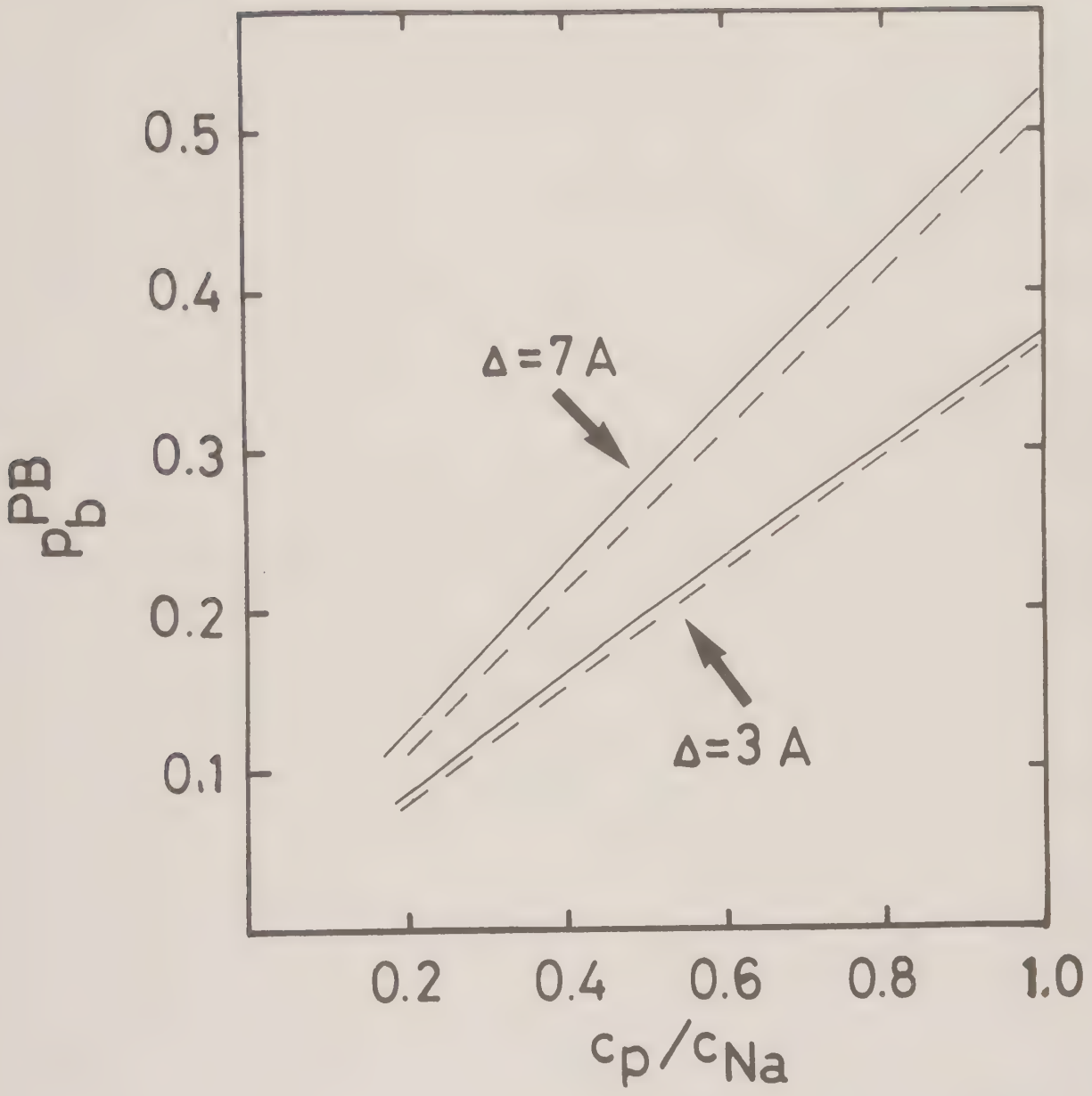

Figure 5.

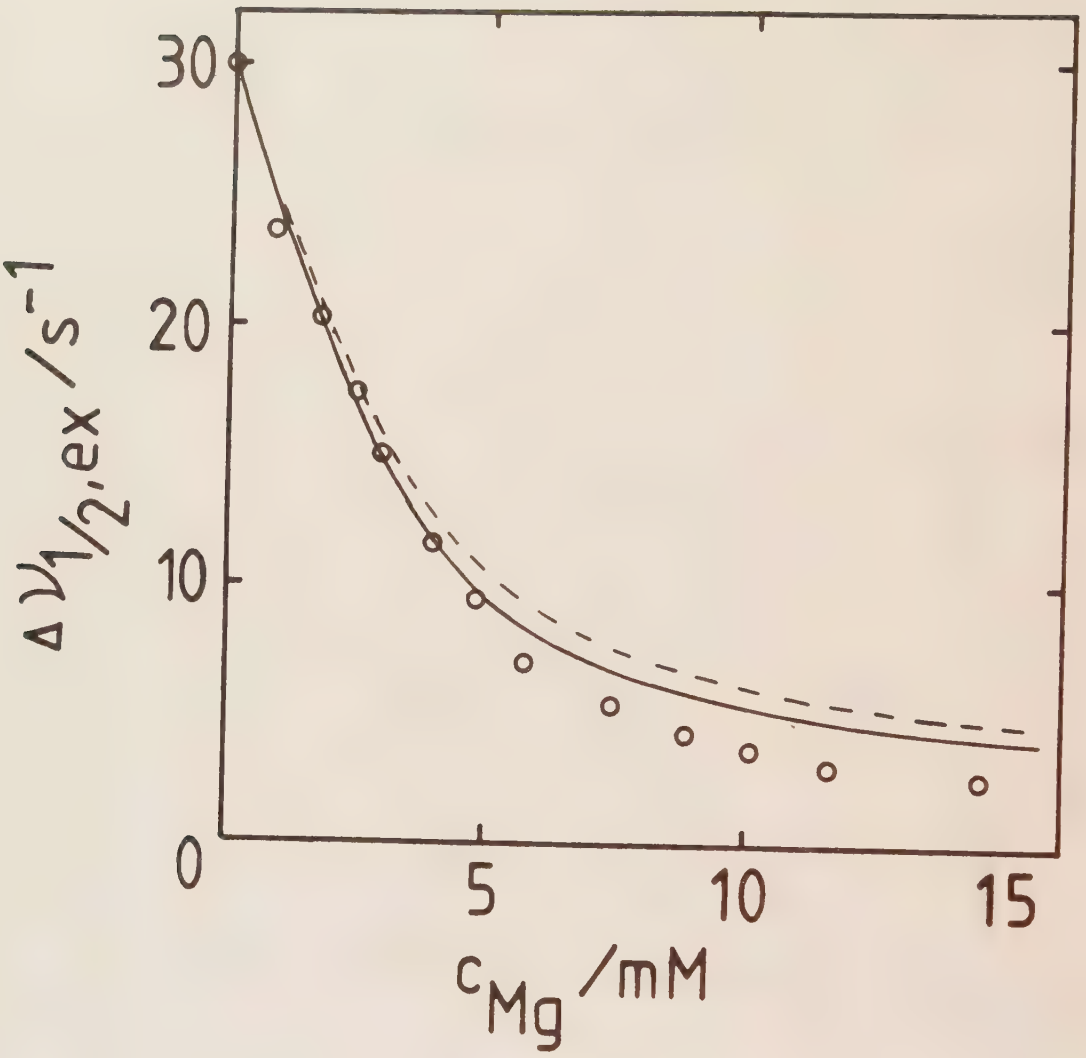

Figure 6.

III

J.C.S. Faraday I, 1980, 76, 1287–1295

Enthalpies of Proton Dissociation of Poly(Acrylic Acid)

Comparison Between Experiment and Theory for a Polyelectrolyte System

By Guðmundur Gunnarsson* and Håkan Wennerström*

Department of Physical Chemistry 2, Chemical Center,
University of Lund, P.O.B. 740, S-220 07 Lund, Sweden

and

Gerd Olofsson and Anatolei Zacharov†

Thermochemistry Laboratory, Chemical Center, University of Lund,
P.O.B. 740, S-220 07 Lund, Sweden

Received 30*th July*, 1979

Enthalpies of proton dissociation ΔH_a of poly(acrylic acid) at three different temperatures have been determined as a function of the degree of dissociation α. Despite the apparent increase in pK_a with increasing α, the enthalpy of proton dissociation decreases with increasing α, reaching an almost constant value around $\alpha = 0.3$, which possibly reflects that above this value of α ion condensation behaviour applies.

The experimental values are compared with a theoretical calculation of ΔH_a based on a solution of the Poisson–Boltzmann equation. The model correctly predicts that ΔH_a decreases with increasing α and the calculated ΔH_a is of the right order of magnitude and shows the correct α-dependence. The decrease in ΔH_a with increasing polyion charge is coupled with the anomalous temperature dependence of the dielectric permittivity of water.

The recent renewed interest in polyelectrolyte systems stems partly from the finding that electrostatic theories give a surprisingly accurate and simple description of a number of properties related to counterion distribution. The concept of counterion condensation has turned out to be fruitful.[1-5] However, most experimental tests are related to properties of the free energy. Due to the simplifying assumptions in the theories one might suspect that their success could be due in part to a cancellation of errors, giving a type of enthalpy–entropy compensation. If this is the case such a cancellation might not occur in the separate enthalpies or entropies. Thus an investigation of enthalpy changes associated with ionic processes in polyelectrolyte systems should provide a basis for a stronger test of the electrostatic theories.

Škerjanc *et al.*[6-9] studied enthalpies of dilution of synthetic polyelectrolyte systems and showed that the Poisson–Boltzmann equation, applied to the cylindrical cell model, gave a qualitative rationalization of the experimental results. Crescenzi *et al.*[10, 11] measured enthalpies of proton dissociation for a number of polycarboxylic acids at 25 °C. A comparison with electrostatic theories was also made. From measurements of enthalpies of mixing of polyelectrolyte and simple electrolyte solutions, Boyd *et al.*[12] concluded that the additivity rule [13] does not apply to enthalpies of mixing but that the infinite line charge model [14] gave predictions consistent with the experimental results. In the present paper we report experimental determinations of enthalpies of proton dissociation, ΔH_a, of poly(acrylic acid) as a function

† On leave from Chemical-Technological Institute of Ivanovo, Ivanovo, U.S.S.R.

of the degree of ionization α at three different temperatures and at constant counterion concentration. The experimental results are compared with theoretical calculations of the α-dependence of ΔH_a and a molecular interpretation is attempted.

EXPERIMENTAL

Solid poly(acrylic acid) [—$CH_2CH(COOH)$—]$_n$ (Aldrich-Europe) with an average molecular weight of 250 000, showing a glass transition temperature T_g = 106 °C, was used without further treatment. The purity was checked by acidimetric titration and was better than 97.0±0.5 wt %.

The sodium polyacrylate+poly(acrylic acid) (NaPA+PAH) solutions were prepared by neutralizing a stock solution of PAH with aqueous NaOH to the desired degree of neutralization α; solid NaCl and water was then added to give solutions containing 0.05 mol kg^{-1} of Na^+ and 0.05 monomol kg^{-1} of (PAH-PA^-). (Polymer concentrations are expressed as monomol kg^{-1} of carboxyl and carboxylate groups.) Solutions were prepared with $\alpha[= m_{PA}/(m_{PA}+m_{PAH})]$ = 0.10, 0.20, 0.30, 0.40, 0.60 and 0.80 with an uncertainty in α of < 0.005.

The molality of the HCl solution used was found from acidimetric titrations to be 0.5101±0.0004 mol kg^{-1}. Good quality demineralized water was used to prepare all solutions.

The calorimetric measurements were performed using an LKB-8721 reaction–solution calorimeter with a 100 cm^3 glass reaction vessel. The experiments were performed and evaluated as described in ref. (15).

RESULTS

In the calorimetric measurements 0.4×10^{-3} mol HCl (0.8 g of a 0.5 mol kg^{-1} solution) was added to 100.7 cm^3 of a solution containing $0.05\alpha_1$ mol kg^{-1} NaPA + $0.05(1-\alpha_1)$ mol kg^{-1} PAH + $0.05(1-\alpha_1)$ mol kg^{-1} NaCl. The measured enthalpy changes ΔH_{obs} are summarized in table 1, where α_1 and α_2 denote the degree of dissociation in the initial and final solutions, respectively.

TABLE 1.—OBSERVED ENTHALPY CHANGES ΔH_{obs} FOR THE ADDITION OF 0.8 g OF 0.5 mol kg^{-1} HCl TO 100.7 cm^3 SOLUTION CONTAINING $0.05\alpha_1$ mol kg^{-1} NaPA+$0.05(1-\alpha_1)$ mol kg^{-1} PAH+0.05 $(1-\alpha_1)$ mol kg^{-1} NaCl

		ΔH_{obs}/kJ mol^{-1}		
α_1	α_2	2.85 °C	25.12 °C	50.17 °C
0.10	0.04	−2.79	−0.46	1.93
0.20	0.12	−1.86	0.98	3.64
0.30	0.22	−0.34	2.11	4.67
0.40	0.32	0.27	2.75	5.01
0.60	0.52	0.73	3.20	5.46
0.80	0.72	1.12	3.48	5.79

The pH of the initial and final solutions was measured and the amount of HCl not reacting with the polyacrylate ion was estimated. Only at the two lowest values of α was the amount of free HCl significant, ≈ 20 % in experiments with α_1 = 0.10 and ≈ 2 % with α_1 = 0.20. The values of ΔH_a shown in table 2 have been corrected for this effect.

The observed enthalpy changes are the sum of the enthalpy of protonation of polyacrylate ion and the enthalpy of dilution of HCl. The best strategy for deriving

a useful and well-defined protonation enthalpy is to evaluate the enthalpy change ΔH_1 for the process

$$\begin{aligned}\mathrm{HCl(aq)} + 12.6\{[\alpha\mathrm{NaPA} + (1-\alpha)\mathrm{PAH} + (1-\alpha)\mathrm{NaCl}] \,.\, 1100\ \mathrm{H_2O}\} \rightarrow \\ 12.6\{[(\alpha - 1/12.6)\ \mathrm{NaPA} + (13.6/12.6-\alpha)\mathrm{PAH} + \\ (13.6/12.6-\alpha)\mathrm{NaCl}] \,.\, 1100\ \mathrm{H_2O}\};\quad \Delta H = \Delta H_1 \end{aligned} \tag{1}$$

where $\alpha = \alpha_1$ in our experiments.

We then have

$$\Delta H_1 = \Delta H_{\mathrm{obs}} - \Delta H_{\mathrm{dilln}}(\mathrm{HCl}) \tag{2}$$

where $\Delta H_{\mathrm{dilln}}(\mathrm{HCl})$ denotes the enthalpy change for the infinite dilution of 0.51 mol kg^{-1} HCl. Values of $\Delta H_{\mathrm{dilln}}(\mathrm{HCl})$ were calculated from results of previous calorimetric measurements on dilution of HCl from 0.51 to 0.005 mol kg^{-1} [15] and from enthalpies of dilution and apparent molar heat capacities reported by Parker [16] as −0.852, −1.176 and −1.601 kJ mol^{-1} at 2.85, 25.00 and 50.17 °C, respectively.

TABLE 2.—DIFFERENTIAL ENTHALPIES OF DISSOCIATION ΔH_a OF POLY(ACRYLIC ACID) AT VARIOUS DEGREES OF DISSOCIATION AND TOTAL PAH CONCENTRATION OF 0.05 monomol kg^{-1} AND Na^+ ION CONCENTRATION OF 0.05 mol kg^{-1}

$\bar{\alpha}$ \ T/°C	ΔH_a^a/kJ mol^{-1} 3.00	25.00	50.00
0.07	2.45	−0.86	−4.26
0.16	1.01	−2.19	−5.32
0.26	−0.54	−3.29	−6.28
0.36	−1.14	−3.91	−6.65
0.56	−1.60	−4.37	−7.05
0.76	−1.99	−4.64	−7.37

[a] Experimental uncertainty in ΔH_a is ± 0.09 kJ mol^{-1} expressed as twice the overall standard deviation of the mean.

A discussion of the enthalpy of proton dissociation $\Delta H_a = -\Delta H_1$ expressed in kJ $(molH^+)^{-1}$ follows.

The dissociation reaction can be written in a simplified form as

$$\begin{aligned}\frac{1}{n}[(1-\alpha_2)\mathrm{PAH} + \alpha_2\mathrm{PA^-}]_n + (1-\alpha_2)\mathrm{Cl^-} \rightarrow \frac{1}{n}[(1-\alpha_1)\mathrm{PAH} + \alpha_1\mathrm{PA^-}]_n + \\ (1-\alpha_1)\mathrm{Cl^-} + (\alpha_2-\alpha_1)\mathrm{HCl(aq)};\quad \Delta H = \Delta H_a(\alpha_2-\alpha_1). \end{aligned} \tag{3}$$

The enthalpy change ΔH_a thus approaches the differential enthalpy of proton dissociation as α_2 approaches α_1. In our experiments the change in the degree of dissociation $(\alpha_2-\alpha_1)$ is 0.08 except at $\alpha_1 = 0.10$ where it is 0.06. The values of ΔH_a thus found are summarized in table 2. The mean degree of dissociation $\bar{\alpha} = (\alpha_2+\alpha_1)/2$ is shown in the first column and values of ΔH_a at the three indicated temperatures are given in columns two to four. Values of the average heat capacity changes $\Delta C_{p,a}$ at the mean temperatures $\bar{T} = (T_1+T_2)/2$ and various degrees of dissociation are shown in table 3.

TABLE 3.—DIFFERENTIAL HEAT CAPACITY CHANGES $\Delta C_{p,a}$ OF PROTON DISSOCIATION OF POLY(ACRYLIC ACID) AT VARIOUS DEGREES OF DISSOCIATION AND TOTAL PAH CONCENTRATION OF 0.05 monomol kg^{-1} AND Na^+ ION CONCENTRATION OF 0.05 mol kg^{-1}

$\bar{\alpha}$ / $\bar{T}$/°C	$\Delta C^{a}_{p,a}$/J K^{-1} mol^{-1}					
	0.07	0.16	0.26	0.36	0.56	0.76
14.0	−150	−146	−125	−126	−126	−120
37.5	−136	−125	−120	−110	−107	−109

[a] Estimated uncertainty in $\Delta C_{p,a}$ is ± 5 J K^{-1} monomol^{-1} (*cf.* footnote to table 2).

To illustrate the α-dependence, values of ΔH_a at the three temperatures are plotted against α in fig. 1. The dissociation enthalpies decrease rapidly as α increase up to ≈ 0.3. The decrease is most pronounced at 3 °C, amounting to −3.0 kJ mol^{-1} for an increase in α from 0.07 to 0.26, the corresponding change being −2.0 kJ mol^{-1} at 50 °C. At higher α, ΔH_a changes only slightly the decrease being ≈ −0.8 kJ mol^{-1} for an increase in α from 0.36 to 0.76 at all three temperatures.

Values of $\Delta C_{p,a}$ observed at the lowest α values are close to those found for monocarboxylic acids.[17] At higher α, $\Delta C_{p,a}$ is less negative and becomes constant above α ≈ 0.3-0.4.

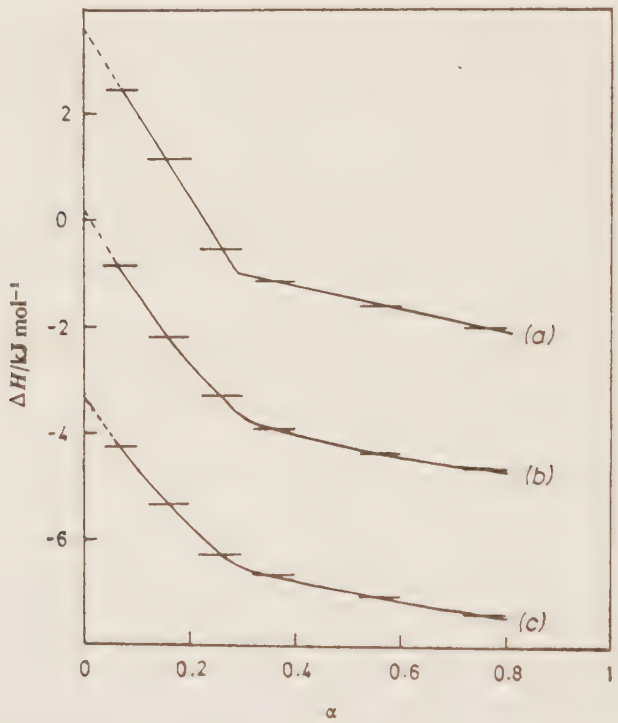

FIG. 1.—Enthalpy of dissociation of poly(acrylic acid) at various degrees of dissociation and Na^+ ion concentration of 0.05 mol kg^{-1}. The total concentration of poly(acrylic acid) was 0.05 monomol kg^{-1}. (*a*) 3, (*b*) 25 and (*c*) 50 °C.

While ΔH_a decreases with increasing α, the apparent pK_a increases and the acid becomes weaker. Thus the enthalpy and the free energy change in opposite senses with changes in α. This applies to the dissociation of poly(acrylic acid) in pure water [10] as well as in dilute NaCl solution (as observed in the present study).

It is not possible to compare the present results at 25 °C with those of Crescenzi *et al.*[10] in quantitative terms because of the different experimental procedures. We have chosen to keep the sodium ion concentration constant, while the measurements of ref. (10) were performed with no added simple salt or with a constant concentration of 0.5 mol kg^{-1} NaCl. Nevertheless, both series of measurement show that ΔH_a decreases with increasing α and that the largest changes occur in the region $0 < \alpha < 0.3$. Furthermore, the enthalpy changes are largest in the absence of a simple electrolyte.

ELECTROSTATIC MODEL

The most straightforward model of a straight chain polymer polyelectrolyte is that of a (infinite) cylinder with a smeared-out charge.[2, 14, 18-20] Within this model a polyelectrolyte at finite concentration can be simulated using the cell model so that the polymer cylinder, radius r_c, is surrounded by an additional cylinder, radius r_f, containing the aqueous dielectric medium, the counterions and added salt. The value of r_f is chosen to give the correct overall concentration of the polymer. The Poisson–Boltzmann equation can be applied to this system and for cylindrical symmetry it takes the form

$$\varepsilon_r\varepsilon_0 \frac{1}{r}\frac{d}{dr}\left(r\frac{d\Phi}{dr}\right) = -\rho = -e\sum_i z_i C_i(r) = -e\sum_i z_i C_{i0}\exp(-z_i\Phi/kT) \tag{4}$$

where the sum extends over the different ionic species i in the solution. ε_r is the relative permittivity, ε_0 the permittivity of a vacuum, Φ the electrostatic potential, ρ the charge density, z_i the valency of ion i, $C_i(r)$ its local concentration and C_{i0} a constant determined by $\Phi(r)$ and the total concentration of the ion i. Eqn (4) has been solved numerically for the relevant boundary conditions determined by the experimental conditions in the calorimetric measurements. For further details of the numerical procedure see ref. (21).

The free energy per unit volume V associated with the electrostatic interactions can be divided into one part associated with the electrical field (for an electroneutral system)

$$G_f = \frac{1}{2}\frac{\varepsilon_r\varepsilon_0}{V}\int_V (\nabla\Phi)^2\,dV \tag{5}$$

and one part, G_{mix}, due to the entropy of the counterion distribution

$$G_{mix} = -\frac{TS_{mix}}{V} = \frac{kT}{V}\sum_i [\int_V C_i(\ln C_i - 1)\,dV - n_i(\ln \bar{C}_i - 1)] \tag{6}$$

where $\bar{C}_i$ is the mean concentration of ion i. The total free energy is [22]

$$G_{el} = G_f + G_{mix}. \tag{7}$$

In eqn (5)-(7) volume changes have been neglected so that Helmholtz' and Gibbs' free energies are equivalent. The free energy can also be determined *via* a charging procedure. However, within the approximations made above, the result is equivalent [22] to eqn (4)-(6) and, in the present case, involves more elaborate calculations which are less susceptible to a molecular interpretation.

From a knowledge of G_{el} the electrostatic contribution to the enthalpy can be calculated using the Gibbs–Helmholtz equation. This gives (see Appendix)

$$H_{el} = \frac{1}{2}\frac{\varepsilon_0}{V}\left(\varepsilon_r + T\frac{\partial \varepsilon_r}{\partial T}\right)\int_V (\nabla\Phi)^2\, dV = G_f\left(1 + \frac{T}{\varepsilon_r}\frac{\partial \varepsilon_r}{\partial T}\right). \quad (8)$$

When ε_r is temperature independent, $G_f = H_{el}$, while G_f in general contains both enthalpy and entropy contributions. The relative magnitude of enthalpy and entropy contributions is constant for a given medium at a given temperature and is thus independent of the particular nature of the polyelectrolyte.

COMPARISON BETWEEN THEORETICAL AND EXPERIMENTALLY DETERMINED ENTHALPIES

The experimentally determined enthalpy changes can be divided into two parts: ΔH_s(mon) equal to the proton dissociation of an isolated carboxyl group and ΔH_{el} arising from the interactions with other ionic groups on the polyelectrolyte and with

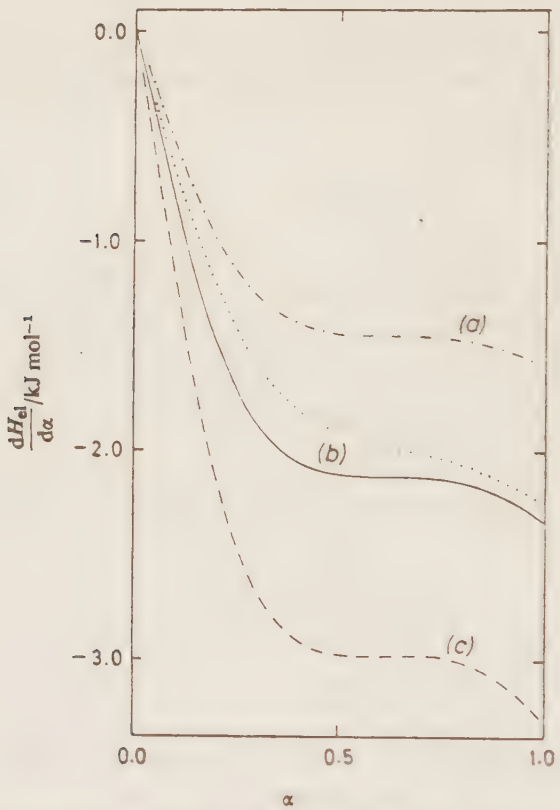

FIG. 2.—Calculated $\partial H_{el}/\partial\alpha$ as a function of α for poly(acrylic acid). The radius of the cylinder, r_c, was taken as 2 Å except for (. . . .) where it was taken as 3 Å. The distance between charges was taken as 2.5 Å. The radius of the outer cylinder, r_f, was adjusted to make the poly(acrylic acid) concentration the same as in fig. 1. The salt concentration was as in fig. 1. Values of ε_r were taken from C. G. Malmberg and A. A. Maryott, *J. Res. Nat. Bur. Stand.*, 1956, **56**, 1. (*a*) 3, (*b*) 25 and (*c*) 50 °C.

the counterions. The enthalpy (per mol of monomer) can thus be written [*cf.* reaction (3)] as

$$\Delta H_a = \Delta H_a(\text{mon}) + (\alpha_2 - \alpha_1)^{-1}[H_{el}(\alpha_2) - H_{el}(\alpha_1)] \approx \Delta H_a(\text{mon}) + \frac{\partial H_{el}}{\partial \alpha}. \quad (9)$$

Here only the second term is α-dependent. Furthermore, $\partial H_{el}/\partial\alpha|_{\alpha=0} = 0$ so that $\Delta H_a(\alpha \to 0)$ should approach the value relevant for the monomer.

From the solutions of the Poisson–Boltzmann equation the derivative $\partial H_{el}/\partial\alpha$ has been calculated as a function of α using eqn (8) for the three different temperatures. The results are shown in fig. 2. A comparison with the experimental results presented in fig. 1 reveals that: (*a*) Both experimental and theoretical values of $\partial H_{el}/\partial\alpha$ are negative. (*b*) The theoretical model predicts a qualitatively correct α-dependence of $\partial H_{el}/\partial\alpha$ with a sharp kink in the curve around $\alpha \approx 0.3$ which corresponds to the critical charge density for which the ion condensation behaviour is supposed to appear.[2] (*c*) There is no quantitative agreement, although the order of magnitude of the enthalpy values are correct showing that the main contribution to G_{el} is entropic. (*d*) The predicted temperature dependence of $\partial H_{el}/\partial\alpha$ appears to be qualitatively incorrect. This might reflect problems associated with the polymer conformation which, particularly at low α, should also locally deviate from a straight chain.

In summary, the electrostatic model provides an important insight into the behaviour of the enthalpies of proton dissociation; in particular it gives an explanation of the unexpected sign of $\partial H_{el}/\partial\alpha$. However, some features remain unexplained, in particular the temperature dependence of $\partial H_{el}/\partial\alpha$.

MOLECULAR INTERPRETATION

On the basis of eqn (5)-(8) it is possible to obtain some insight into the different molecular contributions to the enthalpy and free energy changes. For a dielectric medium in which only the electronic polarization contributes to ε_r, so that ε_r is temperature independent, G_f in eqn (5) is purely an enthalpy. For a solvent consisting of simple dipoles ε_r is, to a good approximation, inversely proportional to T and

$$1 + \frac{T}{\varepsilon_r}\frac{\partial \varepsilon_r}{\partial T} = 0$$

so that G_f is purely an entropy. In this case the sum of the ion–solvent, the solvent–solvent and the ion–ion interaction energies are constant independent of the distance between the ions and the only varying contribution to G_f is the entropy due to the orientation of the solvent dipoles. One of the many intriguing consequences of the strong structure formation in water is that the effective water–water repulsion between oriented water molecules is less than that in a simple dipolar fluid, resulting in an anomalous temperature dependence of ε_r so that

$$1 + \frac{T}{\varepsilon_r}\frac{\partial \varepsilon_r}{\partial T} < -1.$$

Consequently, when H_{el} is negative G_f is always positive: when G_f increases H_{el} decreases and *vice versa*. This would then be the molecular interpretation of the finding that ΔH_a decreases with increasing α, in spite of the fact that ΔG_a increases, as demonstrated by the increase in the apparent pK_a of the carboxylic acids.

A continuum model of the aqueous medium cannot be strictly applied down to distances of a typical molecular dimension. As an example of this difficulty, fig. 3 illustrates how different volume elements contribute to the integral determining the

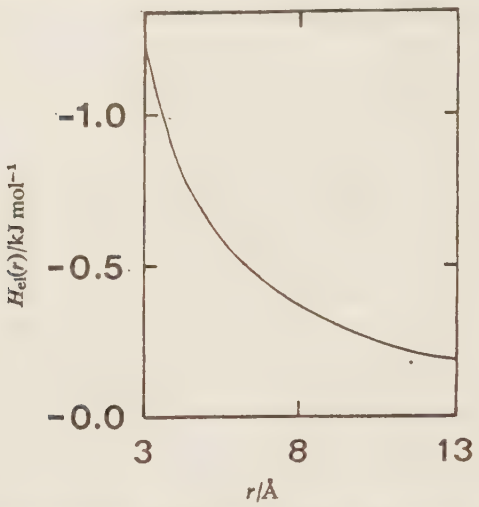

FIG. 3.—Contribution to the enthalpy H_{el} from the different regions in the polyelectrolyte system. The figure shows the value of the integral

$$H'_{el}(r) = \left(1+\frac{T\partial\varepsilon_r}{\varepsilon_r\partial T}\right)\pi\varepsilon_r\varepsilon_0\int_r^n\left(\frac{d\Phi}{dr}\right)^2 r\,dr$$

as a function of the lower limit of integration. At r_c, $H'_{el}(r_c) = H_{el}$; $r_c = 3$ Å, $T = 25$ °C and $\alpha = 0.8$. Other parameters as in fig. 2.

enthalpy in eqn (8). Nearly half of the enthalpy has its origin at distances < 3 Å from the polyelectrolyte cylinder. Nevertheless, a quantitative analysis of the electrostatic effects in polyelectrolyte solutions, based on a continuum model of water, seems to provide important insight into enthalpy changes in the system.

APPENDIX

DERIVATION OF EQN (8)

Combining eqn (6) and (7) one has

$$H_{el} = G_{el} - T\frac{\partial G_{el}}{\partial T} = G_f - T\frac{\partial G_f}{\partial T} + \frac{T^2}{V}\frac{\partial S_{mix}}{\partial T}. \tag{A1}$$

The derivatives on the right hand side can be evaluated explicitly from eqn (5) and (6)

$$\frac{\partial G_f}{\partial T} = \frac{\varepsilon_0}{2V}\frac{\partial\varepsilon_r}{\partial T}\int(\nabla\Phi)^2\,dV + \frac{\varepsilon_r\varepsilon_0}{V}\int\nabla\Phi\cdot\frac{\partial}{\partial T}(\nabla\Phi)\,dV \tag{A2}$$

and

$$\begin{aligned}\frac{\partial S_{mix}}{\partial T} &= -k\sum_i\int\frac{\partial C_i}{\partial T}\ln C_i\,dV = k\sum_i\int\frac{\partial C_i}{\partial T}\frac{z_i e\Phi}{kT}\,dV \\ &= \frac{1}{T}\int\frac{\partial\rho}{\partial T}\Phi\,dV = -\frac{1}{T}\varepsilon_0\frac{\partial\varepsilon_r}{\partial T}\int\nabla^2\Phi\cdot\Phi\,dV - \frac{\varepsilon_r\varepsilon_0}{T}\int\frac{\partial}{\partial T}(\nabla^2\Phi)\Phi\,dV \\ &= \frac{\varepsilon_0}{T}\frac{\partial\varepsilon_r}{\partial T}\int(\nabla\Phi)^2\,dV + \frac{\varepsilon_0}{T}\varepsilon_r\int\nabla\Phi\cdot\frac{\partial}{\partial T}(\nabla\Phi)\,dV\end{aligned} \tag{A3}$$

using eqn (4) repeatedly and applying Green's theorem. Combining eqn (A1)-(A3) gives finally

$$H_{el} = G_f\left(1+\frac{T}{\varepsilon_r}\frac{\partial \varepsilon_r}{\partial T}\right). \tag{8}$$

[1] F. Oosawa, *Polyelectrolytes* (Marcel Dekker, New York, 1971).
[2] G. S. Manning, *Ann. Rev. Phys. Chem.*, 1972, **23**, 117.
[3] G. S. Manning, *Quart. Rev. Biophys.*, 1978, **11**, 181.
[4] J. J. van der Klink, L. H. Zuiderweg and J. C. Leyte, *J. Chem. Phys.*, 1974, **60**, 2391.
[5] H. Wennerström, B. Lindman, G. Lindblom and G. J. T. Tiddy, *J.C.S. Faraday I*, 1979, **75**, 663.
[6] J. Skerjanc, D. Dolar and D. Leskovsek, *Z. Chem.*, 1967, **56**, 207, 218.
[7] J. Skerjanc, D. Dolar and D. Leskovsek, *Z. Chem.*, 1970, **70**, 31.
[8] D. Dolar and J. Skerjance, *J. Chem. Phys.*, 1974, **61**, 4106.
[9] J. Skerjanc, D. Kozak, S. Hocevar, G. Vesnaver, B. Jus and D. Dolar, *Biophys. Chem.*, 1977, **6**, 9.
[10] V. Crescenzi, F. Debber and F. Quadrifoglio, *J. Polymer Sci. A*-2, 1972, **10**, 257.
[11] V. Crescenzi, F. Delben, F. Quadrifoglio and D. Polar, *J. Phys. Chem.*, 1973, **77**, 539.
[12] G. E. Boyd, D. P. Wilson and G. S. Manning, *J. Phys. Chem.*, 1976, **80**, 808.
[13] A. Katchalsky, *Pure Appl. Chem.*, 1971, **26**, 327.
[14] G. S. Manning, *J. Chem. Phys.*, 1969, **51**, 924, 934.
[15] G. Olofsson and I. Olofsson, *J. Chem. Thermodynamics*, 1977, **9**, 65.
[16] V. P. Parker, *Thermal Properties of Aqueous Uni-Univalent Electrolytes* (NSRDS NBS, U.S. Government Printing Office, Washington D.C., 1965).
[17] G. Olofsson, to be published.
[18] R. Fouoss, A. Katchalsky and S. Lifson, *Proc. Nat. Acad. Sci.*, 1951, **37**, 579.
[19] T. Alfrey, P. W. Berg and H. Morawetz, *J. Polymer Sci.*, 1951, **7**, 543.
[20] L. Kotin and M. Nagasawa, *J. Chem. Phys.*, 1969, **51**, 924.
[21] H. Gustavsson and G. Gunnarsson, to be published.
[22] R. A. Marcus, *J. Chem. Phys.*, 1955, **23**, 1057.

(PAPER 9/1204)

IV

MICELLAR SIZE DISTRIBUTIONS FOR IONIC AMPHIPHILES

by

Gudmundur Gunnarsson
Division of Physical Chemistry 2,
Chemical Center, P.O.B 740
S-220 07 Lund, SWEDEN

and

Håkan Wennerström
Division of Physical Chemistry,
Arrhenius Laboratory,
University of Stockholm,
S-106 91 Stockholm, SWEDEN

Running title: Micellar size distributions.

SUMMARY

A model is presented for the aggregate size distribution in micellar solutions of ionic amphiphiles. The micelle formation is treated as due to a balance between electrostatic and hydrophobic interactions. The electrostatic free energies are calculated using the Poisson-Boltzmann equation and the cell model. It is found that the model can account for both the cooperativity of the micelle formation process, the order of magnitude of the polydispersity in the size distribution, the difference in micelle sizes with monovalent and divalent counterions, the growth in micelle size at high amphiphile concentrations and at addition of salt. Thus a series of properties related to the micellar size distribution are described in a semiquantitative way. A general quantitative agreement with experiment is, however, not obtained. This is particularily evident when comparison is made with data obtained from kinetic measurements.

INTRODUCTION

The formation of micellar aggregates by amphiphilic molecules is due to a compromise between the low solubility of apolar molecules in water and the strong affinity of polar groups for water[1-3]. Qualitatively one expects that the cooperativity in the association process arises from the hydrophobic effect in the same way as for a nonpolar substance that has reached beyond its solubility limit in water. However, in the amphiphile systems there is the restriction that the polar heads prefer to remain in contact with the water at the aggregate surface. This implies that the aggregates can not grow indefinitely in three dimensions[3,4] and for the typical micelle forming amphiphiles the aggregates usually takes a spherical or rod like shape[5,6]

Although the general mechanism behind the formation of micelles and liquid crystalline phases is rather well understood, less is known about the finer details that govern the sizes and shapes of the micelles. Many properties of micellar solutions can be described and understood without a detailed description of the aggregate size distribution, by using only a value for the critical micelle concentration (cmc) and an assumed single aggregate size[1,2]. However, more detailed experiments show that such a description is but a first approximation and a more refined model is needed for in the interpretation of the data. This is particularly apparent in connection with micellar kinetics studies but it also applies to thermodynamic and spectroscopic measurements at concentrations around the cmc and under conditions where the micelles change shape. A further aspect is that the phase separation model and models with a fixed aggregation number accepts without explanation that the aggregate formation is strongly cooperative up to a certain aggregation number while the cooperativity is negligible for the further growth. These features of the aggregation process make the micelle

formation rather unique and it is a severe test on quantitative models that they can properly account for these effects.

In this paper we present a model for micelle size distribution for ionic amphiphiles, attempting to within one model describe both the premicellar aggregation and the micellar growth that occurs at higher amphiphile and/or salt concentrations. The treatment is an extension of our previous description of micellar systems[7] using only a single micelle size. The electrostatic effects were treated using the non-linearized Poisson-Boltzmann (P-B) equation and the cell model[8,9] to account for the effect of micelle-micelle interactions. The same basic model has also been shown to account for the phase equilibria between micellar solutions and liquid crystalline phases[10].

The organization of the paper is that the basic model is first described. Then we present the formal treatment of electrostatic effects in the cell model with a distribution of cell sizes, including calculations of the chemical potentials. The following section is devoted to computational procedures and approximations. The model is then applied to size distributions in the vicinity of the cmc. We then calculate aggregation numbers and size distributions at varying amphiphile and salt concentrations. Parameters relevant for the description of the kinetics of the micelle formation[11] are then calculated and compared with experiments.

Our aim has been to keep the model conceptually simple and include only a few physical interactions, the hydrophobic and the electrostatic, in the model free energy, while treating the thermodynamic consequences in detail. Our model is similar to that of Tanford[12] in its basic physical assumptions but particularly the electrostatic effects are treated in greater detail.

It contrasts the recent work of Nagarajan and Ruckenstein[13], where many contributions to the free energy were considered.

BASIC MODEL

The total micellar solution, containing N micellar aggregates with aggregation numbers n=2,3....., is divided into N electroneutral cells each containing one micelle. Each cell also contains a certain amount of electrolyte and water so that the sum over the N cells corresponds to the total content of each species in the system (cf. Fig. 1). The sizes of the cells and their electrolyte content are chosen so that the chemical potentials of the amphiphile (with counterion), of the water and of added salt are uniform throughout the system. The chemical potentials of the components are derived from a model expression for the free energy. The free energy has contributions from essentially only two interactions; the electrostatic and the hydrophobic.

The electrostatic contributions to the free energy are calculated on the basis of the non-linearized Poisson-Boltzmann equation. The electrostatic free energy G_{el} can be written as the sum of an energy E_{el} and an entropy term TS_{el}[14]

$$G_{el} = E_{el} - TS_{el} \tag{1}$$

where E_{el} is determined the energy of the field

$$E_{el} = \varepsilon_r \varepsilon_0 \int (\nabla \Phi)^2 dV/2 \tag{2}$$

and the entropy terms arise from the non-uniform ion distribution

$$TS_{el} = kT\{\int c_i \ln c_i \, dV - \Sigma n_i \ln \tilde{c}_i\} \quad (3)$$

where n_i is the amount of ion i, c_i its local concentration and $\tilde{c}_i$ its average concentration. (See Appendix for a complete list of symbols used.)

For small and intermediate aggregation numbers the micelles can adopt a roughly spherical shape but due to the constraint that all the polar groups should reside at the micelle surface the aggregates tend preferably to a rod-like shape for large aggregation numbers. The solution of the electrostatic equations is considerably more cumbersome for such an aggregate with lower symmetry and we have instead adopted an interpolation scheme using solutions to the electrostatic equations for the allowed spheres and a cylinder of the same radius as the length of a fully extended hydrocarbon chain. The contribution to the free energy from the hydrophobic effect is divided into two parts, one of which represents the free energy gain in transferring the apolar chains from an aqueous environement completely into hydrocarbon environment. This contribution is independent of the particular aggregate that is formed and its size can be estimated from experimental cmc values. It has furthermore a characteristic dependence on chain length with an increment of approximately 1.2 - 1.3 kT per added CH_2-group[7,12]. However, in a micellar aggregate there is appreciable contact between water and alkyl chains which leads to a reduction of the gain in hydrophobic energy on aggregate formation. It is a rather general finding[12,15] that this energy contribution can be treated as approximately proportional to the water-hydrocarbon contact area. For larger aggregates the contact area can be calculated directly from the surface of the sphere or rod but as the aggregates become smaller the deviations from the idealized spherical shape becomes more and more important and a correction has to be applied. Thus we can ex-

press the aggregate dependent part of the hydrophobic energy as $\gamma A_n f_n$ where A_n is the area of the n:th aggregate calculated for its idealized geometry and f_n is the correction factor for the area calculation. Previous studies[5,10] indicate that f_n should approach unity when n corresponds to the value for a proper micelle, while for n = 1 $\gamma A_n f_n$ should cancel the constant part in the hydrophobic energy. Between these two extremes f_n should decrease monotonically. These conditions determine the general behavior of f_n and the undetermined feature is how rapidly f_n decays to one with increasing n.

THE TOTAL FREE ENERGY OF A MICELLAR SOLUTION

The total free energy G of the micellar system consists of contributions from the free energies G_0^n of the N_n cells with aggregates of size n and a contribution from the entropy of mixing of the cells

$$G = \sum_n N_n G_0^n + G_{mix}^{cell} \tag{4}$$

The entropy of mixing contribution is zero if all cells are identical, i.e. for a monodisperse micelle distribution, and it takes the form

$$G_{mix}^{cell} = kT \sum_n N_n \ln Y_n \tag{5}$$

The micelle size distribution is specified by the fraction Y_n of aggregates of size n

$$Y_n = N_n / \Sigma N_n \tag{6}$$

and the Y_n are the quantities we are aiming at calculating.

The free energy for a cell contains contributions from the different interactions but also entropy terms

$$G_0^n = n\mu_{am}^{o,a} + \sum_i n_i^{w,n} \mu_i^{o,w} + G_{el}^n + G_s^n + G_{mix}^n \qquad (7)$$

Here $\mu_{a,m}^{o,a}$ is the standard chemical potential of the amphiphilic ion in the aggregate and $\mu_i^{o,w}$ and $n_i^{w,n}$, respectively, the standard chemical potential of and the amount of species i in the aqueous region, including the water. G_{mix}^n is the contribution from the ideal entropy of mixing of the ions, mole fraction X_i^n, and the micelle, mole fraction X_m^n, with water in a cell with aggregate size n

$$G_{mix}^n = kT\{ \sum_{i\neq w} n_i^{w,n} (\ln X_i^n - 1) + (\ln X_m^n - 1)\} \qquad (8)$$

The summation over i does not include the water. The electrostatic free energy can be expressed in a computationally convenient form[7] through

$$G_{el}^n = z_{am}\, ne\Phi_A^n - E_{el}^n + kT\Sigma n_i^{w,n} \ln(X_{io}^n/X_i^n) \qquad (9)$$

where $z_{am}e$ is the charge of an amphiphilic ion and Φ_A is the electrostatic potential at the surface of a micelle. The potential has been chosen as zero at the surface of the cell in accordance with the assumed electroneutrality of the cells and X_{io}^n is the concentration of species i at the cell surface.

The aggregate dependent part of the hydrophobic energy is written as

$$G_s^n = \gamma A^n f_n \qquad (10)$$

For the proportionality factor γ the value 0.018 N/m has been used. This value has been shown[10] to be appropriate for the description of the properties of liquid crystalline phases in carboxylic soap-water systems. It is also close to the value used by Tanford[3,12] based on an estimate by Hermann[15] from solubility data for apolar molecules. Missel et al.[5] also found a similar value in the analysis of the sphere to rod transition of dodecyl sulfate micelles. For the factor f_n correcting for the roughness of the aggregate surface several different empirical functional forms were tried, using the constraints that $f_1 \simeq 1.6$ and that $f_n \to 1$ as n increases so that f_n is practically unity for n greater than 60. The qualitative results are not critically dependent on the choice of f_n, but there are clear quantitative differences, particularily when parameters relevant for the kinetic measurements are calculated. In the calculations reported below the following form for f_n has been used

$$f_n = 1 + 0.5 \exp\{-(n/43)^3 + 1/43^3) + 0.1 \exp\{-(n/15)^2 + 1/15^2\} \qquad (11)$$

CHEMICAL POTENTIALS AND THE EQUATION FOR THE MICELLAR SIZE DISTRIBUTION

In a micellar solution the amphiphile molecules are distributed between aggregates of different sizes in such a way that the total free energy of the system is minimized. A convenient way of accomplishing the minimization of the model expression for G is to require that the chemical potentials of all species are uniform throughout the system. Although the expression for G is rather complex it is possible to determine the chemical potentials by a straightforward derivation of G using the results and techniques of refs. 7 and 10. The result is that for an ion i in aqueous region

$$\mu_i^w = \mu_i^{o,w} + kT \ln X_{io}^n \qquad (12)$$

For the water

$$\mu_{H_2O} = \mu^{o}_{H_2O} - kT(\Sigma X^{n}_{io} + X^{n}_{m}) \tag{13}$$

where ΣX_{io} represents osmotic contribution from the ions and X^{n}_{m} the osmotic term from the micelle itself. The expression for the chemical potential of the amphiphile in the aggregate is more complex

$$\mu^{a}_{am} = \mu^{o,a}_{am} + G^{n}_{s}/n + \mu^{n}_{el} + \frac{kT}{n} \ln X^{n}_{m} + \frac{kT}{n} \ln Y_{n} \tag{14}$$

The two last terms arise from the entropies of mixing of the micelles in a cell and of the different cells. The electrostatic part of the chemical potential is (cf. ref. 7)

$$n\mu^{n}_{el} = z_{am} ne\Phi^{n}_{A} - E_{el} - kT\Sigma n^{w,n}_{i} + kT(V^{n}_{1}/V_{H_2O})\Sigma X^{n}_{io} \tag{15}$$

where V^{n}_{1} is the aqueous volume of a cell and V_{H_2O} the volume per water molecule. The electrostatic contribution to the chemical potential is thus only related to the surface potential, but contains also other terms related to the redistribution in the system if a monomer leaves an aggregate.

An amphiphilic ion has the option of either residing in an aggregate, where the chemical potential is given by eq. (14), or it can exist as a monomer in the aqueous region, where the chemical potential is obtained from eq. (12). At equilibrium these two chemical potential should be equal giving the equation

$$\ln Y_{n} = -n(\mu^{o,a}_{am} - \mu^{o,w}_{am}) - G^{n}_{s} - n\mu_{el} - kT \ln X^{n}_{m} + nkT \ln X^{n}_{am,o} \tag{16}$$

where $X^n_{am,o}$ is the monomer amphiphile concentration (mole fraction units) at the cell surface. When all the quantities on the right hand side are determined eq. (16) is the required equation for the size distribution.

To find a simple relation that ensures that the chemical potential of all the species are uniform throughout the system we notice that the osmotic contribution from the micelle itself is usually negligible relative to the contribution from the mobile ions so that $\Sigma_i X^n_{io} >> X^n_m$ in eq. (13) and the contribution from X^n_m can be neglected. In this case a uniform chemical potential is obtained if X^n_{io} is independent of n. This condition ensures a considerable simplification of the solution of the electrostatic problem as will be apparent in the description of the computational scheme.

MICELLE GEOMETRIES AND THE ESTIMATION OF PARAMETERS FOR ROD-LIKE MICELLES

Micelles with aggregation numbers lower than that of the maximum spherical micelle are assumed to be spherical. The aggregation number of the maximum spherical micelle, n_s is given by

$$n_s = 4\pi l^3/(3V_m) \tag{17}$$

where l is the length of a fully extended hydrocarbon chain given by eq. (6-5) in ref. (3). V_m is the volume of a hydrocarbon chain given by eq. (6-4) in ref. (3). The radii of the hydrocarbon cores of the spherical micelles, b^n_h are determined by their aggregation numbers, n and V^n_m through the relation

$$b^n_h = \{nV_m 3/(4\pi)\}^{1/3} \tag{18}$$

The area used in the determination of G_s is then

$$A^n = 4\pi(b_h^n)^2 - nA_o \qquad (19)$$

where A_o is the cross sectional area of a hydrocarbon chain, taken as 21 $Å^2$. Micelles larger than the maximum spherical micelle are assumed to be cylinders with hemisphere capped ends, see figure 1. The radii of the cylindrical and spherical portions of these large micelles are given by the length of a fully extended hydrocarbon chain, 1.

The ionic groups are assumed to stick straight out from the surface of the hydrocarbon core. In the case of sulfates this means that the ionic charges are located 3 Å from the surface of the hydrocarbon core[16]. The charges of the ionic groups are assumed to be smeared out, with the charge density σ_n, on the surface defined by the ionic charges in order to make a solution of the P-B equation feasible.

The quantities μ_n^{el}, X_m^n and $X_{am,o}^n$ in eq. (16) are obtained from a solution of the P-B equation. For spheres and infinite cylinders P-B equation reduces to a one dimensional differential equation which is relatively straightforward to solve numerically. For the hemisphere capped cylinders a two-dimensional differential equation is obtained which greatly increase the computational time. We therefore use only the solutions for the spheres and the cylinder and interpolate for the hemisphere capped cylinders using the following equation for a quantity F_n

$$F_n = F(\infty) + B_F/n + C_F/n^2 \qquad (20)$$

where the constants B_F and C_F are determined from F_{n_s} and F_{n_s-1}. $F(\infty)$ is the value for an infinite cylinder. At large n when the last term in eq. (20) can be ignored this equation is equivalent to the one used by Missel et al.[5].

COMPUTATIONAL PROCEDURE

In order to determine the quantities on the r.h.s. of eq. (16) and finally calculate a micelle size distribution an iterative computational scheme has been used. The essential steps are

i) An initial guess is made for the ion concentrations X_{io} at the surface of the cells. This guess is based on the values obtained when a monodisperse size distribution is assumed[7].

ii) The P-B equation is solved for all spheres and for the infinite cylinder using the values for X_{io} and the boundary condition

$$\left.\frac{d\Phi}{dr}\right|_{b_c^n} = -\frac{\sigma_n}{\varepsilon_r \varepsilon_o} \tag{21}$$

where b_c^n is the radius at the surface of charge.

In order to satisfy this bondary condition the radius of the cell has to be varied in an iterative way. The size of the cell is thus determined by σ_n and the X_{io}:s. Once the P-B equation is solved the electrostatic contribution μ_{el}^n to the chemical potential is calculated.

iii) All the quantities for the hemisphere capped cylinders are calculated using the interpolation procedure of eq. (20).

iv) A value for $\mu_{am}^{o,a} - \mu_{am}^{o,w}$ is guessed. Then all the quantities on the r.h.s. of eq. (16) have been determined and it is possible to solve for Y_n.

v) Once the parameters in the model have been fixed the properties of the system are determined for given values of the total concentrations of the amphiphile and of added salt. By initially assigning values for all X_{io} the system of equations becomes overdetermined and they are in general not all satisfied. In the present scheme the calculated Y_n do not automatically sum up to unity as they should according to eq. (6). If $\Sigma Y_n - 1 > 10^{-5}$ step iv) is repeated and small changes in $\mu_{am}^{o,a} - \mu_{am}^{o,w}$ are used to adjust the conditions so that $\Sigma Y_n = 1$.

vi) The concentrations of amphiphile and salt (if applicable) are calculated from the ion concentration profiles in the cells and from the determined size distribution. The procedure is then repeated from step i) by assigning new values for X_{io} which ultimately results in a distribution function for another concentration.

When the concentrations of positive and negative ions at the cell surface become nearly equal, which occurs at low micellar concentrations, our method of solving the P-B equation breakes down numerically. However, in this limit is the corresponding solution of the P-B equation for an aggregate at infinite dilution an excellent approximation[7]. In this case is

$$n\mu_{el}^{n} = G_{el}^{n} \tag{22}$$

while water and electrolyte activities are assumed to be those of the bulk solution. In this case is the condition $\Sigma Y_n = 1$ automatically satisfied.

RESULTS

The cmc and the cooperativity in the micelle formation

Once the model presented above has been specified, there is only one parameter, $\mu_{am}^{o,a} - \mu_{am}^{o,w}$, in the theory. The relevant value for this parameter will depend on the particular amphiphile and it has a characteristic dependence on alkyl chain length[3]. The property of a micellar system that is most strongly dependent on $\mu_{am}^{o,a} - \mu_{am}^{o,w}$ is the cmc, i.e. the concentration at which micellar aggregates start to appear in measurable amounts. Thus in applying the model to a particular amphiphile the value of $\mu_{am}^{o,a} - \mu_{am}^{o,w}$ is adjusted so that the calculated cmc (see below) is in accordance with the experimentally determined value for monovalent counterions and no added salt. In most of the applications reported below $\mu_{am}^{o,a} - \mu_{am}^{o,w}$ has been chosen as 14.74 kT to give a representation of dodecyl sulfate systems, for which the cmc is around 8.3 mM[17] with monovalent counterions.

A characteristic feature of the micelle formation process is the strong cooperativity leading to the existence of a reasonably well-defined critical micelle concentration and a critical test of the model consists of investigating if it can account for/explain this property. It is shown in figure 2 how the aggregate size distribution varies with total amphiphile concentration in the vicinity of 8.3 mM. A peak in the size distribution around n = 55 is gradually appearing showing that aggregates of this size are formed preferentially, revealing the high cooperativity of the process up to aggregation numbers of approximately 50, while the cooperativity is considerably smaller at still higher aggregation numbers. It is this latter property that makes the micelle formation different from an ordinary phase separation. The sharpness of the onset of micelle formation is more clearly illustrated in

figure 3, which shows a plot of the amount of the amphiphile in micellar aggregates versus the total concentrations. For comparison we show also the points obtained assuming a monodisperse distribution with n = 55.5. The difference between the monodisperse system and the one where all micelle sizes are allowed is small. In many experimental studies one would identify the cmc as the point (marked with arrows in figure 3) where the amount of amphiphile in the micelles appear to reach zero when extrapolated from higher concentrations. However, one should note that the cmc does not have, and should not in our opinion be given, a precise definition[18,19]. If one is indeed interested in the details of the aggregation behavior in a concentration range around the cmc one has to accept that the aggregate formation involves multiple equilibria and a size distribution and that the analogy with a phase separation is not complete.

As shown in figs. 2 and 3 the model does provide a quantitatively reasonable description of the cooperativity of the micelle formation. It is then crucial for the conceptual understanding of the phenomenon to recognize what features in the model that are essential in obtaining the cooperativity. An important observation is that with the area enhancement factor $f_n = 1$, essentially neglecting the fact that the molecular nature of the amphiphile prevents it from obtaining an optimal separation of hydrocarbon and water in the smaller aggregates, the micelle formation is no longer cooperative. The cooperativity in the hydrophobic interaction is no longer large enough to compensate for the increased electrostatic repulsions present in the larger aggregates. The relative size of the hydrophobic and the electrostatic contributions can be changed by increasing γ, but in that case one encounters difficulties in explaing why the aggregation stops at essentially spherical aggregates rather than continuing to much larger aggregates. The conclusion that emerges is then that one essential factor for the cooperative micelle formation is the

difficulty of the oligomeric amphiphile aggregates to reduce the hydrocarbon water contact to the value calculated on the basis of a continuous hydrocarbon medium. For larger aggregates the molecular nature of the amphiphile is of less significance. A complementary or alternative explanation would be to assume that intermolecular interactions within aggregates of intermediate range operate between the alkyl chains so that their effect can not be included in γ until the aggregates have reached a certain size.

Micellar size distribution above the cmc

At concentrations above the cmc there is a tendency for the micelles to grow in size. This is partly due to a simple mass action effect but it is also caused by a reduction of the electrostatic effects opposing the formation of larger aggregates. The electrostatics is also greatly influenced by the valency of the counterions, as is manifested in the much lower cmc for DS with divalent than with monovalent counterions (see figure 3). The addition of salt also leads to a lowering of the cmc through a reduction of the electrostatic repulsions[5,7].

A reasonable characterization of the size distribution is obtained through the weight average aggregation number n_w.

$$n_w = \Sigma n^2 Y_n / \Sigma n Y_n \tag{23}$$

which is, for example, measured in light scattering experiments. The polydispersity of the distribution can be measured by the variance σ^2

$$\sigma^2 = \Sigma n^2 Y_n / \Sigma Y_n - (\Sigma n Y_n / \Sigma Y_n)^2 \tag{24}$$

In the calculations of n_w and σ we have chosen to sum over aggregates corresponding to aggregation numbers larger than the minimum in the size distribution. Except for concentrations close to the cmc this choice is of little significance for the value of n_w and σ.

Figures 4 and 5 show how n_w and σ, respectively, vary with the total concentration of amphiphile for DS with monovalent counterions at three different concentrations of 1:1 salt and for DS with divalent counterions. An interesting feature of these figures is that σ increases with increasing total amphiphile concentration for divalent counterions and for monovalent ions with salt while the trend is the opposite for monovalent counterions without salt. However, even in this case σ will ultimately increase but this occurs at very high concentrations. The calculated values of σ are for the monovalent counterions smaller by a factor of two than the values estimated from the kinetic data[11] while good agreement is found for the systems with divalent counterions[20]. In the presence of additional electrolyte the cmc decreases and the tendency for the micelles to grow in size increases. This is accompanied by an increase in polydispersity.

Parameters from kinetic measurements

The experimental method that appears to provide the most detailed information on micellar size distribution is kinetic measurements[11]. Due to the successful theory of Aniasson and Wall[21] the relaxation times measured by ultrasonic relaxation and T or P-jump experiments can be given a detailed interpretation in terms of parameters dependent on the micellar size distribution. In general two relaxation times, τ_1 and τ_2, can be measured. The shorter τ_1 is a measure of the time required for the rearrangement to a new size distribution under the constraint that the total number of micelles is constant and it can

be written

$$1/\tau_1 = k_- \{\sigma^2 - \frac{1}{n_n} (c_{tot} + c_{mon})/c_{mon}\} \quad (25)$$

where k_- is the off rate constant for a monomer, c_{tot} is the total amphiphile concentration, c_{mon} the monomer concentration and n_n the number average aggregation. The slow relaxation time, which is a measure of the lifetime of the micellar aggregate itself is[11]

$$1/\tau_2 = \frac{1}{R \cdot c_{mic}} \frac{c_{mon} + \overline{n^2_n} c_{mic}}{c_{mon} + \sigma^2 c_{mic}} \quad (26)$$

where c_{mic} is the total concentration of micelles and the "resistance" R is given by

$$R = \frac{1}{k_-} \sum_{2}^{n_n - \sigma} 1/(Y_n c_{mic}) \quad (27)$$

The relaxation times τ_1 and τ_2 can be calculated from a given size distribution except for the rate constant k_-. τ_1 depends mainly on σ^2 and n_n while τ_2 is very sensitive to the size distribution around the minimum at intermediate aggregation numbers. In the model it thus depends crucially on the choice of f_n.

Figures 6 and 7 show how theoretical and experimental[22,23] values of $1/\tau_1$ and $1/\tau_2$, respectively, vary with total amphiphile concentrations. We have adjusted the parameters in f_n to obtain a value of $1/\tau_2$ which is of the right order of magnitude for c_{tot} ca. 10 mM. The decrease in $1/\tau_2$ is qualitatively in agreement with experiment. The slope of $1/\tau_1$ vs. c_{tot} is also in agreement with experiment. The apparent intercept is, however, to large reflecting the too small value of σ.

In Table 1 we show the comparison between experimental[20] and theoretical values of the relaxation times for DS with divalent counterions. The theoretical values of $1/\tau_1$ are in approximate agreement with experiments. The theoretical estimate of τ_2 gives a too strong effect of the change from monovalent to divalent counterions. Experimentally τ_2 increases by 10^3 while the calculated value increases by 10^7. This reflects the difficulties in properly describing the small aggregates, the concentrations of which determine τ_2.

CONCLUSIONS

By considering the effects of the electrostatic and hydrophobic interactions on the micelle size distribution one can obtain a sensitive test of the current models for these interactions. It has previously been shown that many thermodynamic parameters such as cmc values[7,24], monomer activities[7], micelle growth[5] and phase equilibria[10] can be quantitatively accounted for in a scheme where the electrostatic energies are calculated from the Poisson-Boltzmann equation and the hydrophobic free energies are determined as a surface free energy. In the present work this approach has been extended to account for micelle size distributions, which are more sensitive to the finer details in the free energy expressions. The general result is that the model predicts a qualitatively correct behavior of the size distribution. One important observation is that the hydrophobic free energy must be described carefully in order to predict the cooperativity in the micelle formation. It is also found that it is a good approximation to consider only one single aggregation number when treating cmc effects. The results for the kinetic parameters show how very sensitive τ_2 values are to the size distribution.

APPENDIX

List of symbols

A^n	area of the hydrocarbon core of a micelle
b_c^n	radius of teh surface of charges of a micelle
b_h^n	radius of the hydrocarbon core of a micelle
c_{tot}	total concentration of surfactant
c_{mon}	concentration of surfactant in monomeric form
c_{mic}^{mon}	concentration of surfactant in micellar form
c_{mic}	total concentration of micelles
c_i	local concentration of ion i
$\tilde{c}_i$	average concentration of ion i in the aqueous volume of a cell
f_n	correction factor for area calculations
E_{el}^n	electrostatic energy of a cell
G	total free energy of a micellar solution
G_o^n	total free energy in a cell
G_{el}^n	electrostatic free energy of a cell
G_s^n	aggregate dependent part of the hydrophobic free energy
G_{mix}^n	the ideal entropy of mixing of ions in a cell with water in the cell
G_{mix}^{cell}	the entropy of mixing of the cells
k_-	the of rate constant for a monomer from a micelle
l	length of a hydrocarbon chain
n	aggregation number of a micelle. When used as superscript of subscritp the labelled quantity refers to a micelle or a cell with an aggregate of aggregation number n.
n_w	weight average aggregation number
n_n	number average aggregation number
n_s	the aggregation number of the maximum spherical micelle
$n_i^{w,n}$	amount of ion i in the aqueous region of a cell

N	total number of micelles
N_n	number of micelles of aggregation number n
S_{el}	the electrostatic entropy of the ion distribution
V_1^n	aqueous volume of a cell
V_m	volume of a hydrocarbon chain
V_{H_2O}	molecular volume of water
X_i^n	mole fraction of ion i over a whole cell
X_{io}^n	mole fraction of ion i at the cell boundary
X_m^n	mole fraction of micelle in a cell
Y_n	fraction of aggregates of size n
z_{am}	the valency of the amphiphile ion
z_c	the valency of the counterion
Φ	electrostatic potential
Φ_A^n	electrostatic potential at the micellar surface
γ	proportionality constant relating G_s^n and $f_n A^n$
ε_o	permittivity of vacuum
ε_r	relative permittivity
$\mu_i^{o,x}$	standard chemical potential of species in environment x
μ_i^x	chemical potential of species i in environment x
μ_{el}^n	electrostatic contribution to the chemical potential of the amphiphile in a micelle
σ^2	the variance of a distribution
σ_n	the charge density of a micelle
τ_1	fast relaxation time measured in kinetic experiments
τ_2	slow relaxation time measured in kinetic measurements

REFERENCES

1. H. Wennerström and B. Lindman, Phys. Rep., 1979, 52, 1.
2. B. Lindman and H. Wennerström, Top. Curr. Chem., 1980, 87, 1.
3. C. Tanford, The Hydrophobic Effect, 2nd ed. (John Wiley, New York, 1980).
4. J.N. Israelachvili, D.J. Mitchell and B.N. Ninham, J. Chem. Soc. Faraday Trans., 2, 1976, 72, 1525.
5. P.J. Missel, N.A. Mazer, G.B. Benedek and C.Y. Young, J. Phys. Chem., 1980, 84, 1044.
6. S. Ozeki and S. Ikeda, J. Colloid Interface Sci., 1980, 77, 219.
7. G. Gunnarsson, B. Jönsson and H. Wennerström, J. Phys. Chem., 1980, 84, 3114.
8. T. Alfrey, P.W. Berg and H. Morawetz, J. Polymer Sci., 1951, 7, 543.
9. R.M. Fuoss, A. Katchalsky and S. Lifson, Proc. Natl. Acad. Sci. USA, 1951, 37, 579.
10. B. Jönsson and H. Wennerström, J. Colloid Interface Sci., 1981, 80, 482.
11. E.A.G. Aniasson, S.N. Wall, M. Almgren, H. Hoffmann, I. Kielmann, W. Ulbricht, R. Zana, J. Lang, and C. Tondre, J. Phys. Chem., 1976, 22, 905.
12. C. Tanford, J. Phys. Chem., 1974, 78, 2469.
13. R. Nagarajan and E. Ruckenstein, J. Colloid Interface Sci., 1979, 71, 580.
14. R.A. Marcus, J. Chem. Phys., 1955, 23, 1057.
15. R.B. Hermann, J. Phys. Chem., 1972, 76, 2754.
16. D. Stigter, J. Phys. Chem., 1974, 78, 2480.
17. P. Mukerjee and K.J. Mysels, Critical micelle concentrations of aqueous surfactant systems, NSRDS-NBS 36. Washington D.C.: US Government printing office.
18. R. Nagarajan and E. Ruckenstein, J. Colloid Interface Sci., 1977, 60, 221.
19. A. Ben-Naim and F.H. Stillinger, J. Phys. Chem., 1980, 84, 2872.
20. W. Baumuller, H. Hoffmann and W. Ulbricht, C. Tondre and R. Zana, J. Colloid Interface Sci., 1978, 64, 418.
21. E.A. Aniansson and S. Wall, J. Phys. Chem., 1974, 78, 1024.
22. R. Folger, H. Hoffmann and W. Ulbricht, Ber. Bunsenges. Phys. Chem., 1974, 78, 986.
23. M. Teubner, S. Diekman and M. Kahlweit, Ber. Bunsenges. Phys. Chem., 1978, 83, 1278.
24. D. Stigter, J. Colloid Interface Sci., 1974, 47, 473.

FIGURE CAPTIONS

Figure 1 — Representation of a micellar solution in the cell model. The system is divided into cells, each containing one aggregate, monomeric surfactant, counterions, added salt and water.

Figure 2 — The variation in the micelle size distribution around the cmc. The amount micellized amphiphile is plotted versus aggregation number. The value of $\mu_{am}^{o,a} - \mu_{am}^{o,w}$ is chosen so that the cmc $\approx$ 8.3 mM corresponding to a sodium dodecyl sulfate system.

Figure 3 — The concentration of amphiphile in micellar form plotted versus the total amphiphile concentration. Solid line: monodisperse distribution (n = 55.5) in the cell model; .... polydisperse distribution in the infinite dilution approximation; X polydisperse distribution in the cell model. The arrows indicate the cmc obtained by extrapolating from higher concentrations the curve for the polydisperse distribution. For the dodecyle sulfate system the cmc so determined is 8.30 mM with monovalent counterions and 2.34 mM with divalent counterions.

Figure 4 — Calculated weight average aggregation numbers versus total amphiphile concentration. Curves are calculated using the infinite dilution approximation while the crosses indicate values calculated in the cell model.

Figure 5 — Calculated standard deviation in the micelle size distribution versus total amphiphile concentration.. Symbols as in Figure 4.

Figure 6

Comparison between experimental and calculated values for τ_1 at different, total amphiphile concentrations for sodium dodecyl sulfate. The theoretical values are obtained by using $k_- = 10^7\ sec^{-1}$ (see ref. 11) and the cell model. Experimental values from ref. 21.

Figure 7

Comparison between experimental (from ref. 22) and calculated values for the relaxation time τ_2 at different amphiphile concentrations. Theoretical values are obtained using the cell model and $k_- = 10^7\ sec^{-1}$.

Table 1. Experimental and theoretical values of $1/\tau_2$ and $1/\tau_1$ for dodecyl sulfate (DS) with monovalent counterions.

Conc. of DS (mM)	$1/\tau_1$		$1/\tau_2$		Method
	$NiDS_2$	$CoDS_2$	$NiDS_2$	$CoDS_2$	
4.0	4.83	3.40	0.976	1.31	Experiment[a]
4.2	5.79	3.86	$1.57 \cdot 10^{-4}$	$1.0 \cdot 10^{-4}$	Theory[b]
8.0	11.36	8.00	10.20	14.29	Experiment[a]
19.3	37.56	25.04	$2.10 \cdot 10^{-5}$	$1.40 \cdot 10^{-5}$	Theory[b]

a) From ref.

b) Value calculated by using $k_- = 2.6 \cdot 10^6$ sec^{-1} for $CoLS_s$ and $k_- = 3.9 \cdot 10^6$ sec^{-1} for $NiLS_2$, see ref.

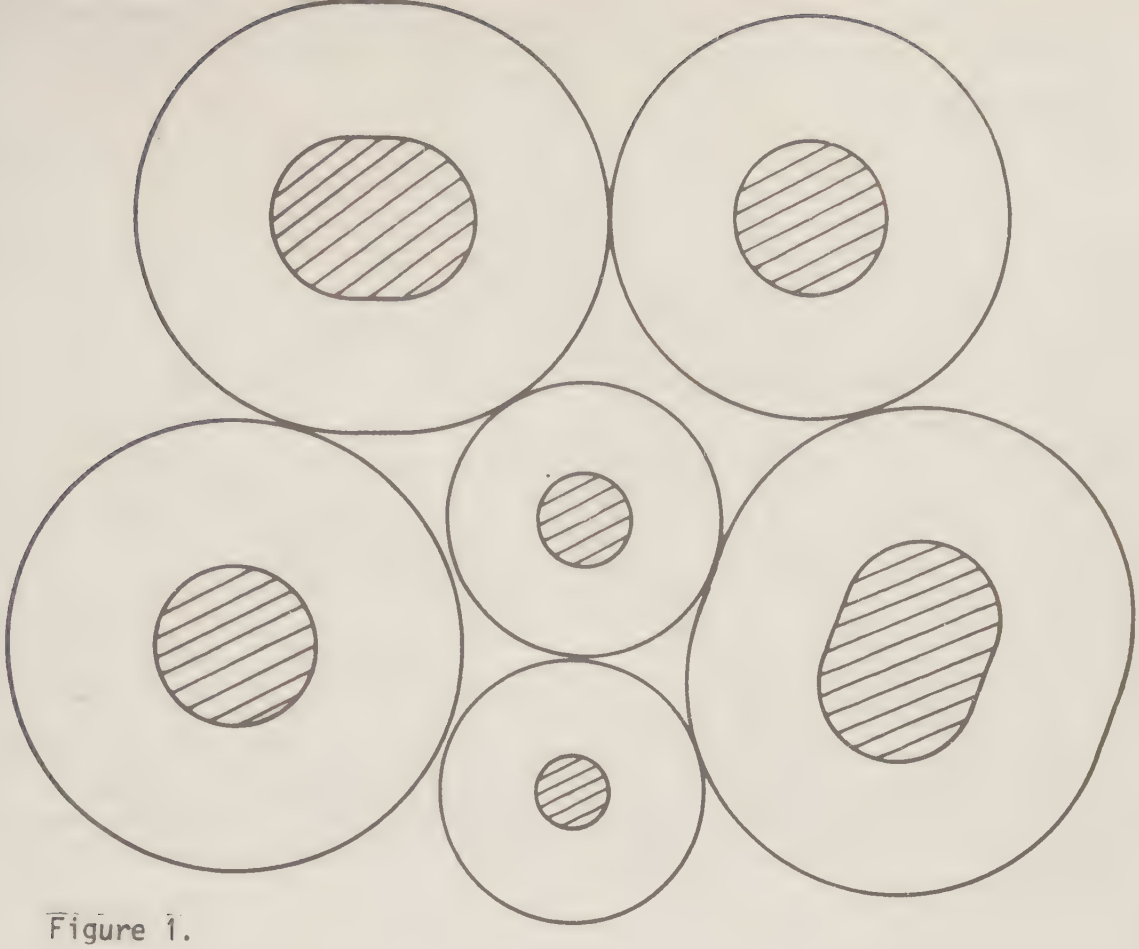

Figure 1.

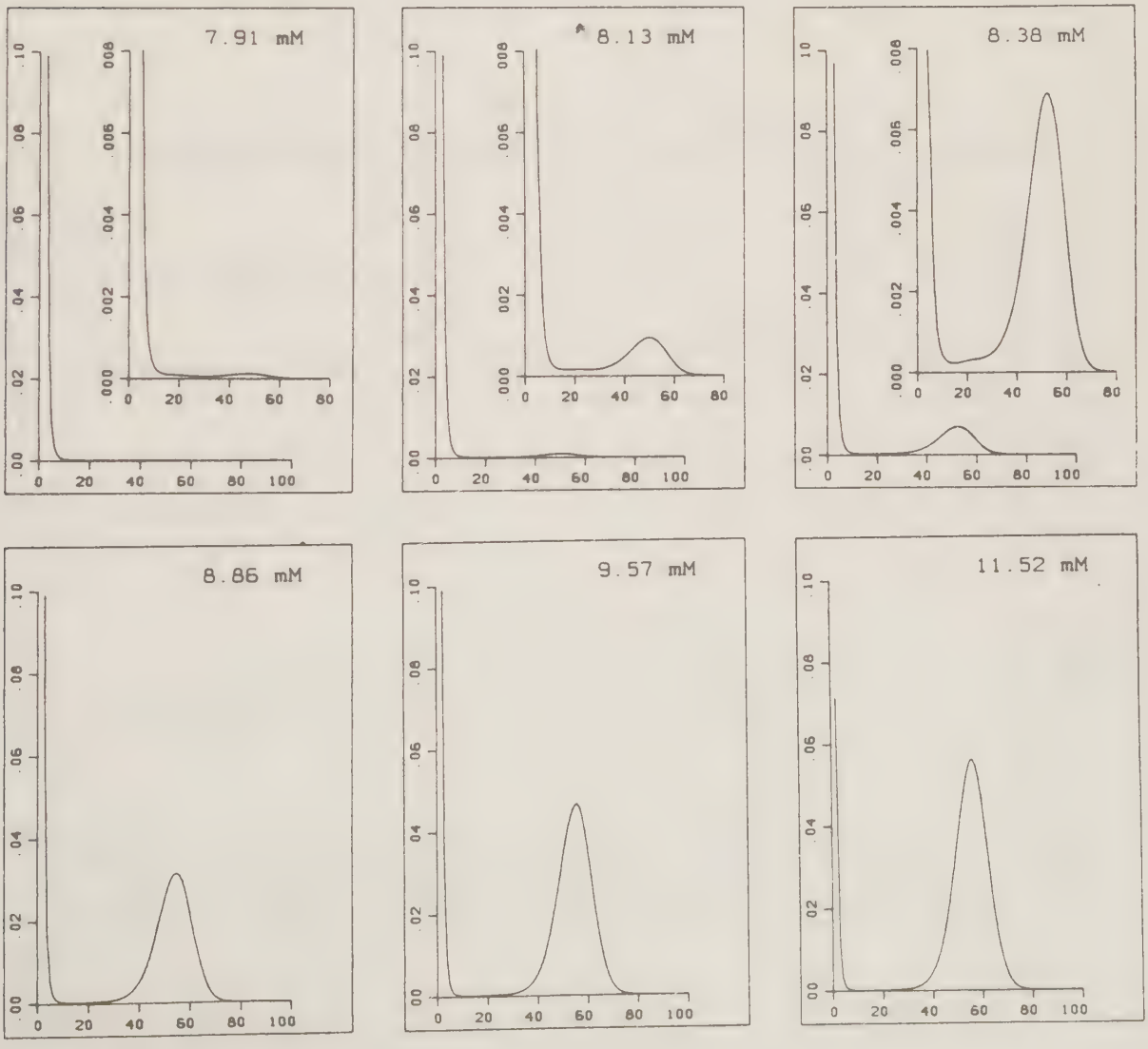

Figure 2.

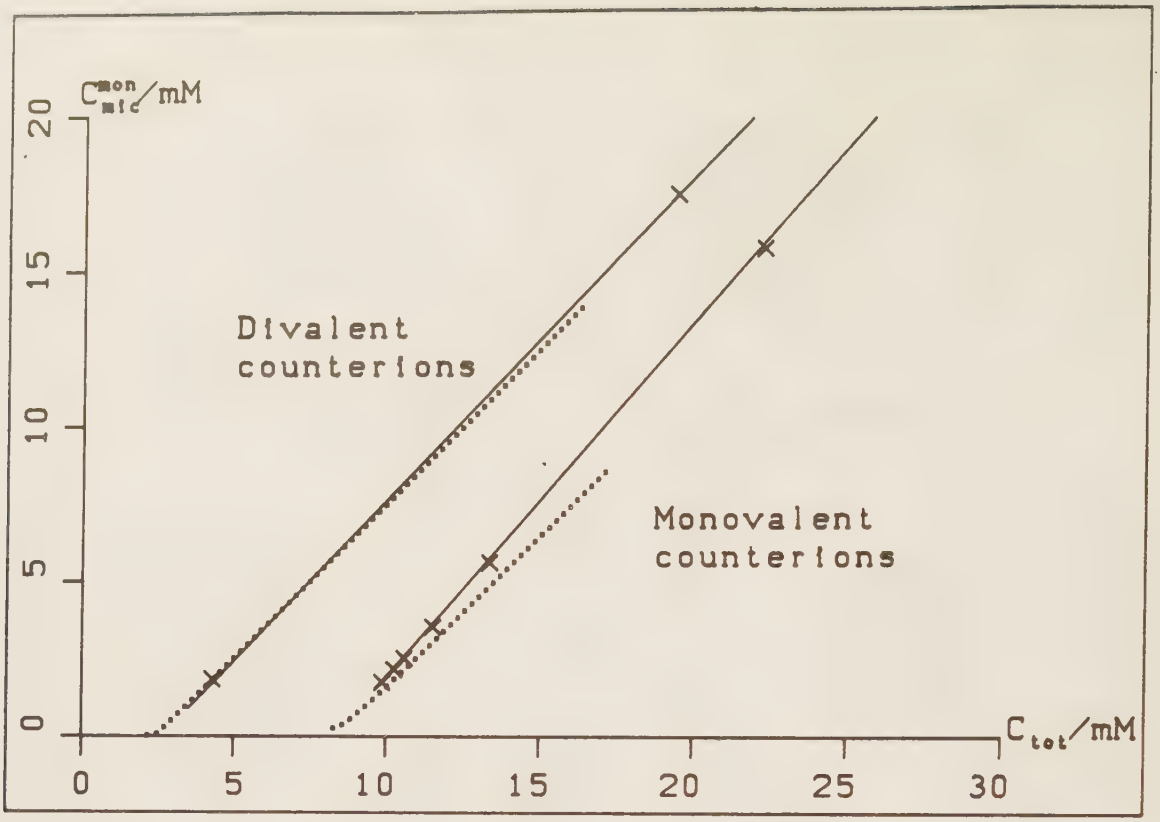

Figure 3.

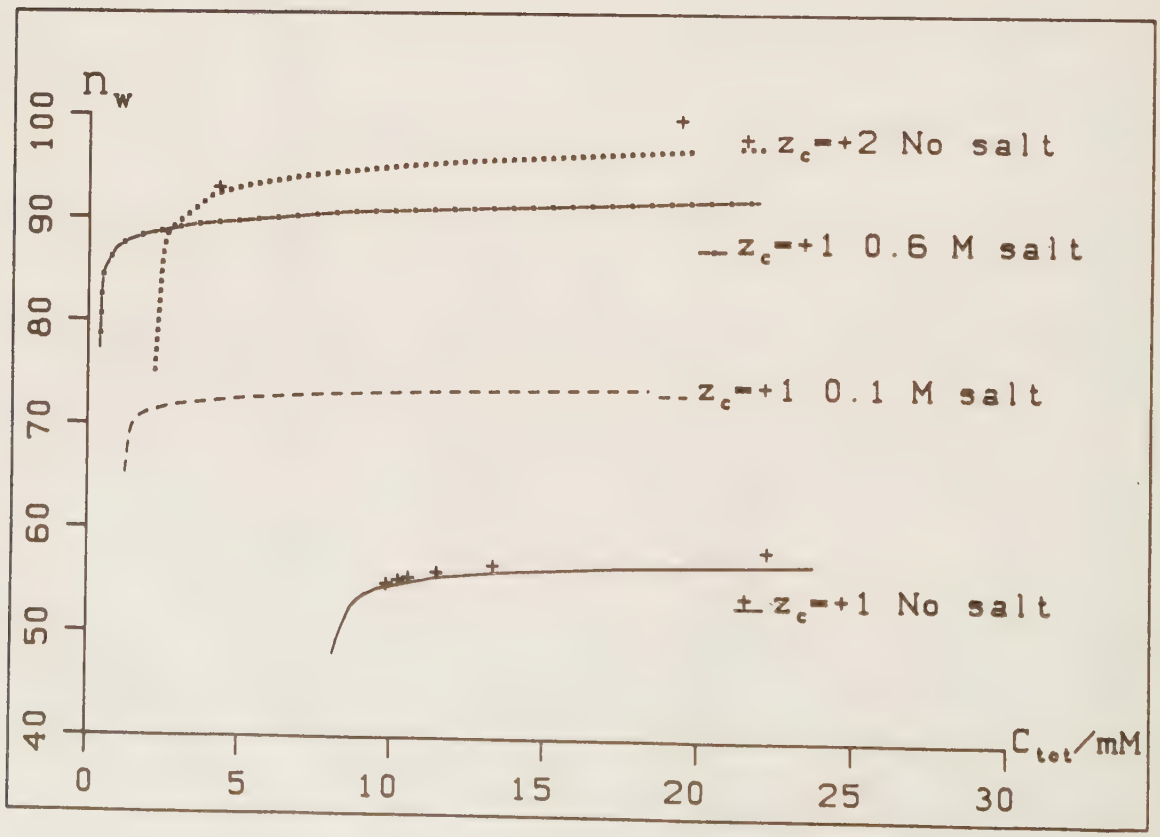

Figure 4.

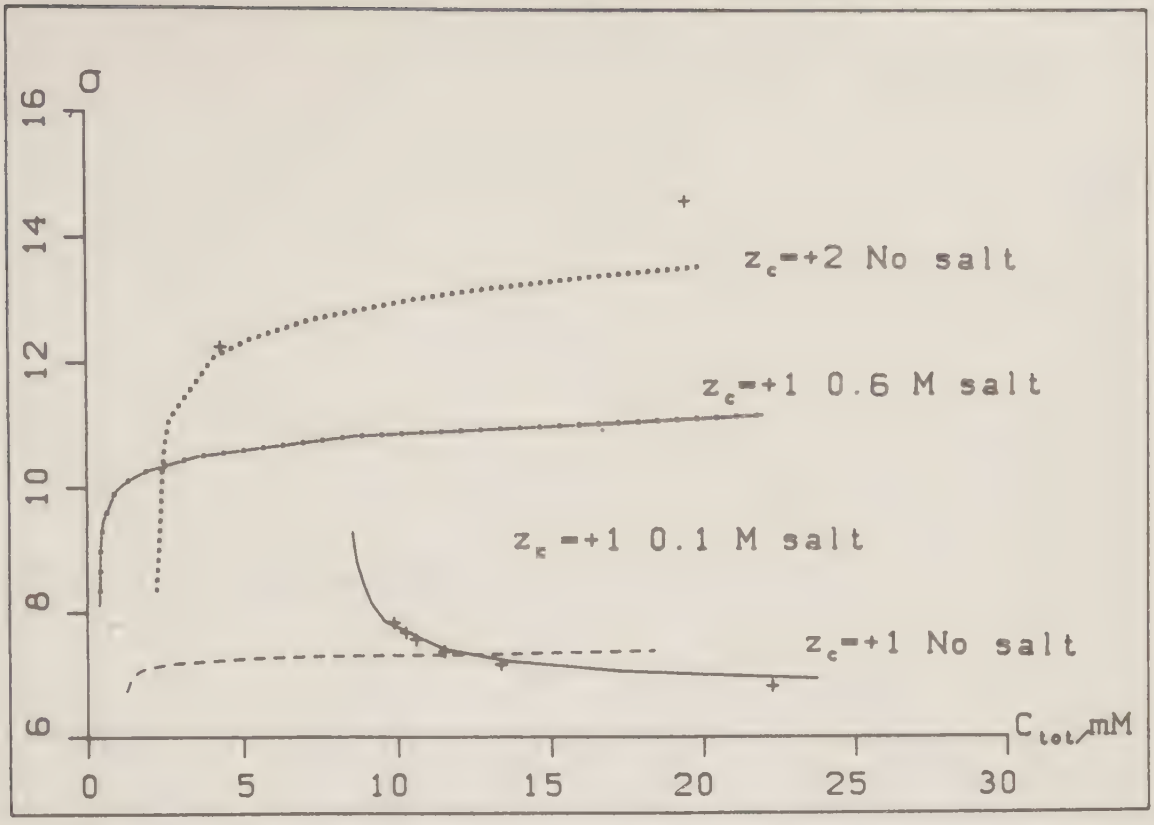

Figure 5.

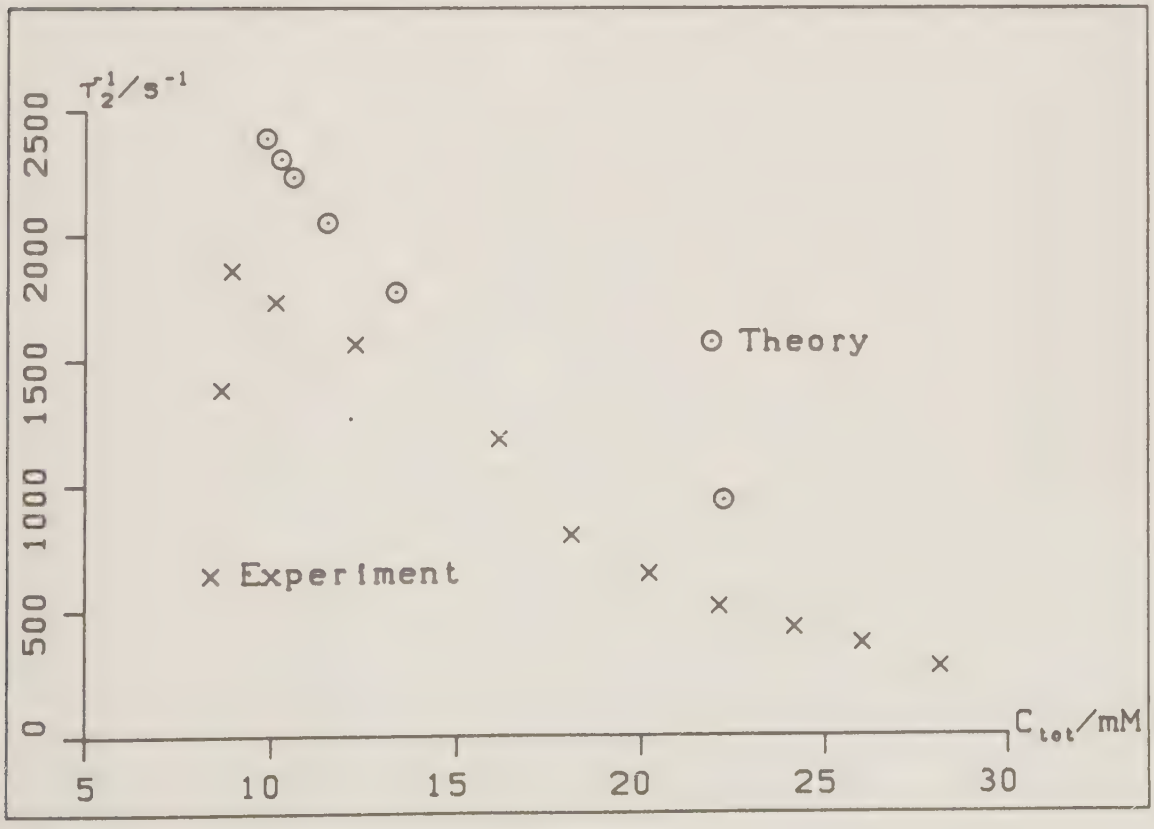

Figure 6.

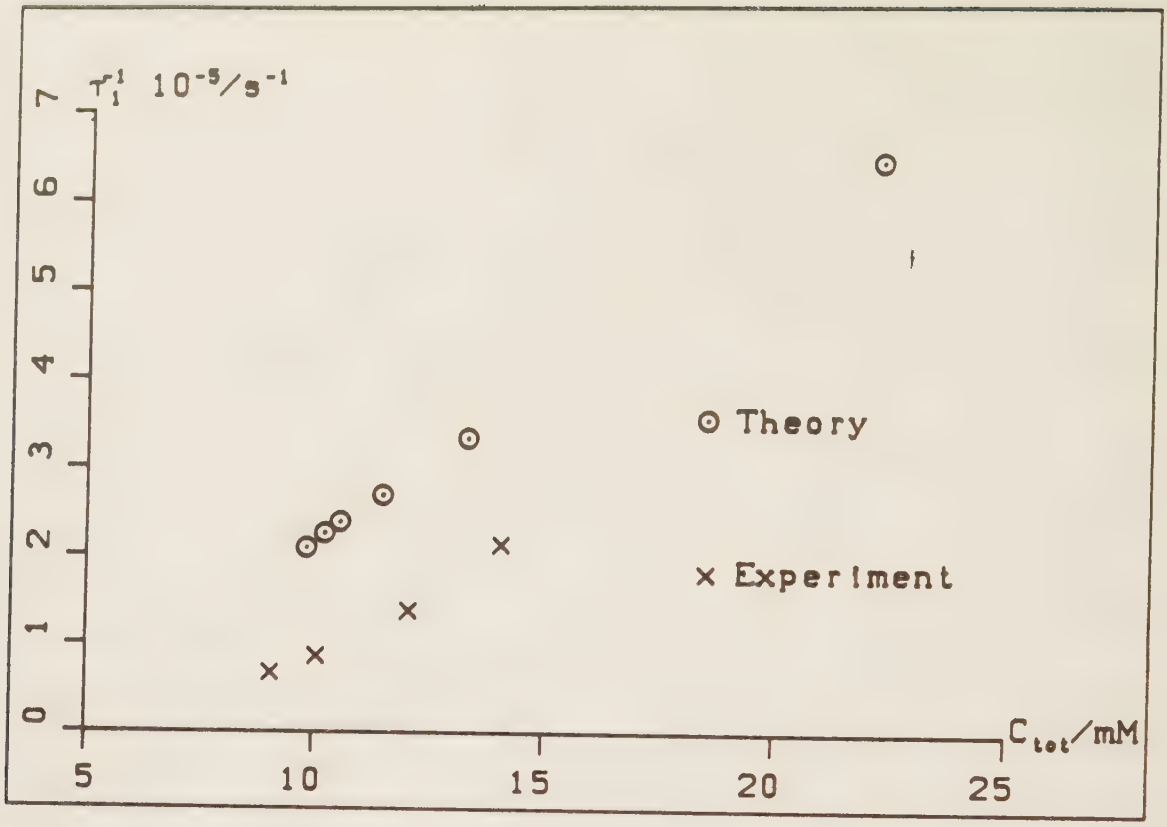

Figure 7.

KEMICENTRUM
reprocentralen Lund